



**JNCC Report
No: 635**

**A Natural Capital Approach to Landscape Planning: a Pilot Project in
Colchagua Valley - Technical Report**

**Trippier, B., Jones, A., Jones, G., Barbosa, O., Colson, D., Duran, P., Godoy, K.,
Harris, M., Harrison, S., Tierney, M., Smith, M. & Wright, E.**

**September 2019
(Revised November 2021)**

© JNCC, Peterborough 2021

ISSN 0963 - 8091



For further information please contact:

Joint Nature Conservation Committee
Monkstone House
City Road
Peterborough PE1 1JY
www.jncc.gov.uk

This report should be cited as:

Trippier, B., Jones, A., Jones, G., Barbosa, O., Colson, D., Duran, P., Godoy, K., Harris, M., Harrison, S., Tierney, M., Smith, M. & Wright, E. 2021. A Natural Capital Approach to Landscape Planning: a Pilot Project in Colchagua Valley – Technical Report, Chile (Revised November 2021). *JNCC Report No. 635*, JNCC, Peterborough, ISSN 0963-8091.

JNCC EQA Statement:

This report is compliant with the JNCC Evidence Quality Assurance Policy
<http://jncc.gov.uk/default.aspx?page=6675>.

Please note:

This document was republished in November 2021 to correct part of the definition of the soil water content equation given in the original version (P. 24).

Summary

This technical report outlines the methodologies and outputs produced from the pilot investigation into Natural Capital mapping in the Colchagua Valley in Central Chile. The aims of the project were to demonstrate how the use of earth observation data together with local knowledge can help to better understand natural capital stocks in the region that support wine production and the role vineyards play in ecosystem service delivery.

Working with lead partners at Programa Vino Cambio Climático y Biodiversidad Chile (VCCB) part of the Institute of Ecology and Biodiversity (IEB-Chile) at the Universidad Austral de Chile and engaging with local viticulture businesses through workshops, key ecosystem services of importance to vineyards were highlighted. High resolution Sentinel earth observation data were used to create a habitat map for the region of interest. Different modelling approaches were undertaken to quantify and map the delivery of water supply and quality, soil erosion and fire susceptibility. The models were run under several scenarios to estimate how service delivery varies with sustainable management practices and under climate change scenarios. The modelled outputs were used to train a Bayesian belief network, which alongside stakeholder knowledge, developed an overall network depicting structured probabilistic outcomes relating to how management measures affected the probable delivery of the key ecosystem services. Outputs have been displayed in a user-friendly interactive manner using an R shiny online application, where stakeholders can query the modelled results and explore the impacts that management trade-offs have at an individual field scale.

Contents

1	Project Introduction.....	1
2	Habitat Map	2
2.1	Introduction	2
2.2	Colchagua Valley.....	2
2.3	Earth Observation Data	3
2.3.1	Identification of Sentinel-2 data	3
2.3.2	Identification of Sentinel-1 data	4
2.3.3	Pre-processing of Sentinel data	4
2.4	Classification of habitat map.....	4
2.5	Field data collection	5
2.6	Habitat map outputs	6
2.6.1	Habitat map	6
2.6.2	Probability map.....	8
2.6.3	Accuracy.....	8
3	Soil loss	10
3.1	Introduction	10
3.2	Data sources	10
3.2.1	Climate data	10
3.2.2	Predicted future climate data.....	11
3.2.3	Rainfall erosivity (R)	11
3.2.4	Soil erodibility (K)	11
3.2.5	Slope length (L) and Slope steepness (S).....	12
3.2.6	Land Cover (LC).....	12
3.2.7	Biophysical table	12
3.2.8	Watersheds	13
3.3	Results.....	13
3.4	Using Sediment Delivery Ratio to inform the BBN	15
3.4.1	Management scenarios	15
3.4.2	Climate scenarios.....	15
3.4.3	Buffer scenario	15
3.4.4	Topsoil loss within the vineyard.....	16
3.4.5	Eroded upslope soil.....	16
4	Fire Susceptibility	16
4.1	Introduction	16
4.2	Data Sources	16
4.2.1	Topographic Data.....	17
4.2.2	Climate Data.....	17

4.2.3	Biological Variables	17
4.2.4	Habitat map	17
4.2.5	Anthropogenic Variables	17
4.2.6	Burned Area Data.....	18
4.3	Fire Susceptibility Model.....	18
4.4	Informing the BBN	19
4.5	Result	21
5	Water quality and supply	23
5.1	Introduction.....	23
5.1.1	The Soil and Water Assessment Tool (SWAT) Model.....	23
5.2	Data sources	25
5.2.1	Landscape.....	26
5.2.2	Climate	26
5.3	Model configuration	27
5.3.1	Watershed delineation.....	27
5.3.2	HRU creation.....	28
5.3.3	Station data and Weather generator	29
5.4	Baseline modelling	29
5.5	Climate change scenarios	39
5.6	Management scenarios to inform the BBN	41
5.6.1	Buffer strips	41
5.6.2	Fertiliser and Pesticide use	41
5.6.3	Winter grazing by cattle.....	43
6	Bayesian Belief Network modelling	44
6.1	Introduction.....	44
6.2	Conceptual Ecological Model	44
6.3	Bayesian Belief Network Development	45
6.4	Relationship Evidence	48
6.4.1	Measured and modelled data.....	48
6.4.2	Literature review and stakeholder workshops	49
6.4.3	Constructing the Conditional Probability Tables (CPTs)	51
6.5	Applying the BBN	51
7	Conclusion and next steps	54
7.1	Potential Steps for Model Improvement	55
8	References	56
Appendix 1 – Implementing the Living Maps Method (LMM) in the Colchagua Valley		64
1	Datasets.....	64
1.1	Sentinel-1	64
1.2	Sentinel-2	65

1.3 Digital Elevation Model (DEM)	66
1.4 Bioclim.....	66
1.5 Open Street Map data	66
2 Training Data	66
3 Method	66
3.1 Segmentation	67
3.2 Random Forest Classifier most significant variables.....	67
Appendix 2 – SWAT modelling HRU parameters	70
1 Plant growth definitions	70
2 Snow parameters	71
Appendix 3 – Stakeholder workshops	74

1 Project Introduction

Through the South Atlantic Research Outreach Programme, the Joint Nature Conservation Committee (UK) has collaborated with The Wine, Climate Change and Biodiversity Program (Programa Vino, Cambio Climático y Biodiversidad [VCCB]) which is a scientific initiative of the Institute of Ecology and Biodiversity and the University Austral of Chile. The initiative works to show that biodiversity conservation and the development of the Chilean wine industry are compatible endeavours. VCCB works closely with 17 vineyards in the Colchagua Valley, central Chile.

The *Natural Capital Approach to Landscape Planning: a Pilot Project in Colchagua Valley*, builds upon long standing work undertaken by VCCB and partner vineyards since 2008 (VCCB, 2008). The project draws upon the natural capital work that JNCC has undertaken with the UK Overseas Territories in the South Atlantic region (JNCC 2019). The project combines industry knowledge with ecosystem sciences and looks to disentangle and quantify the interactions between land management, biotic and abiotic factors, and the effects on ecosystem services relevant to wine producing businesses.

In 2017, Chile exported 9% of its wine to the United Kingdom, with a value of US\$203 million. Projects such as this are critical to the UK and its trading partners in understanding how emerging science and technology can be translated for use by businesses and underpin sustainable supply chains that deliver long-term value, whilst protecting the ecosystems that support the global economy.

The Colchagua Valley is part of Chile's Mediterranean biome that can be found between the regions of Coquimbo (29°02') and Bío-Bío (38°30'). It plays an important role in the productivity of Chile's agriculture and viticulture. The biome is considered a priority for biological conservation as it represents 16% of the continental surface of Chile, yet hosts 50% of Chilean flora and more than half of the country's endemic species (Barbosa & Godoy 2014).

Like many of the world's ecosystems, the Chilean Mediterranean biome is affected by land conversion to agriculture and urban development. The wineries, who are the stakeholders in this project, have been working with VCCB since 2008, exploring ways in which their businesses can sustainably manage their land to conserve habitats in both their vineyards and the surrounding areas, enhancing the local biodiversity.

The project goes to demonstrate how ecosystem mapping and modelling can be established in-line with user requirements and provide tools that help bring environmental data into decision making processes.

Evidence-based environmental management is critical for avoiding supply chain disruption and potential infrastructure damage, such as identifying fire risks and implementing avoidance strategies. Better understanding of catchment processes can lead to informed land management planning and predicting factors such as water stress and pollution risk that are vital to the future sustainability of any business.

The high-level project objectives are:

- Demonstrate how Earth Observation data, ecosystem modelling and local ecological knowledge can be combined to inform ecosystem-based management.
- Work with the wine industry to identify where the application of mapping and modelling outputs can offer commercial benefits through sustainable supply chains.

- Strengthen future collaboration between the United Kingdom and Partners in the South Atlantic region.

The project is funded by the United Kingdom's Department for the Environment, Farming and Rural Affairs (DEFRA).

2 Habitat Map

2.1 Introduction

Habitat maps are a key component to understanding the distribution and extent of features across the landscape, and are a requirement in facilitating better management practices, natural capital accounting, ecosystem service mapping, interpreting and targeting biodiversity monitoring and delivering policies; such as those related to UN Sustainable Development Goals. There are many global land cover and land use products available, but these often do not provide enough detail to perform analyses on a regional level. A land cover map was available for the Colchagua Valley (Martínez 2014), but the map is out of date, and excluded recent land use change; such as those in the forestry and viticulture sectors. Therefore, an updated habitat map was required to carry out the ecosystem service mapping and modelling.

Earth Observation (EO) has been extensively used to provide a synoptic view of land use, cover and change at a variety of scales. New sensors are being developed and launched at an increasing rate, with some mission making data accessible through open source licensing; such as the Copernicus Programme's Sentinel data¹. EO is a valuable resource when no other data are available but is most powerful when combined with field data and a variety of other data sources to create products that provide critical information, particularly for evidence-based decision making.

2.2 Colchagua Valley

The Colchagua Valley is located in central Chile in the General Libertador Bernardo O' Higgins region, 130 km south of capital Santiago. The valley is carved by the Tinguiririca River flowing from the headwaters in the glaciated Andean Mountains to the east, down to the lowland grasslands towards the Pacific coast in the west. As a result, the valley experiences a Mediterranean climate bordered by mountain ranges, with glacial melt being an important water source throughout the year (Bravo *et al.* 2017). The Colchagua valley is located between 34°15'S and 34°50'S and 72°00'W and 70°15'W with a strong agriculture-based economy famed for its winegrowing, which dates back to 1542 (Viñas de Colchagua 2012). The area of interest for the habitat mapping covered an area of approximately 6900.8 km², defined by the main watersheds of interest (see section 5) and encompassing all of the VCCB stakeholder vineyards.

¹ Copernicus is an Earth Observation Programme headed by the European Commission (EC) in partnership with the European Space Agency (ESA). Copernicus provides a unified system through which vast amounts of data are fed into a range of thematic information services designed to benefit the environment, the way we live, humanitarian needs and support effective policy-making for a more sustainable future < https://www.esa.int/Our_Activities/Observing_the_Earth/Copernicus/Overview3>.



Figure 2.1. Area of interest for the Colchagua Valley habitat mapping.

2.3 Earth Observation Data

Copernicus datasets have been identified as a key data source for this project because of their open access and their spatial resolution of 10 metres. In comparison with other open access EO datasets, Sentinel-2 covers the globe more frequently than other observing systems, and is an operational mission as opposed to research based. The Sentinel-2 mission also endeavours to continue to provide open datasets for the future, with a further two satellites planned for launch to join the constellation. For the mapping work, both Sentinel-1, a radar mission, and Sentinel-2, an optical mission, were used to capture as many features in the landscape as possible. Further information on the Sentinels is contained in Appendix 1.

2.3.1 Identification of Sentinel-2 data

As an optical constellation of satellites, Sentinel-2 imagery is limited by cloud cover. To secure cloud-free data of the area of interest in Colchagua, an investigation was required to identify suitable images. Seasonal changes and differences were considered as these variations can be critical to habitat identification and separation of classes. For example, leaf flushes and snow cover vary between seasons. We examined all images acquired by the satellite in 2018, and identified cloud-free images from the following dates for use in the analysis:

- 25th March 2018
- 28th July 2018
- 21st October 2018
- 10th December 2018

This provided approximately quarterly scenes and are considered sufficient to identify most significant seasonal changes.

2.3.2 Identification of Sentinel-1 data

As a radar constellation, Sentinel-1 is not constrained to the same limitations as Sentinel-2, because this radar remote sensing tool can image Earth's surface through cloud cover and during periods of darkness. This means that all images are potentially usable, to capture the seasonal changes and differences four images were chosen with dates that correspond as closely as possible to the Sentinel-2 images. The dates of these images were:

- 25th March 2018
- 23rd July 2018
- 27th October 2018
- 14th December 2018

2.3.3 Pre-processing of Sentinel data

Once the required scenes were identified, the Sentinel imagery were pre-processed using processing chains that have been established through previous project work at JNCC (Sentinel-2: Jones *et al.* 2017; and Sentinel-1: Minchella 2018). To fully exploit the valuable information contained within Sentinel data, users are required to undertake a series of complex pre-processing steps to turn the data from a 'raw' unprocessed format into a state that can be analysed. To enable wider use and exploitation of EO data, JNCC are promoting the systematic and regular provision of Analysis Ready Data (ARD). This aligns with the Committee on Earth Observation Satellites (CEOS) work on facilitating access to satellite data through the international CEOS Analysis Ready Data for Land (CARD4L) project. This notion of accepted standards is recognised by JNCC and the wider CEOS community as a vital step for repeatable and comparable analytical work. The use of ARD allows immediate analysis for end-users and removes complex pre-processing. The processing for Sentinel-2 was carried out using cloud computing facilities available from Amazon Web Services (AWS). The processing chain steps include:

- Geometric correction
- Atmospheric correction
- Radiometric correction

Sentinel-1 data are transformed into backscatter products from data collected in the Interferometric Wide (IW) swath mode and processed from the Ground Range Detected (GRD) version of the data made available by the European Space Agency (ESA). These Sentinel-1 data contain data in both VV and VH polarisations. The raw scenes were terrain corrected, radiometrically normalised and processed to Gamma-0 backscatter coefficient in decibels (dB) using the open-source image analysis software SNAP Toolbox (ESA SNAP).

2.4 Classification of habitat map

The classification method chosen for the generation of the habitat map was the Living Map Method (LMM) (Kilcoyne *et al.* 2017). The habitat classes mapped are defined in section 2.6.1. The LMM developed a code base that allowed users to implement a machine learning

approach to classification, with the flexibility to integrate numerous different data types, including earth observation data. The availability of a ready-made code base that is straight forward to adapt provides an advantage over other similar open-source tools, as it removes the time needed to write code for implementation. Other reasons for choosing the LMM method include:

- Utilises machine learning algorithms which are increasingly used in mapping applications utilising earth observation data;
- Can be carried out on pixel-based and object-based analyses;
- All steps can be carried out using open-source software;
- The code is available under an Open Government License;
- JNCC had a minor role in supporting the development of the code, and hence had good familiarity with the method;
- Can be repeated across different areas and a variety of datasets with little adaption to code;
- Iterations of maps can be generated quickly, efficiently, and it is highly repeatable.

For details on the datasets, classes and method, including data preparation, segmentation, training datasets creation and outputs, see Appendix 1 of this report.

2.5 Field data collection

Following the completion of the first draft of the broad habitat map (see Appendix 1), further data were required to validate the outputs and re-iterate the classification process if necessary. To generate a field survey, a set of points from each class was randomly generated using the outputs of the first draft habitat map. Figure 2.2 shows the location of these points, which were manually checked to ensure no proposed field data collection point overlapped with training points used to generate the classification algorithm. Due to time constraints and accessibility in the upper Andean region of the area of interest, only points considered within a smaller area of interest, as agreed upon by project partners at Austral University of Chile, were visited and recorded (or as many of these as possible). Figure 2.2 shows the points randomly generated and those that the field team were able to visit feasibly during the field campaign conducted in January 2019. This introduces some bias and spatial correlation to the validation set, which becomes more evident and is discussed in detail in section 2.6.3.

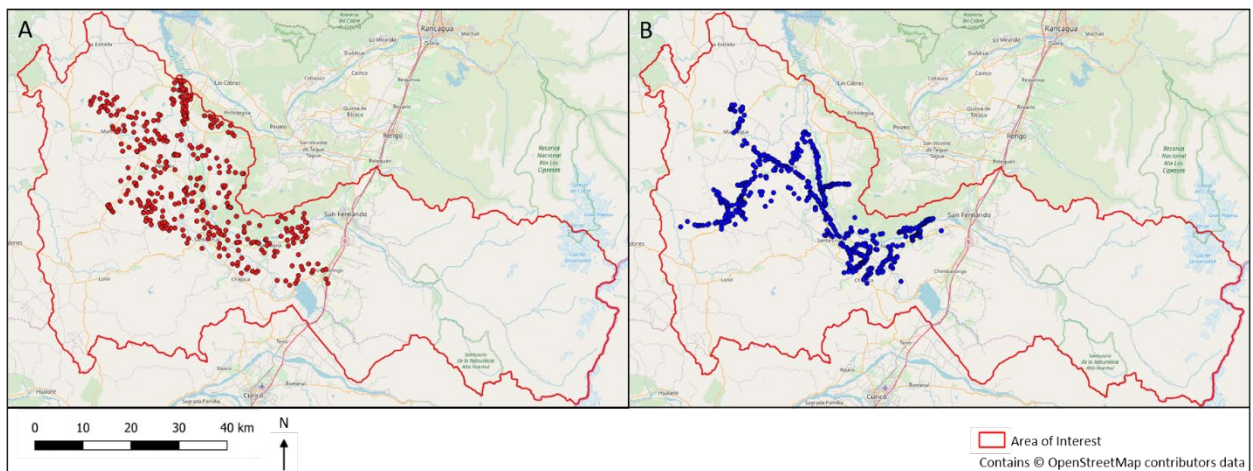


Figure 2.2. Location of points to visit during the field campaign. A) Points to visit B) Points visited.

2.6 Habitat map outputs

2.6.1 Habitat map

Table 2.1 shows the classes present in the habitat map. These classes were chosen in relation with the 2013 land cover map to provide continuity and are defined in relation to habitats of interest for the ecosystem service mapping.

Table 2.1. Habitat class names and descriptions.

Class Name	Class Description
Agricultural land	All areas used as vineyards and for fruit production.
Alluvial plain	A landform created by deposition of material eroded higher up the catchment.
Central Andean Steppe	Montane grassland and shrublands ecoregion in the high elevations of the southern Andes mountain range.
Crop grassland	All areas used to grow crop such as maize on a rotational basis (i.e. not permanent crop types), and areas used for grazing.
Glaciers	A slowly moving mass or river of ice formed by the accumulation and compaction of snow on mountains or near the poles.
Lakes	Areas of water bodies, including naturally formed lakes and reservoirs.
Native forest	A forest composed of indigenous trees and not classified as forest plantation.
Plantation	A forest established by planting and/or seeding in the process of afforestation or reforestation. It consists of introduced species in most cases.
Rivers	A river channel that includes a permanent flow of water.
Rocky outcrops	An area of bedrock that is exposed. Covers varying types of rock.
Scrubland	An area of land consisting of scrub vegetation.
Seasonal meadows	An area consisting of grassland that appears on a seasonal basis.
Snow cover	An area that is permanently covered in snow.
Trees & Scrub	Areas of trees, woodland and scrub that occur on the fringes of field boundaries, river banks and in urban areas.
Urban	Built infrastructure, including houses, farm buildings, roads and any other built structures, tarmac, concrete or gravel.

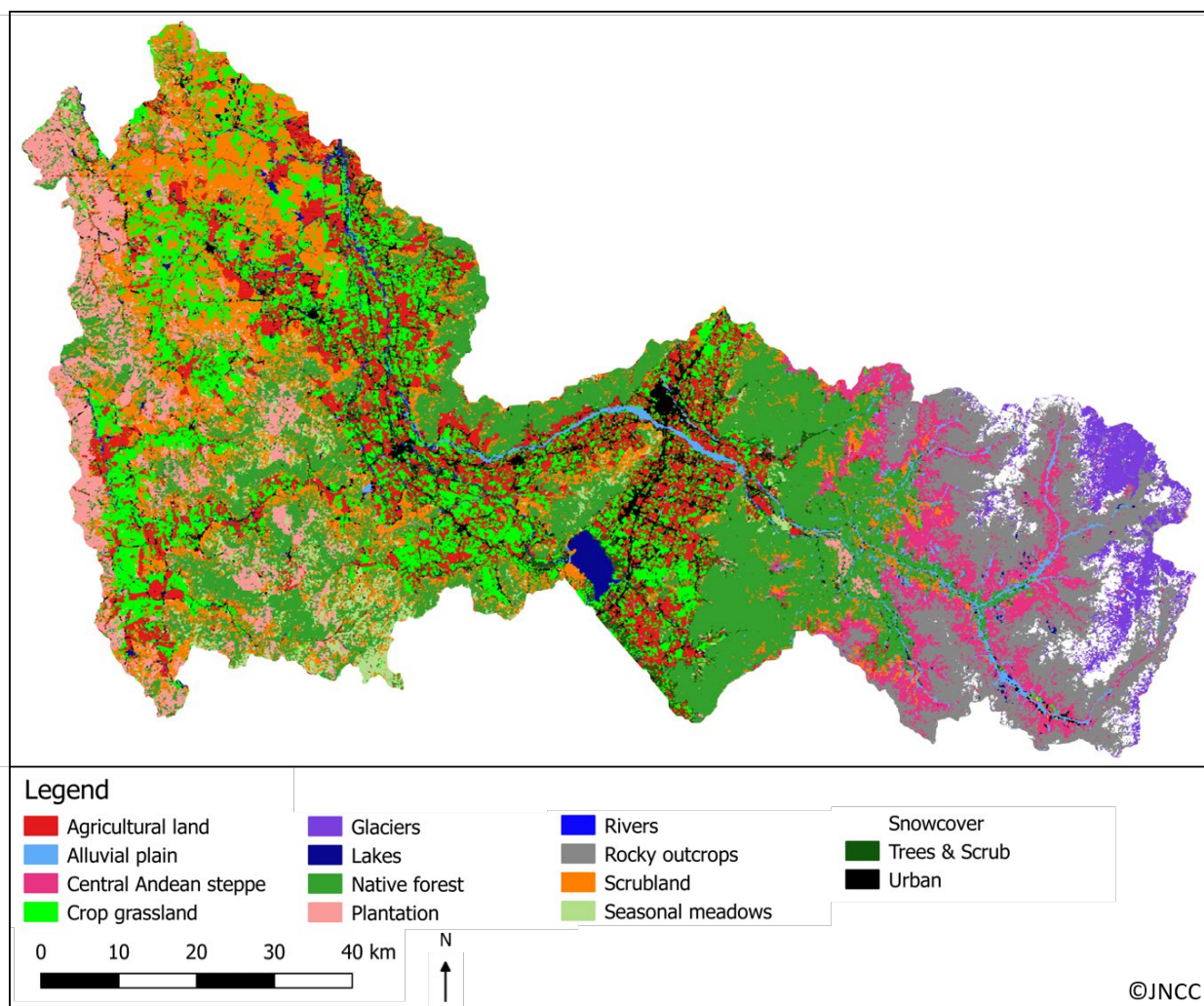


Figure 2.3. Habitat map of Colchagua Valley 2018.

2.6.2 Probability map

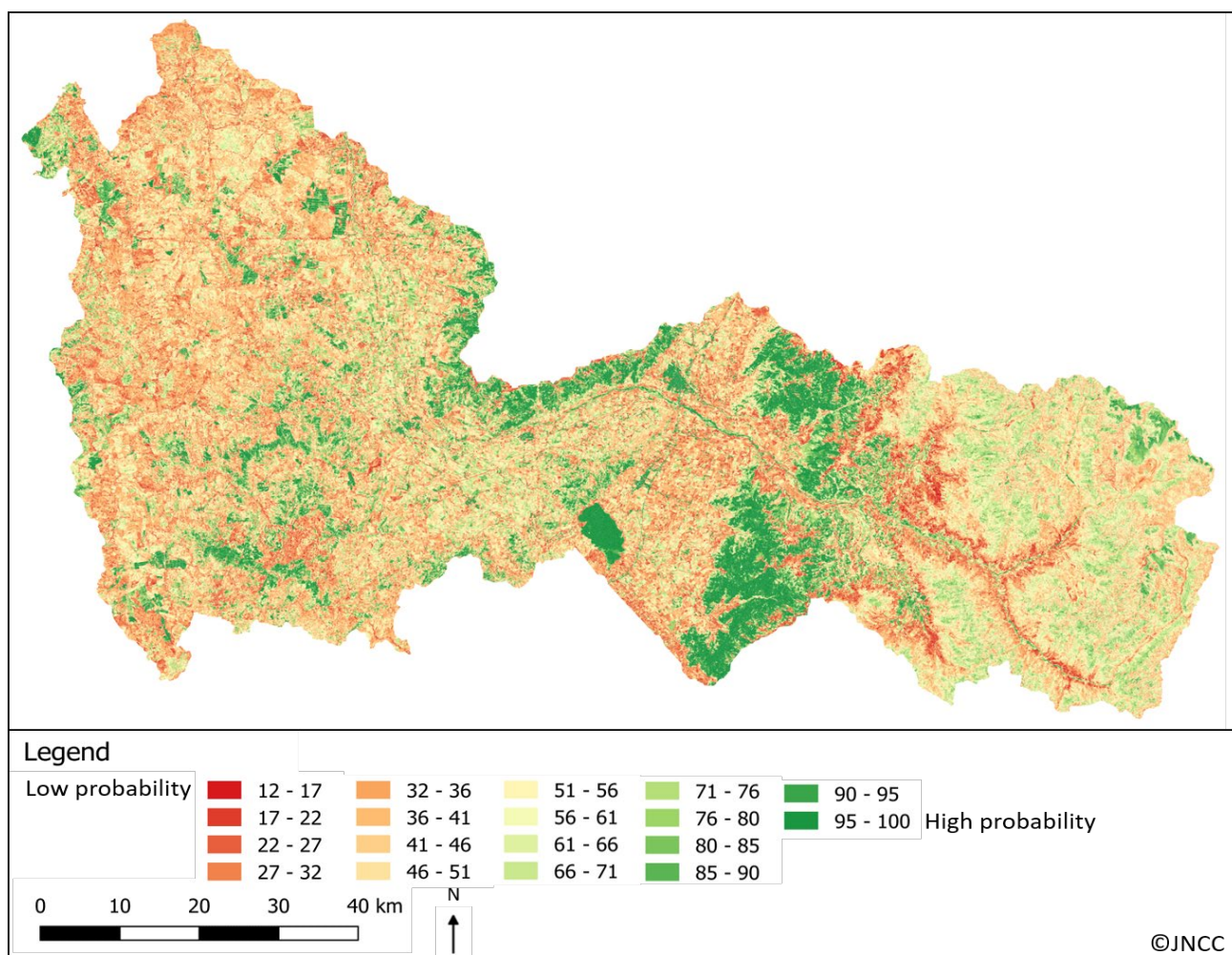


Figure 2.4. Probability of classes being the identified class output, generated from the random forest algorithm when predications from individual trees are aggregated based on a voting system.

Figure 2.4 shows the classification probability, attributed to each object. These figures suggest that there is greater confidence in the forest and water-based classes, such as lakes and rivers. It is likely that classes within the agricultural regions of the valley have a lower probability due to the variety of habitats which can appear similar in the EO data. For example, an object classified as crop grassland will have similar characteristics to seasonal meadows, agricultural land and scrubland classes in EO data, meaning that the probability of the object belonging to a single class is reduced. The presence of mosaic habitats will also reduce the probability value, so Figure 2.4 can be used to interpret the uniformity and variety of the landscape in addition to providing a level of confidence spatially of the classified output.

2.6.3 Accuracy

To analyse the accuracy of the outputs, the data collected during the field visit were used to generate an error matrix of the habitat map. The overall estimated accuracy of the map, which gives us an indication of how many of the field data were classified correctly, is 78 %.

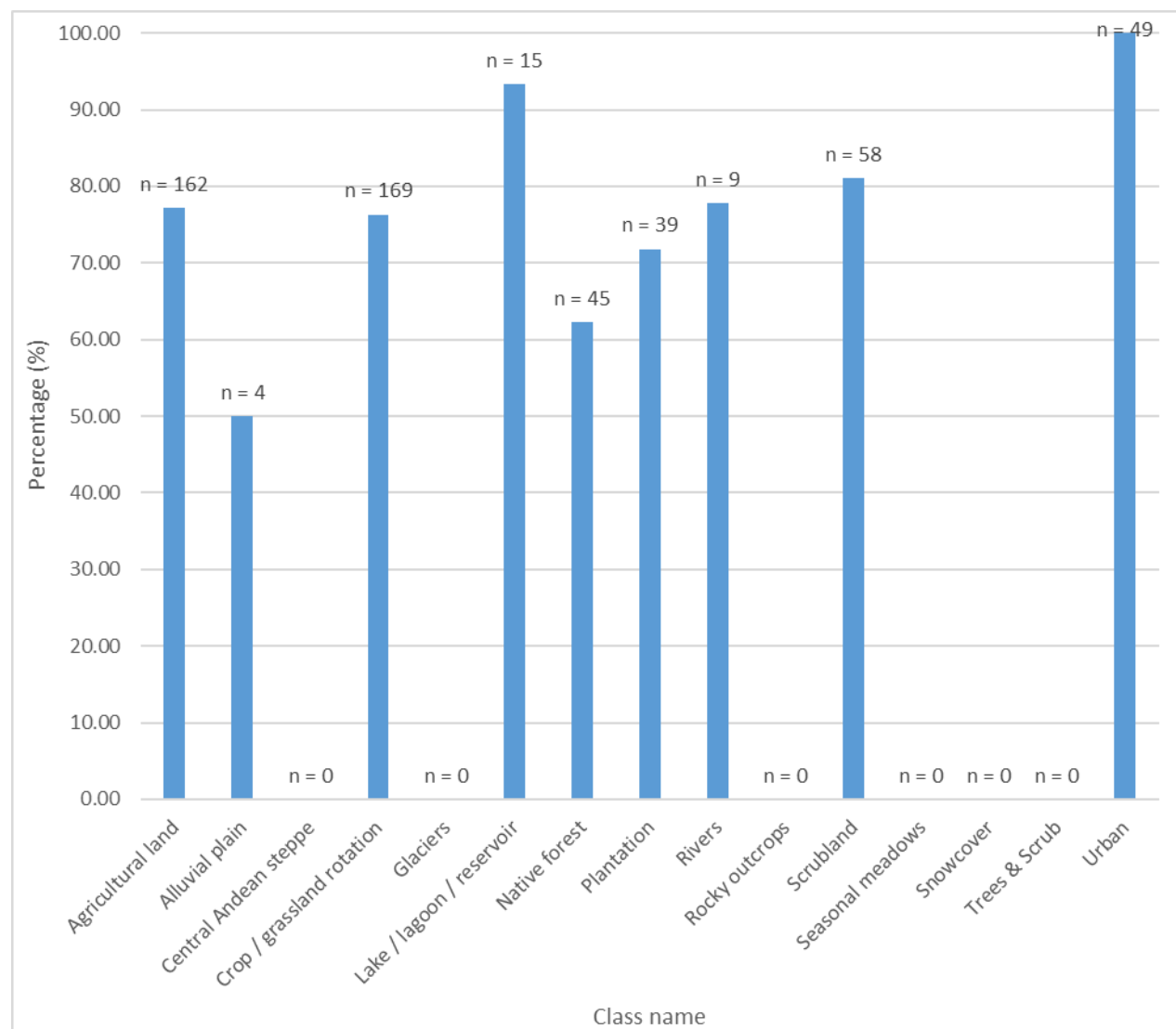


Figure 2.5. A graphical output of the user's accuracy from the error matrix, where 'n' is the number of field validation points available per class. Overall estimated accuracy of the map is 78%.

In order to interpret these results, an assessment of the error matrix is required (Figure 2.5). It should be noted that these estimates of accuracy have variable certainty associated with them due to differing field data sample numbers. For example, no validation points were collected for a number of classes, therefore, the estimated accuracy is unknown. The overall accuracy therefore, does not provide any indication of accuracy of classes without any field data, and should be interpreted as such, and used with caution. For classes with validation points, it is important to note the spatial distribution of the data is centred around the north west region of the area of interest, meaning the accuracy of other areas within the map are less certain. It is also worth mentioning classes Agricultural land, Crop / grassland rotation and scrubland are showing accurate user accuracies despite the random forest algorithm providing low probabilities for these classes in Figure 2.4. This means that the classification algorithm has performed better than expected when identifying classes that have similar characteristics with several other classes, such as Agricultural land and Crop / grassland rotation.

3 Soil loss

3.1 Introduction

Viticulture stakeholders within the project region identified priority ecosystem services that their vineyards either delivered or might affect. Topsoil was recognised as a major ecosystem service for the growth of the vines, and erosion of topsoil can be a significant ecosystem service loss. In addition, the import of nutrients due to erosion of soils upslope from the vineyards is also recognised as detrimental to grape growing. To evaluate the movement of soil both from within and above vineyards we used the Sediment Delivery Ratio (SDR) model of InVEST 3.5.0 (Stanford University 2019) to calculate revised universal soil loss equation (RUSLE). We used this over the inbuilt sediment module in the SWAT model (used to assess water supply and quality in Section 5) as the outputs are at a higher resolution (10 m pixel, rather than SWAT's Hydrological Response Units) which is more appropriate for vineyard land management, and because it is well suited to change management parameters, the outputs of which were used to inform the follow-on Bayesian Belief Network (see Section 5).

The SDR model is designed to map the overland sediment generation and subsequent delivery to waterways, however as part of this the model outputs the total potential soil loss per pixel calculated from the RUSLE:

$$A = RKLSCP$$

where A is the rate of soil loss ($\text{ton ha}^{-1} \text{yr}^{-1}$), R is the annual rainfall erosivity factor ($\text{MJ mm ha}^{-1} \text{h}^{-1} \text{yr}^{-1}$), K is the soil erodibility factor ($\text{t ha yr ha}^{-1} \text{MJ}^{-1} \text{mm}^{-1}$), L is the slope length factor, S is the slope steepness factor, C is the cover and management factor, and P is the supporting practices factor (Renard *et al.* 1997). RUSLE does not include wind erosion, nor rill and gully erosion or landslips, and therefore the results are viewed as indicative and not absolute.

3.2 Data sources

The data inputs for the model are outlined below. All spatial data were georeferenced to WGS84 UTM zone 19S (EPSG:32719) and cropped to the area of interest. Data processing and transformations were performed in R version 3.4.4 (R Core Team 2018). For additional non-spatial inputs², default values were retained. For more details on the SDR model and the default values, please see the documentation from The Natural Capital Project (2019).

3.2.1 Climate data

Global layers of monthly minimum temperature, maximum temperature, mean temperature, mean windspeed, and total precipitation were downloaded from WorldClim v2.0 (<http://worldclim.org/version2>) at 30 arc second resolution.

The WorldClim global layers were used as a continuous raster of the entire region. Local weather station data from the Colchagua Valley were only available as point data, and at inconsistent time intervals. However, we chose to rescale the global layers based on local data to ensure layers were: i) more accurate to local conditions; ii) more up-to-date (WorldClim rasters represent year 2000 conditions), and; iii) consistent with the point data used in SWAT modelling (Section 5.2.2): Daily weather station data ranging from late-2017

² Threshold flow accumulation, Borselli k parameter, Borselli IC_0 parameter and SDR_{max} .

to late-2018 (early-2015 to late-2018 for precipitation) were averaged per month. For each full month of weather data per station, WorldClim values corresponding to the location of that station were extracted. Station values were divided by the extracted WorldClim values to achieve a scaling factor for each station-month combination. All scaling factors were then averaged to produce a single scaling factor, and the original WorldClim raster layers were then multiplied by this factor to produce a new layer scaled by the local data. This process was repeated for each variable of interest independently.

3.2.2 Predicted future climate data

Global monthly raster layers of predicted minimum temperature, maximum temperature, and total precipitation for the year 2070 were downloaded from WorldClim v1.4 (<http://www.worldclim.org/CMIP5v1>), for the model HadGEM2-ES and representative concentration pathways 4.5 and 8.5, to represent a moderate and high greenhouse gas concentration pathway (see also section 3.4.2). WorldClim v1.4 was used as predicted data under climate change are not yet available for WorldClim v2.0. These layers underwent scaling in the same way as the present-day climatic variables, using 20-year mean (2061-2080) monthly values of minimum temperature, maximum temperature, and precipitation, derived from modelled station data.

3.2.3 Rainfall erosivity (R)

The rainfall erosivity factor is an index to describe the rainfall erosivity power, and the effect of raindrop impact on runoff. It is ideally derived as a proportional rainstorm parameter, based on storm energy and maximum intensity within a 30-minute period, and further validated against local erosion data to check suitability for the local region. As this requires long-term rainfall intensity and erosion data which are frequently not available, there are derived equations based on the correlation between rainfall erosivity (R) and total precipitation. Here we follow Renard and Freimund (1994) using the equation:

$$R = 0.04830 P^{1.61}$$

where P is a mean annual precipitation below 850 mm, and

$$R = 587.8 - 1.219 P + 0.004105 P^2$$

where P is a mean annual precipitation of 850 mm or above. This is a standard method, and appropriate when there are no validation data. These equations were applied to the precipitation rasters generated in section 3.2.1, to produce a 30 arc second resolution raster of rainfall erosivity in MJ mm ha⁻¹ h⁻¹ yr⁻¹.

3.2.4 Soil erodibility (K)

Soil erodibility is a measure of the susceptibility of soil particles to detachment and transport by rainfall and runoff and is largely based on the texture of the soil. Soil profile data were taken from the Harmonized continental SOTER-derived database (SOTWIS) (ISRIC 2019) at a resolution of 30 arc seconds, which gives the proportion of clay, silt and sand of the soil. The soil texture R package (Moeys 2018) was used to classify the FAO (2006) soil type based on the soil size and texture proportions.

The soil erodibility factor (K) (ton ha h (ha MJ mm)⁻¹) was then derived per soil class based on the OMAFRA fact sheet (2015), as recommended by the SDR documentation (The

Natural Capital Project 2019). Within the region the K factor ranged from 0.45 – 0.67, with a median of 0.45 for both the whole region and the vineyards.

3.2.5 Slope length (L) and Slope steepness (S)

Both slope length (L) and slope steepness (S) factors are derived by the InVest SDR model from the DEM (Appendix 1). The altitude within the region ranges from 54 – 4971 m, the mean altitude of the vineyard areas is 302 m (± 209 m). The mean slope was 13.5° ($\pm 12.9^\circ$) and 9.8° ($\pm 10.0^\circ$) for the region and vineyards respectively.

3.2.6 Land Cover (LC)

The habitat map produced from Sentinel 2 data by JNCC for this project (Figure 2.3) did not disaggregate vineyards from other types of similar agriculture such as orchards and table grapes, so these were added manually to the map using vineyard property boundary data provided by partners at VCCB. All areas falling within boundaries that had been classified as 'Agricultural land' were reclassified as 'Vineyard' as a separately assigned 16th land class, and the full map was rasterised to a 10 m resolution.

3.2.7 Biophysical table

The table attributes a C factor and P factor value per land cover class, which is applied spatially by joining to the land cover map. The cover management factor is used within RUSLE to reflect the effect of cropping and management practices on annual soil loss and is most often used to compare relative impacts of differing management plans. To be calculated specifically requires detailed data on prior land use, surface roughness, soil moisture and parameters of the vegetation itself. This is difficult to acquire outside of experimental conditions and at the landscape level, so the C factor has been estimated for Colchagua based on the methodology of Panagos *et al.* (2015). The results of their literature review give a range of derived C factor per land cover class. This can then be corrected for local conditions based on vegetation density using the following formula:

$$C_{LC} = \min(C_{LCit}) + \text{range}(C_{LCit}) \times (1 - F_{cover})$$

where $\min(C_{LCit})$ and $\text{range}(C_{LCit})$ are the minimum and range respectively of the C factor values retrieved from the literature for each land cover class, and F_{cover} is the % of soil covered by any type of vegetation derived from Copernicus Global Land Service (2019) data. F_{cover} was extracted using the land cover map shapefile, and the mean value per land cover class was applied in the above formula.

Panagos *et al.* (2015) literature review is European focused, but given the lack of local data, European data were deemed to be more appropriate than globally averaged data due to the similarities in climate. In addition, the inclusion of local F_{cover} improves specificity to the area of interest.

The support practice factor (P) specifies the ratio of soil loss in comparison to upslope and downslope tillage and is principally affected by practices such as contouring and terracing (and not the tillage system itself which is incorporated into the C factor). As with the C factor the value is applied per land cover class. For the purposes of this study P factor was defined as 1 to assume no special practices, and management effects are therefore only captured by the C factor.

3.2.8 Watersheds

Watershed delineation was based on HydroBASINS (Lehner & Grill 2013) level 12 sub-basins for the region, and the extent of the soil model was based on all sub-basins which intersect the land cover map. However, results are presented at the higher resolution pixel level rather than at sub-basin level to better represent soil erosion within the vineyard level.

3.3 Results

The map of estimated soil loss is shown in Figure 3.1. Although the modelled results are given in $\text{ton ha}^{-1} \text{yr}^{-1}$, there are no local data available to validate the outputs. Therefore, the results are mapped qualitatively, based on Table 3.1.

Table 3.1. Soil loss tolerance rates (OMAFRA Factsheet 2015).

Soil Erosion Class	Potential Soil Loss ($\text{ton ha}^{-1} \text{yr}^{-1}$)
Very low (tolerable)	<6.7
Low	6.7 –11.2
Moderate	11.2 –22.4
High	22.4 –33.6
Severe	>33.6

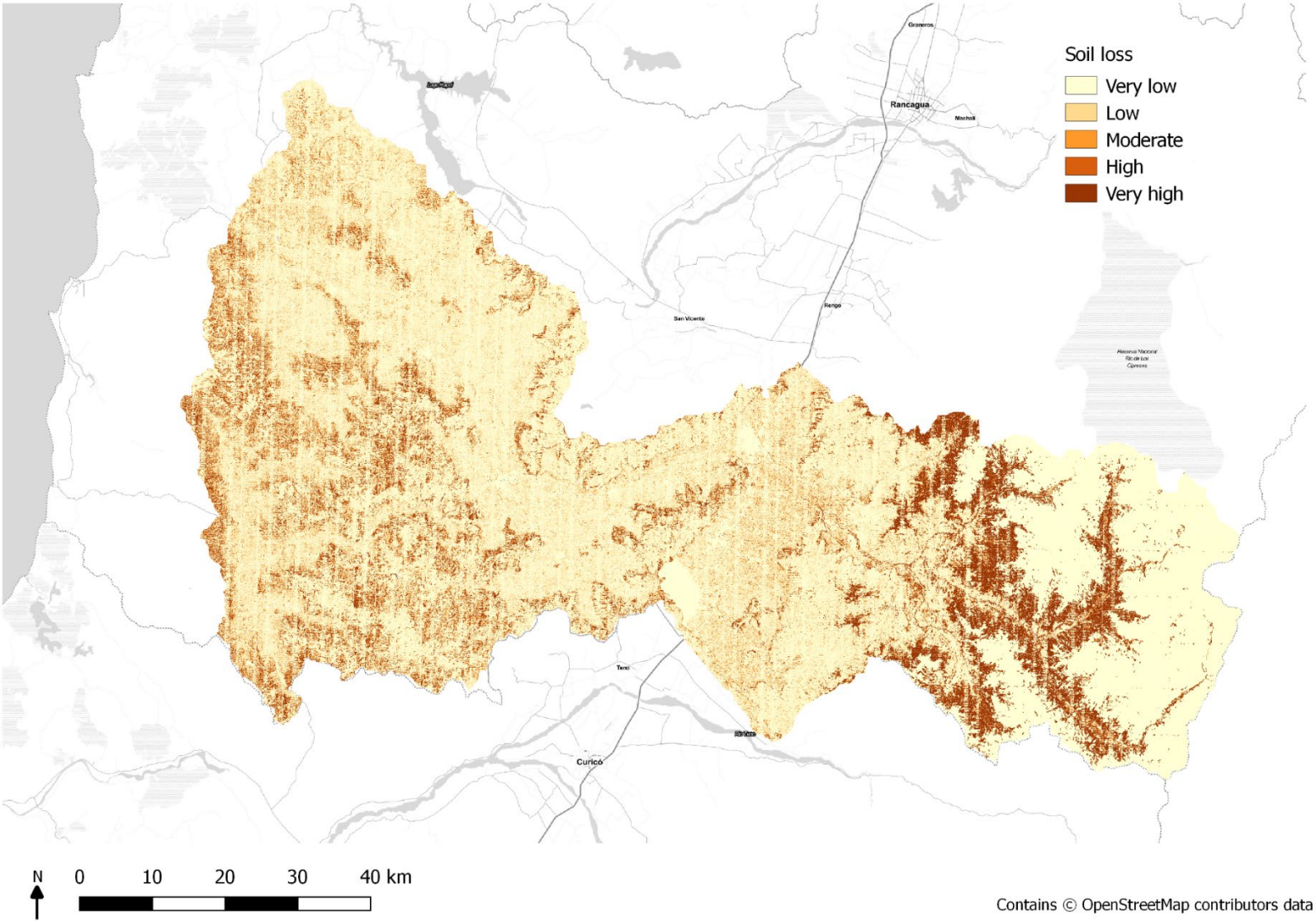


Figure 3.1. Modelled estimated soil loss in the Colchagua Valley.

3.4 Using Sediment Delivery Ratio to inform the BBN

The Viticulture ImplemeNting Ecosystem Services Bayesian Belief Network shows how management practices and future climate may impact soil loss at the field level (section 6). To inform the BBN, the SDR model was re-run after changing parameters for C factor for the Vineyard land cover class (to represent changes in management within the vineyards), climate change projections, and with added native buffer strips within the vineyards.

3.4.1 Management scenarios

Changes to C factor were again based on Panagos *et al.* (2015), and used the following equation:

$$C = C_{LC} \times C_{tillage} \times C_{cover}$$

C_{LC} is calculated as above (see 2.2.7), and a management factor for tillage and cover crop is applied to quantify the effect in differing practices on soil loss. Conventional tillage assumes a $C_{tillage}$ of 1, and a $C_{tillage}$ of 0.35 or 0.25 is appropriate for conservation/ridge tillage and no tillage respectively (OMAFRA Factsheet 2015). A total of 83% of vineyard fields managed by stakeholders of this project (n=18) reported using tillage practices of some sort. As vines are permanent crops, tillage will not be 100% of the field, and therefore the values of 0.35 was used as default but changed to 0.25 to measure the impact on the model outputs of removing tillage practises. The default for C_{cover} was 1, assuming no cover crops used, but an iteration where $C_{cover} = 0.8$ was also used to represent the reduction in soil erosion due to use of cover crops (Panagos *et al.* 2015).

3.4.2 Climate scenarios

Vineyards are interested in understanding how ecosystem services may respond to future climate change, particularly in relation to water management. To look at the implications of future climate change on the region, two scenarios were selected from the Coupled Model Intercomparison Project Phase 5 (CMIP5) evaluations used in the Fifth Assessment Report by the Intergovernmental Panel on Climate Change (IPCC). These were the representative concentration pathways (RCPs) 4.5 and 8.5; which represent two different scenarios and provide a range of predictions. RCP4.5 represents a moderate stabilization scenario under climate change, whereas RCP8.5 represents a very high baseline emissions scenario (van Vuuren *et al.* 2011). Data for these scenarios were taken from WorldClim and scaled as before (section 3.2.2) and used to calculate new R values for model input as above.

3.4.3 Buffer scenario

In previously published guidance to vineyard managers, VCCB encourage the creation of biological corridors of native vegetation around managed agricultural land, at least 9 m wide and connected, so as to encourage biodiversity, prevent soil erosion and aid water quality (Barbosa & Godoy 2014). To demonstrate this, buffer strips of 9 m native forest were added to the stakeholder fields within the dissolved vineyard, crop rotation and seasonal meadows land classes, as these were the land classes within vineyards that a native tree buffer strip would most likely be added to. Adding buffer strips does not affect the management scenario 'C factor' for the 'Vineyard' land cover class but will affect the proportion of 'Vineyard' and 'Native Tree' land cover classes within the vineyard areas, and therefore effect total RUSLE per vineyard. All above scenarios were therefore run using the buffered land cover layer also.

3.4.4 Topsoil loss within the vineyard

Outputs for all nodes of the BBN were extracted to inform the BBN at the Field level (boundaries of the stakeholder vineyard estates): The mean value of the outputs within each field boundary was used for continuous variables, and median used for categorical variables. The vineyards in Colchagua valley are largely planted on flat land, yet RUSLE is heavily influenced by slope. To better capture the risk to soil loss, means were taken from all pixels where slope was greater than 2°. Outputs were extracted for every combination of scenario of management, climate, and buffered land cover. As before soil loss was categorised using Table 3.1.

3.4.5 Eroded upslope soil

To quantify the amount of soil eroding upslope, thus potentially travelling downslope and contributing to the nitrification of the vines, the sum of upslope soil loss was calculated for each vineyard. Upslope buffers of 50 m were created for all regions classified as 'Vineyard' (see also section 6.4.1). These were used to extract the proportion of each land class, plus mean values for precipitation, slope, soil type, and the summed total of soil loss within the buffer, to inform the BBN. Outputs were derived from every combination of scenario of climate and buffered land cover. Exploring 'Tillage' across the landscape was out of scope for the project, this was considered only at vineyards level to inform the Bayesian Belief modelling (see section 6).

4 Fire Susceptibility

4.1 Introduction

Wildfires have increased in both frequency and size in recent years in central Chile (Gómez-González *et al.* 2019), posing a threat to both vineyard infrastructure and production. Here, we employ a species distribution modelling (SDM) type framework following previous studies in Chile and elsewhere (Gómez-González *et al.* 2019; McWethy *et al.* 2018; Duane *et al.* 2015), using historical burn and estimated ignition locations as presence points analogous to species records, to identify environmental and anthropogenic predictors of wildfire. These models are used to predict and map current landscape ignition susceptibility and burn avoidance (how unsusceptible the habitat is to fire) and burn avoidance under management, specifically the planting of buffer strips.

4.2 Data Sources

Unless otherwise specified, all data were georeferenced to WGS84 (EPSG:4326) and cropped to the area of interest covered by the habitat map. Data were often of a lower resolution than the habitat map (see Section 2) but required to be the same resolution for the modelling framework. Data were therefore resampled to the higher 10 m resolution of the habitat map where necessary. Transformation and resampling were performed using bilinear interpolation in the case of continuous variables, and nearest neighbour values in the case of categorical variables, in QGIS 3.4 (QGIS Development Team 2019) and R 3.4.4 (R Core Team 2018).

Environmental and anthropogenic predictor variables considered relevant to habitat ignition susceptibility and burn avoidance were chosen primarily based on previous work both in Chile and other Mediterranean landscapes (Gómez-González *et al.* 2019; McWethy *et al.* 2018; Duane *et al.* 2015). These variable layers were mostly indices of climate (temperature and precipitation), topography, or vegetation type and productivity, which together aimed to

account for factors including available fuel and fuel flammability. Where related layers were highly correlated (Pearson's Correlation Coefficient ≥ 0.75), the most ecological relevant, basal, or highest resolution dataset was used. For example, potential evapotranspiration (PET) was considered but ultimately not included as a predictor variable given that it is highly correlated to precipitation, and the precipitation data in question was both of a higher resolution and more basal (precipitation is used to calculate PET). Population and road proximity metrics were also included as over 99% of ignitions in central Chile are anthropogenically caused (CONAF 2018; Urrutia-Jalabert *et al.* 2018).

4.2.1 Topographic Data

Slope and elevation, which potentially influence the behaviour of topographically driven fires (Duane *et al.* 2015) were included, with slope being calculated from the DEM using QGIS 3.4.

4.2.2 Climate Data

Minimum annual temperature, maximum annual temperature, mean annual temperature, mean annual windspeed, and total annual precipitation were calculated from rescaled WorldClim layers as described in Section 3.2.1.

Temperature seasonality and precipitation seasonality (the seasonal variability in temperature and precipitation) were calculated using the rescaled monthly minimum temperature, maximum temperature, and precipitation layers and the R package *dismo* (Hijmans *et al.* 2017).

Global annual Palmer Drought Severity Index (PDSI) raster layers were downloaded from TerraClimate (<http://www.climatologylab.org/terraclimate.html>) at the highest available resolution (~4 km) for the most recent 10 years for which data were available (2008 – 2017), and averaged to create a single layer of annual PDSI. PDSI describes wetness and dryness relative to the local normal (Palmer 1965) and provide information about potential habitat dryness and flammability.

4.2.3 Biological Variables

MODIS MOD13A1 Normalized Difference Vegetation Index (NDVI, Didan *et al.* 2015) product, used to inform the model of vegetation productivity and condition, was downloaded and processed using the R package *MODIS* (Mattiuzzi & Detsch 2018) for the study area and period 2008-2017, at 500 m resolution. Annual mean NDVI was calculated from this product.

4.2.4 Habitat map

The habitat map produced in Section 2, adapted to include a vineyard class as outlined in section 3.2.6, was included to inform the model of the association between vegetation types and burned areas.

4.2.5 Anthropogenic Variables

Anthropogenic layers, capturing information on population density and the distance of burned and unburned areas to main roads, were included to account for the fact that Chilean wildfires are almost exclusively a result of anthropogenic ignitions (CONAF 2018; Urrutia-Jalabert *et al.* 2018).

A shapefile of Chilean road networks was downloaded from OpenStreetMap (<https://www.openstreetmap.org>; ©OpenStreetMap, licensed under the Open Data Commons Open Database License (ODbL) by the OpenStreetMap Foundation (OSMF)). The roads layer was edited to include only significant roads (listed as 'Motorway', 'Primary', 'Secondary', 'Tertiary', and their respective 'Link' roads). This layer was then rasterised to a 0.0001 decimal degree (~10 m) resolution. A raster layer of distance to these main roads was then calculated. Rasterization and distance calculations were performed in QGIS 2.14.5.

Modelled data of population density per hectare, rescaled to match to UN country-level population estimates, was downloaded from WorldPop (WorldPop 2016).

4.2.6 Burned Area Data

Monthly MODIS burned area product MCD64A1 (Giglio *et al.* 2015) was downloaded and processed using R and the package MODIS at ~500 m resolution. Data used in final analysis spanned the period 2008-2017. For each month, discrete areas of contiguous burned pixels (considered individual fires) were polygonised and used as a mask to identify burned pixels in a version of the month's data resampled to 10 m, with the pixel centroid latitude and longitude values combining from each month to become the 'burned locations' point layer for the burn avoidance analysis.

For each fire, the earliest burned pixel or pixels were also identified, and taken to represent the location of ignition events for that fire. Because the estimated burn dates in MODIS MCD64A1 data have inherent uncertainty (i.e. initial burn date is not always detected with 100% accuracy), we aimed to account for this by considering ignitions occurring close to each other in space and time as one event. Where pixels were within ~10.4 km of each other (the distance travelled by a medium sized fire in 1 day (Johnston *et al.* 2018) based on the advice of the Canadian Forest Fire Behaviour Prediction System (Alexander *et al.* 1984)), they were assumed to represent the same ignition event. Aggregating all earliest burn points from distinct fires in this way resulted in 165 unique potential 'ignition events' associated with the fires experienced by the area of interest in the period 2008-2017. Pixels associated with each of the 165 events were polygonised in turn and used as a mask to extract pixel centroid latitude and longitudes from a 10 m resampled version of the MODIS data, in the same way as for burn locations. This created a layer of 814,604 potential ignition points. One point falling within the area of each 'ignition event' was randomly sampled to produce a layer of 165 unique random points to use as ignition locations during modelling. For both burn and ignition, any points located on snow cover, glacier, river, or lake habitat classes were removed from the dataset of potential points for modelling. All processing was performed in R.

4.3 Fire Susceptibility Model

Landscape level ignition susceptibility and burn avoidance were modelled using a species distribution model (SDM) framework. In this context, the cell centroids of burned cells for the 165 randomly sampled 'ignition points' act as presence points analogous to species presence records, and all other layers act as environmental or anthropogenic predictors defining where burns or ignitions take place. Here we implement a Random Forest regression approach (RF) using the package JNCCsdms (JNCC 2018), which proved to be consistently the most successful of a suite of species distribution models (including Boosted Regression Trees, GLM, GAM, and MaxEnt) implemented in early testing. A regression approach was used in place of a classification approach both to enable the mapping of relative levels of suitability (rather than presence-absence), and because regression techniques have previously been observed to be more successful in SDM contexts (Hijmans

& Elith 2019). Output maps were created by averaging the results of a number of model runs, in this case 10 runs were used as this value had been suggested by previous work examining SDM implementation (Barbet-Massin *et al.* 2012).

Potential ignition points were randomly sampled for each model run as described above, resulting in a layer of 165 randomly placed ignition location points, one for each 'ignition event'. The exact number of ignition points varied between model runs (mean = 158.6), as randomly placed ignition points could fall within an ignition event location but outside of the area of interest, representing an ignition for which there was no habitat map coverage. Note that due to the inability to identify exact ignition point, the habitat ignition susceptibility maps should be considered significantly more uncertain than those for habitat burn avoidance. For the burn avoidance analysis, a subset of 10,000 points representing burned pixels was used rather than the whole burned pixels layer, to avoid computational limitations or excessive processing time.

Since burn and ignition points represent presence-only data, and the modelling framework also requires information on absences (i.e., where fires have not taken place), random pseudo-absence background points were generated for each model run, with the number of points generated equalling the number of presence points used in that run. Pseudo-absence points were generated within unburned or unignited cells for the respective burn and ignition maps. Pseudo-absences were generated in equal number to presences (though typically samples were not exactly even) following suggestions from previous work examining species distribution modelling (Barbet-Massin *et al.* 2012), which suggested equal weighting of presences and absences and equal numbers of each in random forest modelling (though in that case considering classification). Additionally, in the case of ignition susceptibility, the typically used value of 10,000 pseudo-absence points was not used as this resulted in model overfitting, which was avoided by using a lower number of absence points.

Ten models were fitted and used to produce ten rasters (then averaged) of predicted burn avoidance (Figure 4.1) and ignition susceptibility (Figure 4.2), and an additional ten for burn avoidance under the buffer strips management scenario (used to inform the BBN, see section 3.4). These management predictions were created in the same way and using the same parameters as the models run with no management, however the habitat map input layer was replaced with a modified habitat map where 9 m woodland buffers were added to vine, meadow, and crop areas within vineyards to simulate management effects (see section 3.4.3). Averaged outputs were categorised as 'Poor', 'Moderate' and 'Good' for burn avoidance, representing values of <33%, 33-66%, and >66% respectively, and 'Low', 'Moderate' and 'High' for ignition susceptibility, representing values of <33%, 33-66%, and >66% respectively. AUC (area under the receiver operator curve), is also reported as an indicator of the quality of model performance, where an AUC of 1 indicates highly successful model prediction, and 0 indicates highly unsuccessful prediction (Hijmans & Elith 2019).

4.4 Informing the BBN

Average burn avoidance value for both the model with no management and the model under management was calculated for each vineyard-field combination and used to inform the BBN (section 6).

Note that climate change was not included in the fire scenario modelling, as these models failed to produce realistic predicted burn avoidance. There are several possible and likely interacting reasons for this. Input precipitation and temperature seasonality values under climate change often lay outside the range of values the fire model was trained against. Additionally, WorldClim precipitation data demonstrated increases with climate change, in contrast to what is expected of the region (Urrutia-Jalabert *et al.* 2018). Moreover, non-linear

relationships between observed fire and climatic variables may be resulting in unexpected interactions between predicted climate and fire. Due to a lack of confidence in scenario model results, they were not included in the final product, and predictions under climate change were not considered for burn avoidance in the BBN.

4.5 Result

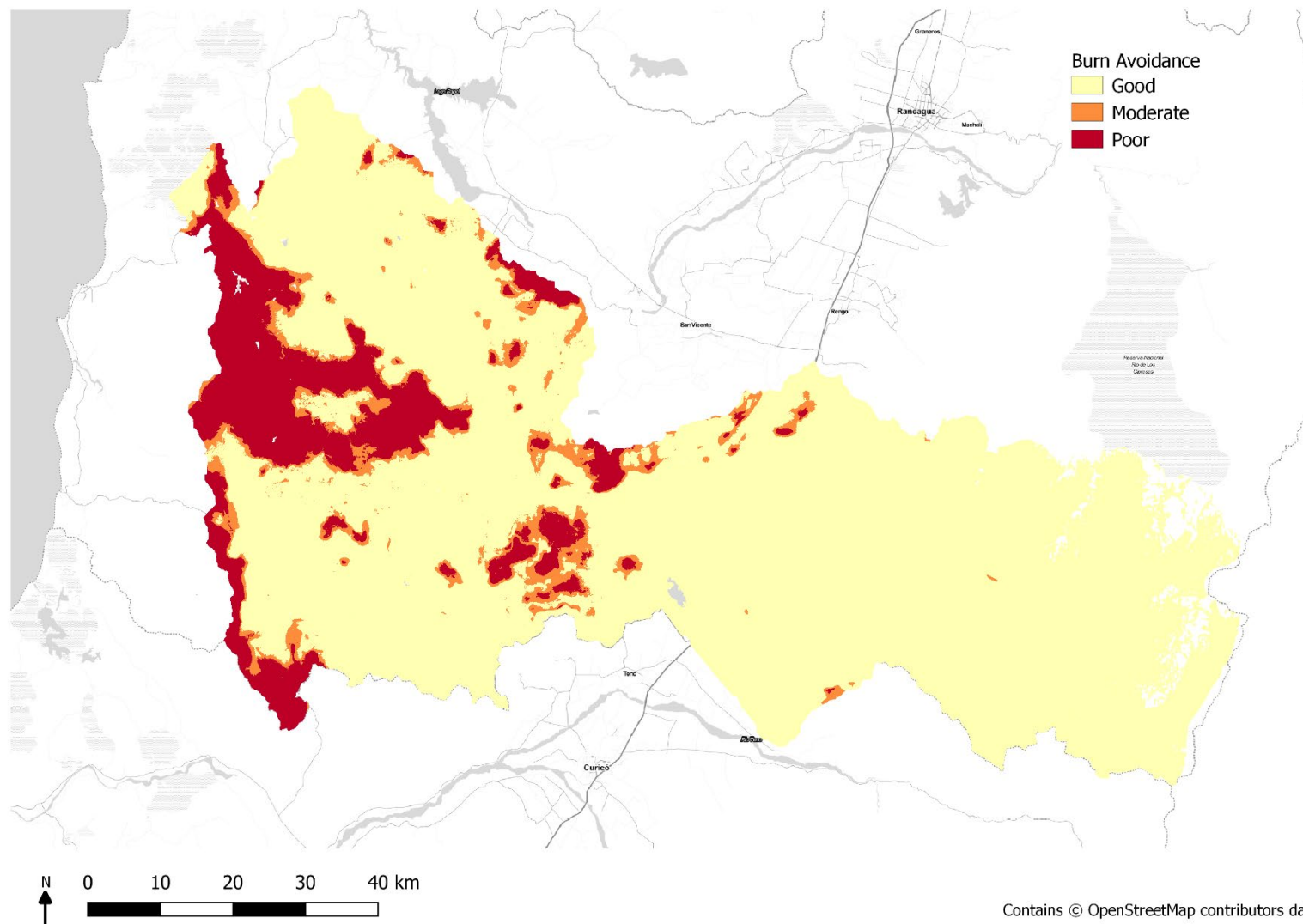


Figure 4.1. Modelled habitat burn avoidance, categorised as Good (>66% avoidance, least likely to burn), Moderate (33-66%) and Poor (<33% avoidance, more likely to burn). Mean AUC = 0.994.

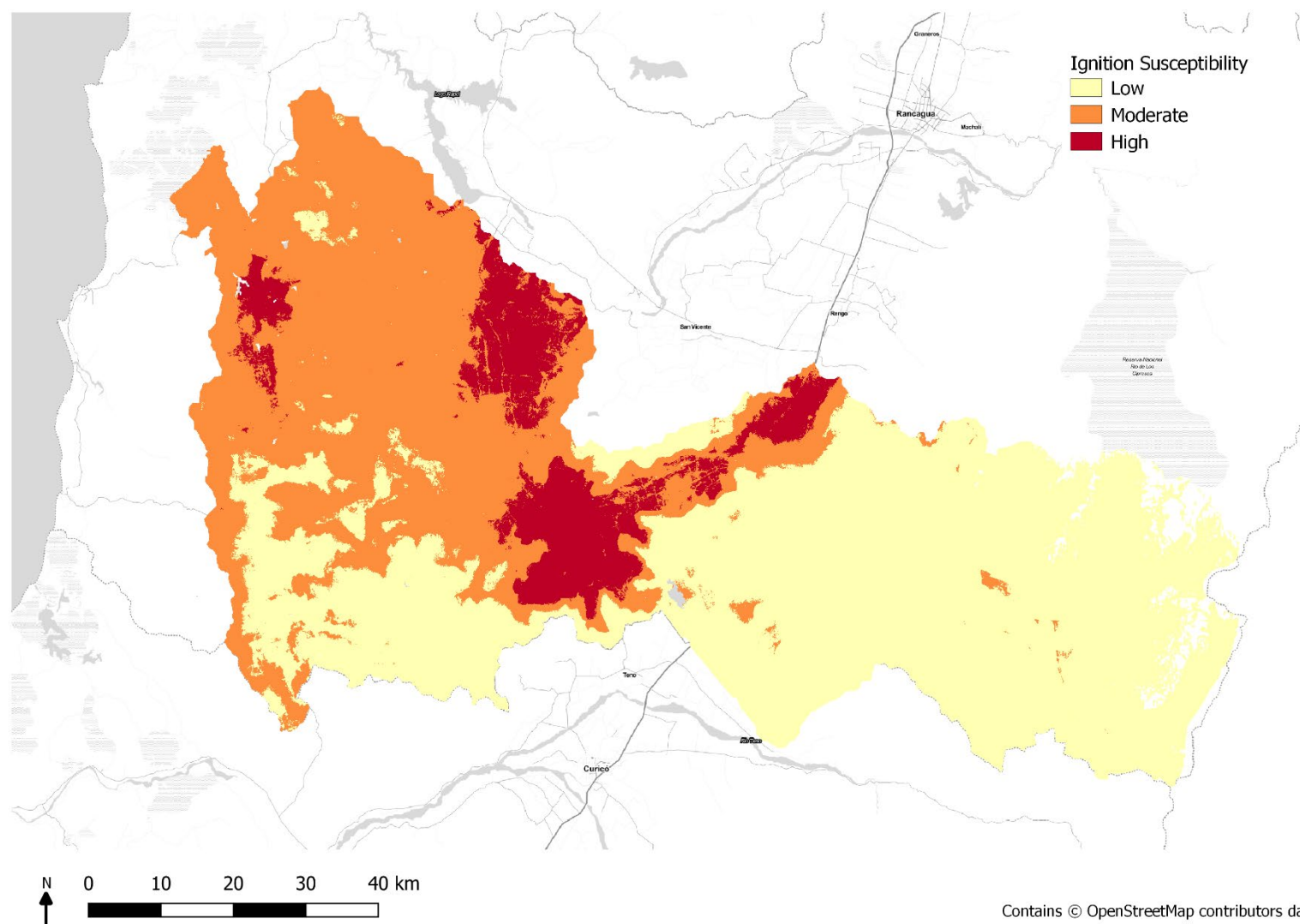


Figure 4.2. Modelled habitat ignition susceptibility, categorised as Low (<33% susceptibility, least likely to ignite), Moderate (33-66% susceptibility) and High (>66% susceptibility, most likely to ignite). Mean AUC = 0.835.

5 Water quality and supply

5.1 Introduction

Water supply and water quality were highlighted as a priority by stakeholders, being essential to grape production and a key concern in terms of water resource management under future climate scenarios and impacts on water quality driven by land management practices. VCCB emphasised stakeholder desires to understand how management strategies involving fertiliser and pesticide application, soil tillage, creation and maintenance of buffer strips and cover crops could affect water resources both now, and under future scenarios.

To understand the processes behind these ecosystem services, the Soil and Water Assessment Tool (SWAT)³ was used to model and map water metrics within the valley. SWAT is a complex semi-distributed model, developed by the US Department of Agriculture, Agricultural Research Service (USDA-ARS) and has been applied globally to assess water and sediment movement within catchments. It is well-established as a robust interdisciplinary watershed modelling tool with an online literature database of case studies where it has been applied worldwide (Gassman *et al.* 2007). Its flexibility allows users to alter land uses and management operations within land parcels, such as crop rotations, fertiliser use and tillage.

Studies have applied SWAT to examine climate change scenarios, water quality assessments and trade-off of different land management practices. This versatility and the robustness of the modelling tool makes it well suited to producing ecosystem service maps and exploring how different management practices can alter their delivery. SWAT was used over other ecosystem service mapping tools as it produces additional intermediary hydrological metrics such as percolation, which are relevant to vineyards. SWAT's inbuilt algorithms to determine snowmelt favour its use over other similar models in highly glaciated watersheds, as a result it has been applied in previous studies of the Chilean Andes (Stehr *et al.* 2008; Omani *et al.* 2017). Although the model is complex and data demanding, and local data in our region of interest are limited, global data layers for specific application in SWAT are available along with guides and literature examples that inform its use and application.

5.1.1 The Soil and Water Assessment Tool (SWAT) Model

SWAT is an open-sourced environmental model for assessing the daily, monthly and annual hydrological and sediment dynamics in a watershed. It is available through the QGIS interface as a python plugin QSWAT, and uses data inputs of elevation, land use and soil maps to delineate a watershed into sub-basins and determine Hydrological Response Units (HRUs). These HRUs are homogenous unique soil type and land use parcels within each sub-basin, which feed into equations for run-off and soil erosion to generate the output statistics for water and sediment yields. Different management conditions can be applied to each HRU and their changing response measured across the landscape. A flow diagram of the SWAT model development is displayed in Figure 5.1.

³ The Soil Water Assessment Tool (SWAT) (2019) is open-sourced software available through Texas A&M University from <https://swat.tamu.edu/>.

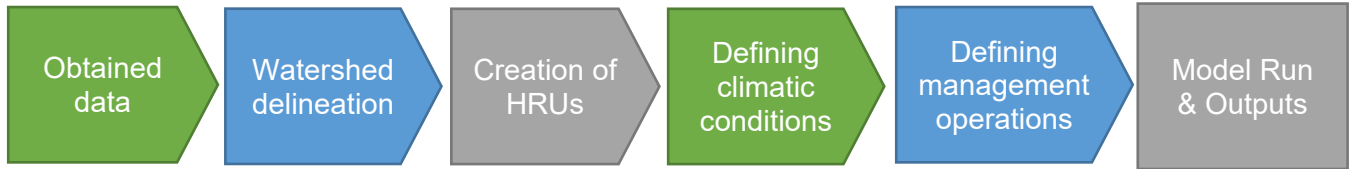


Figure 5.1. Flow diagram outlining the SWAT model development methodology.

To accurately predict movements of nutrients, sediments and water, SWAT models the hydrological cycle to simulate what is occurring across the entire watershed. Firstly, the hydrologic balance is simulated for each HRU within a sub-basin; this is calculated through the water balance equation (Neitsch *et al.* 2011):

$$SW_t = SW_0 + \sum_{i=1}^t (R_{day} - Q_{surf} - E_a - w_{seep} - Q_{gw})$$

where SW_t is the final soil water content (mm H₂O), SW_0 is the initial soil water content on day i , t is the time (days), R_{day} is the amount of precipitation on day i (mm H₂O), Q_{surf} is the accumulated runoff or rainfall excess (mm H₂O), E_a is the amount of evapotranspiration on day i (mm H₂O), w_{seep} is the amount of water entering the vadose zone from the soil profile on day i (mm H₂O), and Q_{gw} is the amount of return flow on day i (mm H₂O).

Calculating input variables to the equation on an HRU basis enables input factors such as evapotranspiration and runoff to reflect the differences between crop and soil types (Neitsch *et al.* 2011). This calculation determines the land phase of the hydrologic cycle and the amount of water deposited onto the land and entering the main channels within each sub-basin division.

The inputs and processes at this stage include climate variables of daily precipitation, minimum and maximum air temperature, wind speed, solar radiation and relative humidity. SWAT uses temperature-index based computation methods to model its hydrological and snowmelt processes, outlined in Neitsch *et al.* (2002). SWAT classifies precipitation input as either rain or snow determined by the average daily temperature and snowfall temperature thresholds. Snowmelt is then governed by a set of parameters which can be assigned to the whole catchment or within elevation bands of individual sub-basins, allowing for flexibility when working in mountainous glaciated watersheds.

Canopy storage, infiltration and evapotranspiration are calculated from the soil and plant types, determined by the land use classes. SWAT uses a modified soil conservation science (SCS) curve number method to calculate the surface runoff volume:

$$Q_{surf} = \frac{(R_{day} - I_a)^2}{(R_{day} - I_a + S)}$$

Where Q_{surf} is the accumulated runoff or rainfall excess (mm H₂O), R_{day} is the rainfall depth for the day (mm H₂O), I_a is the initial abstractions which includes surface storage, interception and infiltration prior to runoff (mm H₂O), and S is the retention parameter (mm H₂O) which varies dependent on changes in soils, land use, slope and management.

Soil erosion is determined through using the Modified Universal Soil Loss Equation (MUSLE), which is well established in models of soil erosion (Dile *et al.* 2018; Williams 1975):

$$sed = 11.8 \cdot (Q_{surf} \cdot q_{peak} \cdot area_{hru})^{0.56} \cdot K_{USLE} \cdot C_{USLE} \cdot P_{USLE} \cdot LS_{USLE} \cdot CFRG$$

Where *sed* is the sediment yield on a given day (metric tons), Q_{surf} is the surface runoff volume (mm H₂O/ha), q_{peak} is the peak runoff rate (m³/s), $area_{hru}$ is the area of the HRU (ha), K_{USLE} is the USLE soil erodibility factor (0.013 metric ton m² hr/m³ -metric ton cm)), C_{USLE} is the USLE cover and management factor, P_{USLE} is the USLE support practice factor, LS_{USLE} is the USLE topographic factor and $CFRG$ is the coarse fragment factor.

The MUSLE equation uses the amount of runoff to simulate soil erosion, supplied by the hydrology model, along with crop management factors and C factor (C_{USLE}) which is a value accounting for the degree of soil loss depending upon crop type, management, and land cover. Other factors used in the soil loss equation are derived from Wischmeier and Smith (1978). The MUSLE equation is used by SWAT as it can provide a finer temporal resolution producing daily outputs and uses runoff factor to calculate erosion, as opposed to the Revised Universal Soil Loss Equation (RUSLE) used in the INVEST sediment delivery modelling, which uses annual precipitation to calculate annual gross erosion using the rainfall energy factor (see section 3).

The nitrogen cycle is also simulated in SWAT through monitoring five pools of nitrogen; NH₄ and NO₃ stored in the soil impacted by calculations of plant uptake, leaching, volatilization, denitrification and erosion, and three pools of organic nitrogen associated with the soil humus, detailed in Neitsch *et al.* (2002). Similarly, the phosphorus cycle is equated through monitoring stored pools of soluble and organic phosphorus in the soil. Additional inputs of fertilisers and pesticides are derived from loading functions and are applied through management operations to the land.

The second phase of the model controls how water, nutrients and sediments move through soil and the stream networks and towards the main outlet (i.e., the Tinguiririca River). Sediment, water flow, nutrient and chemical pathways are equated throughout the stream network taking into account the land management operations within each sub-basin and influencing downstream conditions. Reservoirs within the network are modelled separately within SWAT and their dynamics differ to those of rivers, having significant impacts upon sediment and nutrient storage and water flow. More information on the equations used in calculations can be found in SWAT's technical documentation (Neitsch *et al.* 2011).

The SWAT model uses all of these algorithms to output several intermediary metrics throughout each stage of the hydrological cycle, as well as quantifying the amount of runoff from each HRU and the streamflow, sediment and nutrient concentrations within the stream network. This information can be displayed spatially to map how these metrics vary across the landscape. The model can be rerun under different modelled climatic conditions and management operations to compare how these impact upon the modelled hydrological cycles.

5.2 Data sources

All data were georeferenced to WGS84 UTM zone 19S (ESPG:32719) and cropped to the area of interest detailed in Section 2.2. The SWAT model was built using the QSWAT version 1.7 under 32-bit QGIS version 2.18.27. Data processing and transformations were also performed in this version of QGIS (QGIS Development Team 2019) and in R version 3.4.4 (R Core Team 2018).

5.2.1 Landscape

The modelled watershed in the Colchagua Valley in central Chile was a total area of 6163.95 km² and encompasses all VCCB partner vineyards, key stakeholder in the project. The watershed ranges from a minimum elevation of 55 m to a maximum of 4971 m in the Andean mountains. To delineate the watershed and create topographic layers, a 30 m DEM raster layer (see Appendix 1) was re-projected to the regional projection ESPG:32719 and clipped to the extended watershed boundary (the whole area of interest shown in Figure 5.2). High level watershed delineation boundaries were obtained from Hydrological data and maps based on Shuttle Elevation Derivatives at multiple Scales (HydroSHEDS) developed by the World Wildlife Fund's Conservation Science Program (WWF 2019). The vector layer was available on a global scale developed from high resolution SRTM digital elevation models and broken down into different delineation scales. These are different subdivisions of the land based upon watersheds determined by the elevation and are available at different scales depending upon the topological concept of the Pfafstetter coding system, which ranges from 1 to 12 increasing as the watersheds are further divided to smaller sub-units. A HydroBASINS polygon layer, a subset of the HydroSHEDS database at the 15 second arc resolution (Lehner & Grill 2013), was used at the Pfafstetter Level 7 to determine the main watersheds covering the area of interest and stream network. The area of interest used for the SWAT modelling process differs slightly from the other maps produced in this project, as it is clipped by the boundary of the main watershed delineation so models a slightly smaller region as a result.

The land cover was based on the adapted 16 class map developed for this project (see section 3.2.6). A South American soil tile was obtained from Waterbase (UNU-INWEH 2019) based on the UN Food and Agriculture Organization digitized Soil Map of the World (2003). The soil map (v.3.6) was prepared at a nominal scale of 1:5000000 (65 km² resolution) and cropped to the watershed boundary.

5.2.2 Climate

Local data were provided from five stakeholder weather stations for 2018 with incomplete daily records for variables including; daily air temperature, precipitation, relative humidity, solar radiation and wind speed. Additional stations from the Ministerio de Obras Públicas's Dirección General de Aguas hydrometric network (DAG 2019) were added to improve hydrological estimations.

The climate change scenarios were developed with climate projections from the Coupled Model Intercomparison Project Phase 5 (CMIP5) evaluations used in the Fifth Assessment Report by the Intergovernmental Panel on Climate Change (IPCC). The CMIP5 HadGEM2-ES modelled data were used along with baseline historical climate data from 1979-2005 at 38 km resolution. These were obtained as daily temperature and precipitation station records from 2W2E (2019) which extracted data from the ISI-MIP project, that developed a Climate Change Toolkit for projecting and extracting predictive data under the CMIP5 scenarios (Vaghefi *et al.* 2017) using global historical data CRUTS3.1 from the Climate Research Unit East Anglia (Harris *et al.* 2014). To supply all the required variables into SWAT, daily data for solar radiation, relative humidity and wind speed were extracted for the same period from the National Centers for Environmental Prediction's Climate Forecast System Reanalysis (NCEP-CFSR) global meteorological dataset through SWAT's weather data tool (2019).

The watershed within the area of interest includes a glaciated region of the Andean mountains and consequently snowmelt is a key water resource in the region (Valdés-Pineda 2014). Datasets from Global Land Ice Measurements from Space (GLIMS 2018) were used

to make comparisons with the glacier outlines and snow depth data that were obtained from study stations in Stehr and Aguayo's (2017) supplementary paper.

5.3 Model configuration

5.3.1 Watershed delineation

The stream networks were defined through using the “burn-in” methodology available through the QSWAT interface. For this method, elevations were extracted from the digital elevation data within the DEM then a digitally defined stream network (hydroBASINS 2010) was superimposed onto the DEM to provide hydrographic definition of the streams and watershed boundary delineation. Sub-basins were delineated using standard analytical techniques from the TauDEM suite contained in the SWAT QGIS interface (Dile *et al.* 2018). A minimum upstream contributing area of 50 km² was used for the drainage basin threshold value in defining stream cells. This is the minimum area draining into a stream, therefore helps to define subbasin size. This threshold value is based on a SWAT model for a basin in the nearby Biobio region, which covered a similar sized catchment (Stehr *et al.* 2008). The study area contains two watersheds (from the level 7 Pfafstetter delineation), the main watershed of interest and an added sub-section of the watershed towards the southwest, where some stakeholder vineyards were located outside of the main watershed. The main river outlets, reservoir locations, and inlet for the sub-watershed were based on comparisons with ‘QuickOSM’ base maps plugin available in QGIS (Trimaille 2019) and snapped to 300 m. The overall area modelled was 6163.95 km², with the main watershed size being 5055.60 km². This was divided into 68 sub-basins, shown in Figure 5.2.

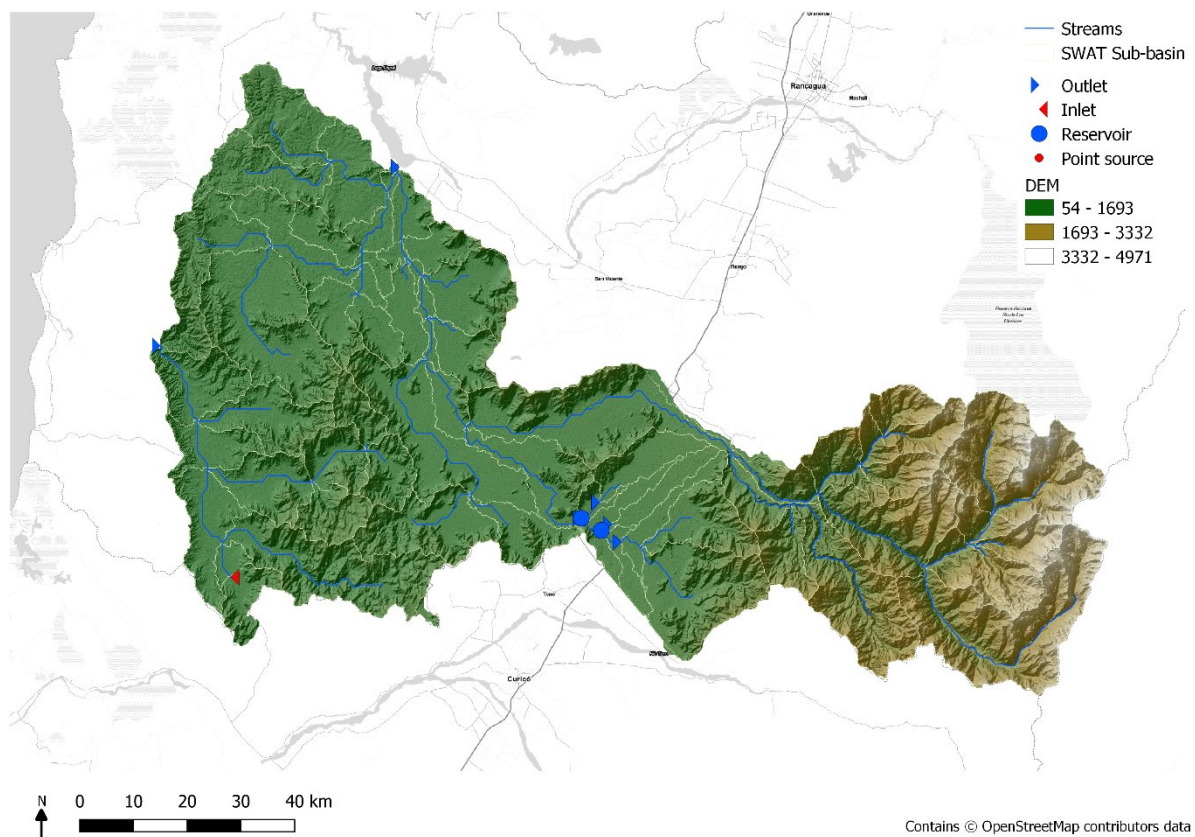


Figure 5.2. Delineated Watershed overlaid on top of the digital elevation model.

5.3.2 HRU creation

The sub-basins were then further divided into Hydrological Response Units (HRUs) defined by unique land-use and soil combinations within each sub-basin. These were defined using the habitat map derived using Sentinel-2 satellite imagery (Section 2) and the global FAO soil tile available through Waterbase. SWAT contains predetermined crop and urban land databases, which define a variety of characteristics such as maximum rooting depth and leaf area index, which are used in the hydrological, soil and nutrient equations.

As local data were unavailable for every parameter for local habitat types, the habitats classed in the habitat map were matched to the nearest crop/land-use classes contained within the SWAT reference database (shown in Appendix 2). These assumptions may create inaccuracies in how plant uptake is modelled within SWAT as classes are based upon North American land classes (where SWAT was developed). If more data on local crop characteristics was made available models could be further refined to provide more accurate outputs based upon local parameters.

Due to lack of local soil data, the global UN FAO soils dataset was used to define the soil characteristics, which was compatible with the built in QSWAT reference database (global_soils and usersoil). Within each sub-basin, unique combinations of soil type and land use cover were used to generate 1036 unique HRUs, shown in Figure 5.3. For each unique HRU, management operations and snow parameters were applied to define crop growth cycles and snowmelt. The HRU parameters of the model are explained in more detail in Appendix 2.

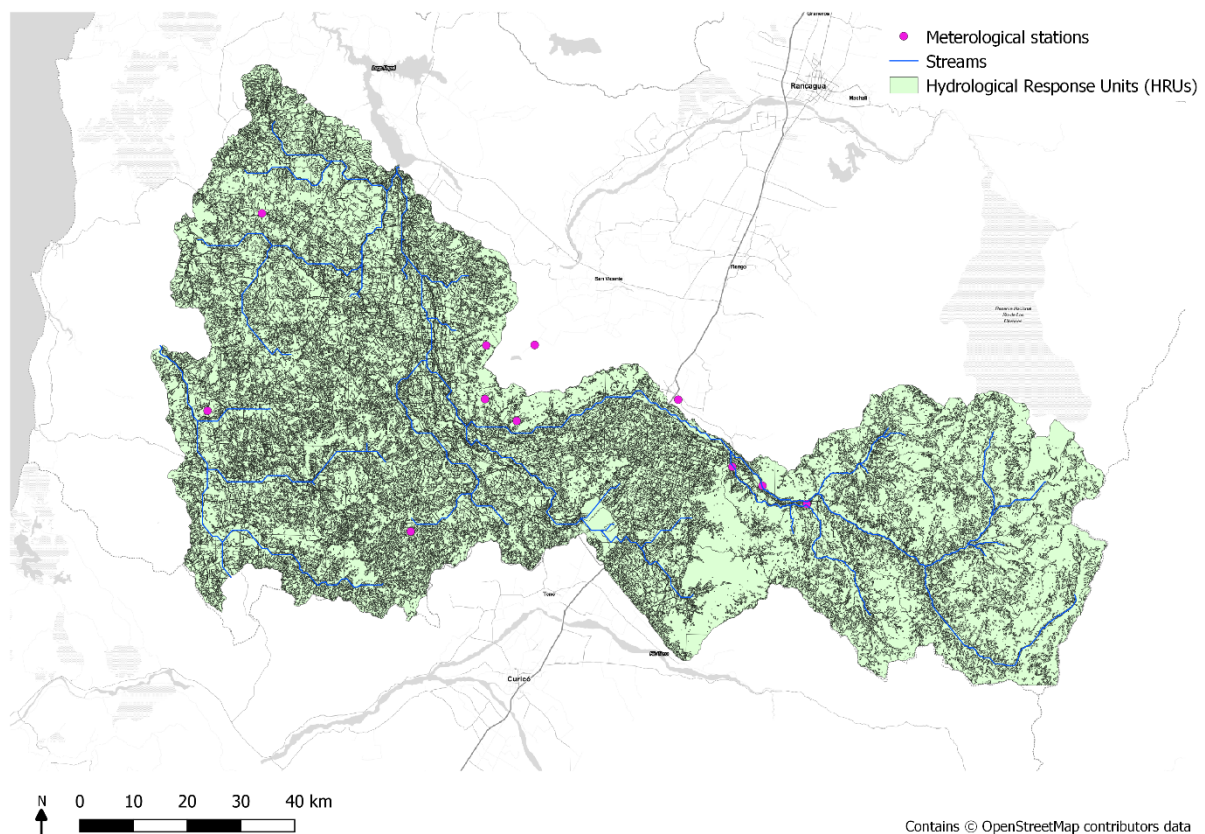


Figure 5.3. A map of the defined actual Hydrological Response Units derived from the land use and soil maps.

5.3.3 Station data and Weather generator

Data from local meteorological stations were prepared in the SWAT input format, converting measurement units using the 'weathermetrics' R package version 1.2.2 (Anderson *et al.* 2016) and Allen *et al.* (1998) conversion factors for solar radiation units from watts per square meter per day ($\text{W/m}^2 \text{ day}^{-1}$) to megajoules per square metre per day $\text{MJ/m}^2 \text{ day}^{-1}$. When employing SWAT modelling it is suggested to run models with at least a 3 to 5 warm-up period to give the simulation processing time to establish basic hydrological flow conditions and processes, particularly for stabilising water levels in reservoirs to ensure accurate modelling (Almendinger 2016). To aid in the conversions of daily station text files and add simulated data for a given warm up period, a weather datafile writing tool was created 'weathergen.R' in R to help speed up processing.

For the two climate change simulations RCP4.5 and RCP.8.5, only station data for daily precipitation and air temperature records were available. To maintain consistency with the baseline model, these were also modelled using a 3-year warm-up period.

In addition to station data, SWAT requires a 'weather generator'. This is a table of stations with monthly average climatic variables it can refer to when local data are missing, and conditions need to be simulated. For each sub-basin the model searches for the closest station with available data, therefore if no station data are available for the period, SWAT will use the simulated station data. To build the weather generator, the historical data used to generate the climate change simulation daily values were used, to maintain consistency. These were daily maximum and minimum air temperatures and precipitation data from CRUTS3.1 for the period 1979-2005. For the remaining climate variables required by SWAT; solar radiation, wind speed and relative humidity, data from Climate Forecast System Reanalysis (CFSR) were obtained for the same time period. CFSR is a long-term dataset from 1979-2014 providing global coverage of daily climatic variables and is regularly used in SWAT modelling studies; a web tool for extracting these data is provided by SWAT (SWAT 2019). Comparison between long-term historical datasets used in CFSR and in Global Climate Models revealed no significant differences in climate trends (Omani 2014), therefore the uncertainty in using these data sources together for creating the weather generator is relatively negligible.

CRUTS stations were compared to the closest CFSR station using a nearest neighbour join, in order to obtain the missing climatic variables (QGIS processing). To calculate the 169 climatic statistical values the model's weather generator requires, another R tool was developed 'swat_wgen.R', which follows the same method as the widely used "WGN Excel macro" developed by Dr. Gabrielle Boisrame available through the SWAT (2019) software pages. The climate statistics of maximum half hour rainfall were assumed to be a third of the daily precipitation value, following community knowledge from the Spatial Science Laboratory of Texas A&M University, which developed the SWAT modelling software (Srinivasan 2013). There are several methods to estimate skewed coefficient of a distribution, so for the skewed precipitation values the statistical package 'e1071' was used in R and method 2 in the 'skewed' function was applied, which closely aligned to the excel SKEW function outputs and commonly used in analytical software such as SPSS (Meyer *et al.* 2019). The 'swat_wgen' tool produced a weather generator table that was then inserted into SWATs reference database and used for all the model simulations.

5.4 Baseline modelling

The SWAT model was run with the prepared meteorological station data and weather generator from long term historical weather statistics. The SWAT model was run firstly to show the baseline conditions, the ecosystem services delivered where no management

measured were applied to the land. For the baseline model, a three-year warm-up period was applied using simulated data, then the model was run for three years from 2016 to 2018 using station data, where available, and printing the results on a yearly basis, using an annual timestep. The average mean values across the run period were used to produce the final plots of water flow and water quality metrics from HRUs into the stream reach, shown in Figure 5.4 – 4.9.

As the model was unvalidated, results are presented categorically with high, moderate and low values. The categorical boundaries for the maps produced were determined from the data ranges of the baseline model, as well as comparisons with literature resources for the ranges of meteorological variables in Central Chile (Boisier *et al.* 2018; Alvarez-Garretón *et al.* 2018). This method of categorising was used due to some of the SWAT algorithms and resulting outputs being unique to SWAT, which in turn means comparisons to other existing high, moderate and low levels are difficult. For instance, the estimated water yield is defined as the total amount of water leaving the HRU into the main channel reach and is a calculated value from the equated surface water runoff, lateral flow, groundwater flow, and transmission loss equations. Similarly, Water Stress days is a calculated value in SWAT equated by:

$$wstrs = 1 - \frac{E_{t,act}}{E_t} = 1 - \frac{w_{actualup}}{E_t}$$

Where *wstrs* is the water stress for a given day, E_t is the maximum plant transpiration on a given day (mm H₂O), $E_{t,act}$ is the actual amount of transpiration on a given day (mm H₂O) and $w_{actualup}$ is the total plant water uptake for the day (mm H₂O). Other calculations of the water stress a plant experiences may vary by using different metrics such as annual runoff as indicators of water stress (Alcamo *et al.* 2007).

The gridded appearance of the output maps reflects the low resolution of the FAO soils data layer used in the model, which does not accurately reflect how the soil compositions vary spatially across that landscape. Within the time constraints of the project it was not possible to conduct a sensitivity analysis to assess the relative influence of data layers, including the soils layer. A summary of the baseline maps is shown in Table 5.2.

As data for the current levels of phosphates and nitrates present within streams were unavailable, it was difficult to determine what the current state of water quality within the region was likely to be. To give an impression of areas that may have naturally higher nitrate and phosphate levels, and therefore at greater potential risk of having poorer water quality, the loading rates of organic nitrogen and phosphorus were mapped. These were calculated through a number of equations used to model the nitrogen and phosphorus cycles based on the land use classes and characteristics of the soil, which are outlined in Neitsch *et al.* (2011). The categorised levels of nitrate and phosphorus present in the water are based on concentration classifications from the ADAS report to DEFRA assessment for the nitrates directive in England (2007) and the UKTAG WFD European standards (2008), shown in Table 5.1 below.

Table 5.1. Classifications for nitrate and phosphorus levels present in water (ADAS 2007; UKTAG WFD 2008).

Average Nitrate concentrations		
Classification for nitrate grade	Grade limit (mg NO ₃ /l) Average	Description
1	<5	Very Low
2	>5 to 10	Low
3	>10 to 20	Moderately Low
4	>20 to 30	Moderate
5	>30 to 40	High
6	>40	Very High

Annual mean Soluble Reactive Phosphorus	
Status	Grade limit (µg/l)
High	<30
Good	>50 to 30
Moderate	>150 to 30
Poor	>500 to 150

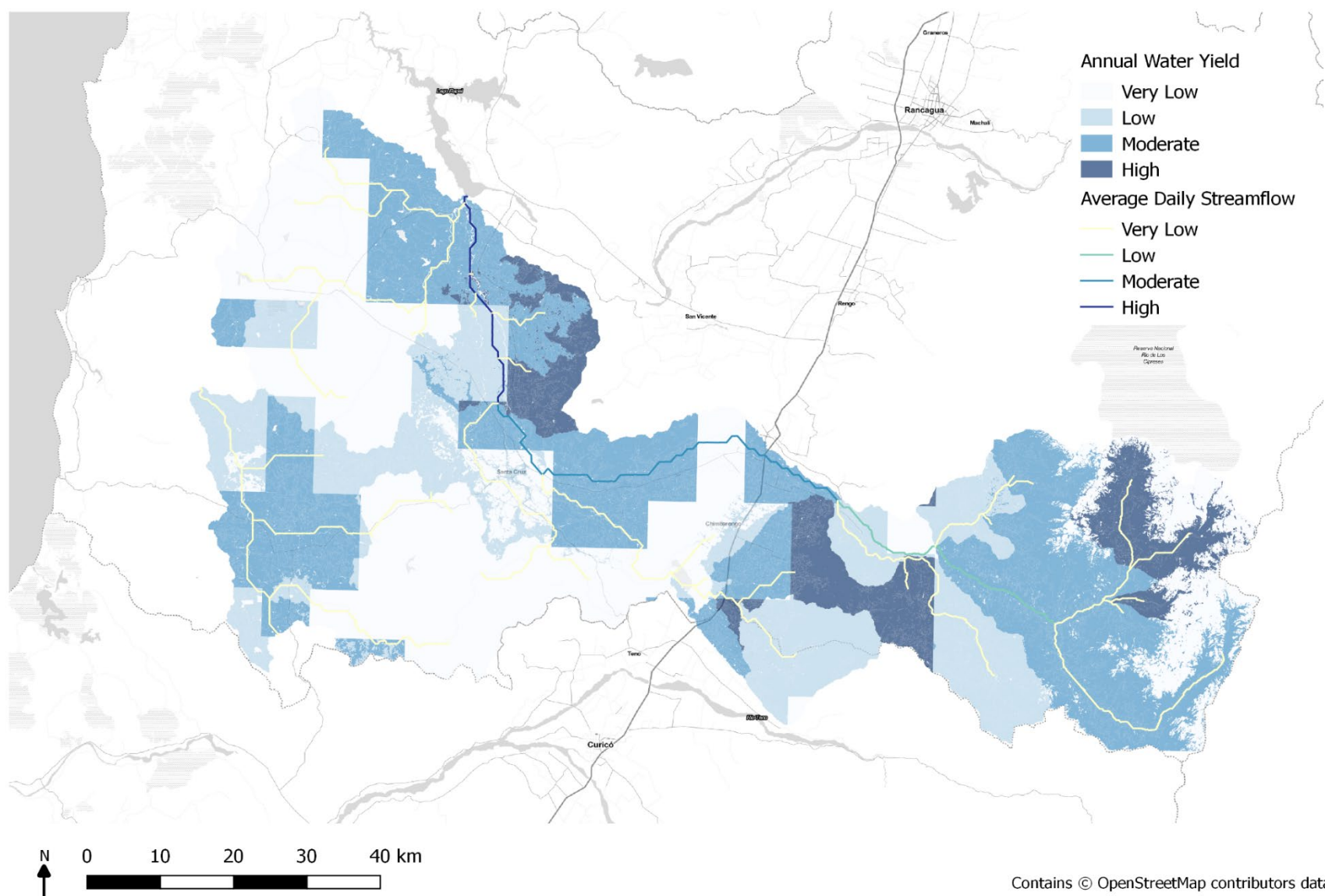


Figure 5.4. Modelled baseline map of annual water yield and average daily streamflow across the modelled period divided across Hydrological Response Units. The gridded appearance of the output maps reflects the low resolution of the FAO soils data layer used in the model.

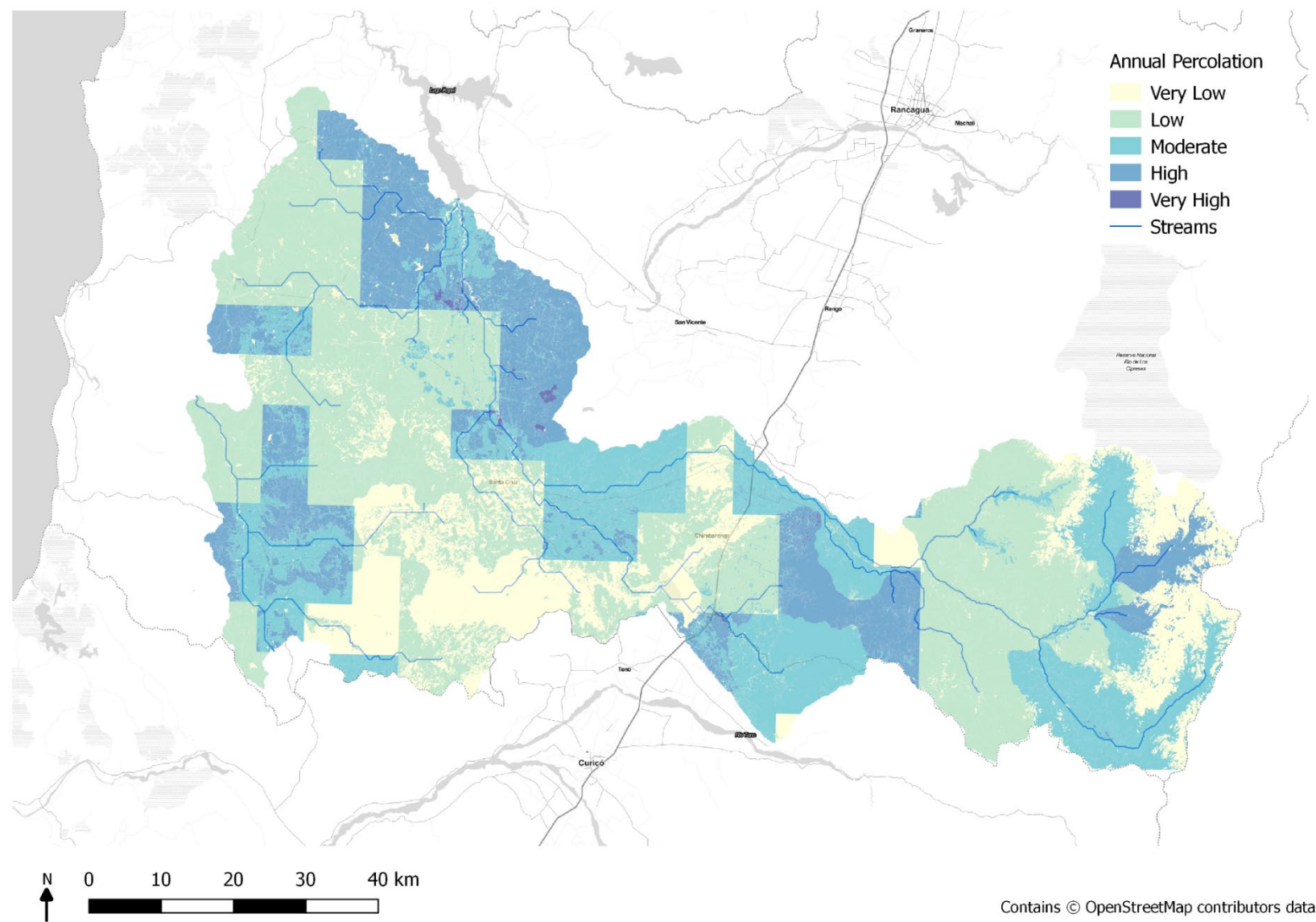


Figure 5.5. Modelled baseline map of annual mean percolation past the rooting depth of the crop.

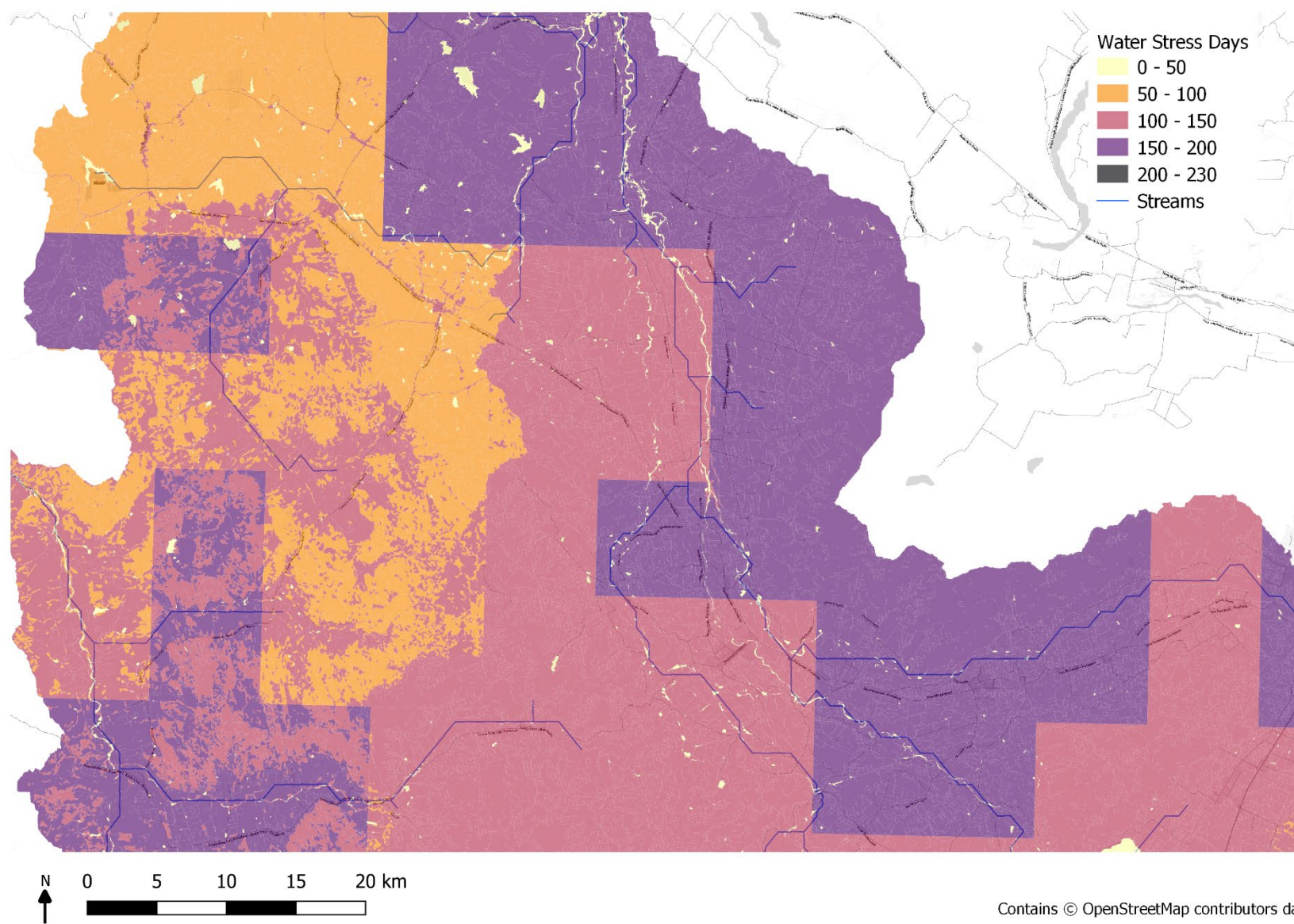


Figure 5.6. Modelled map of annual water stress days for the modelled period, zoomed to the major populated region in the south west of the valley where stakeholder vineyards are predominantly located.

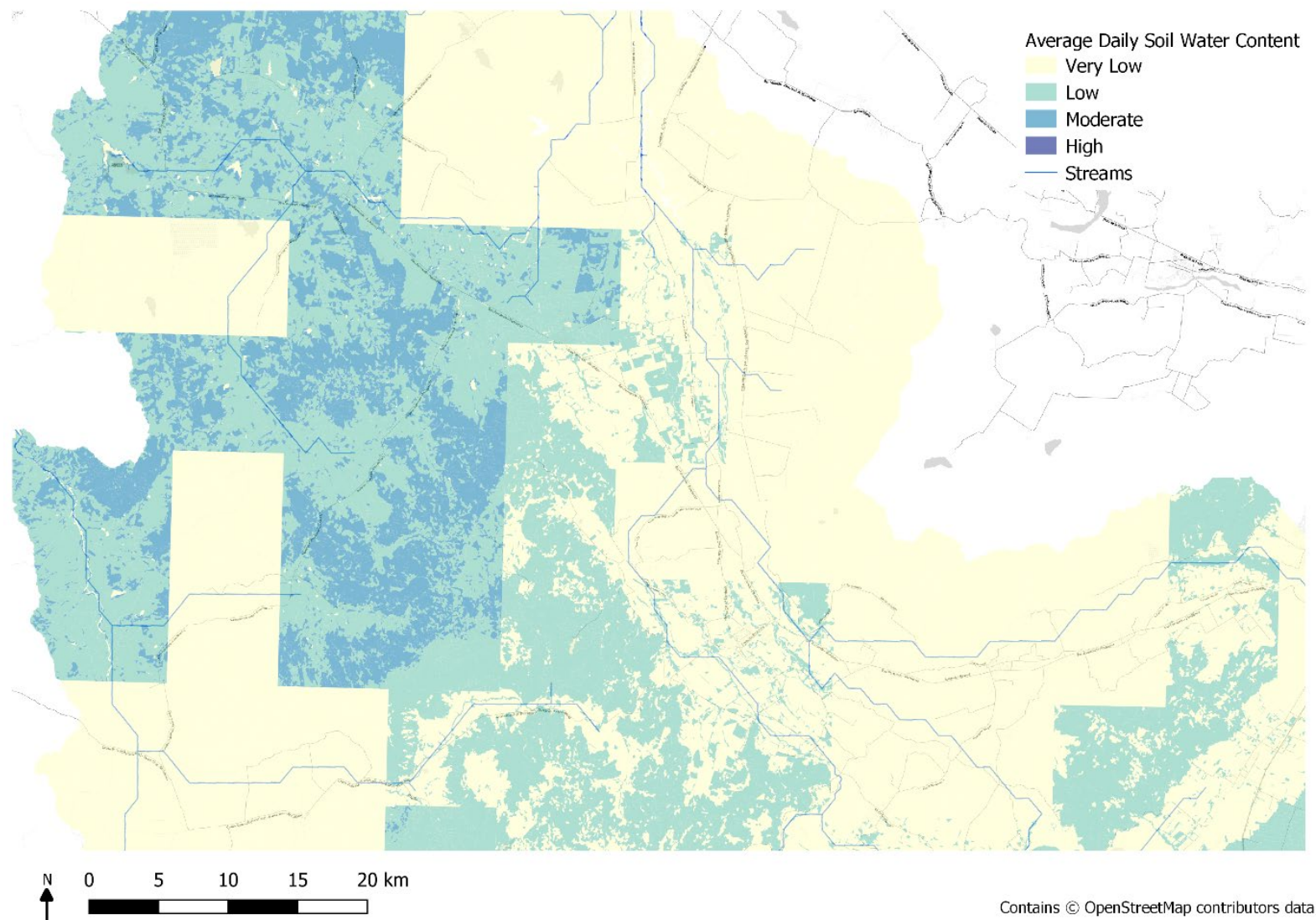


Figure 5.7. Modelled map of the average daily soil water content for the period, zoomed to the major populated region in the south west of the valley where stakeholder vineyards are predominantly located.

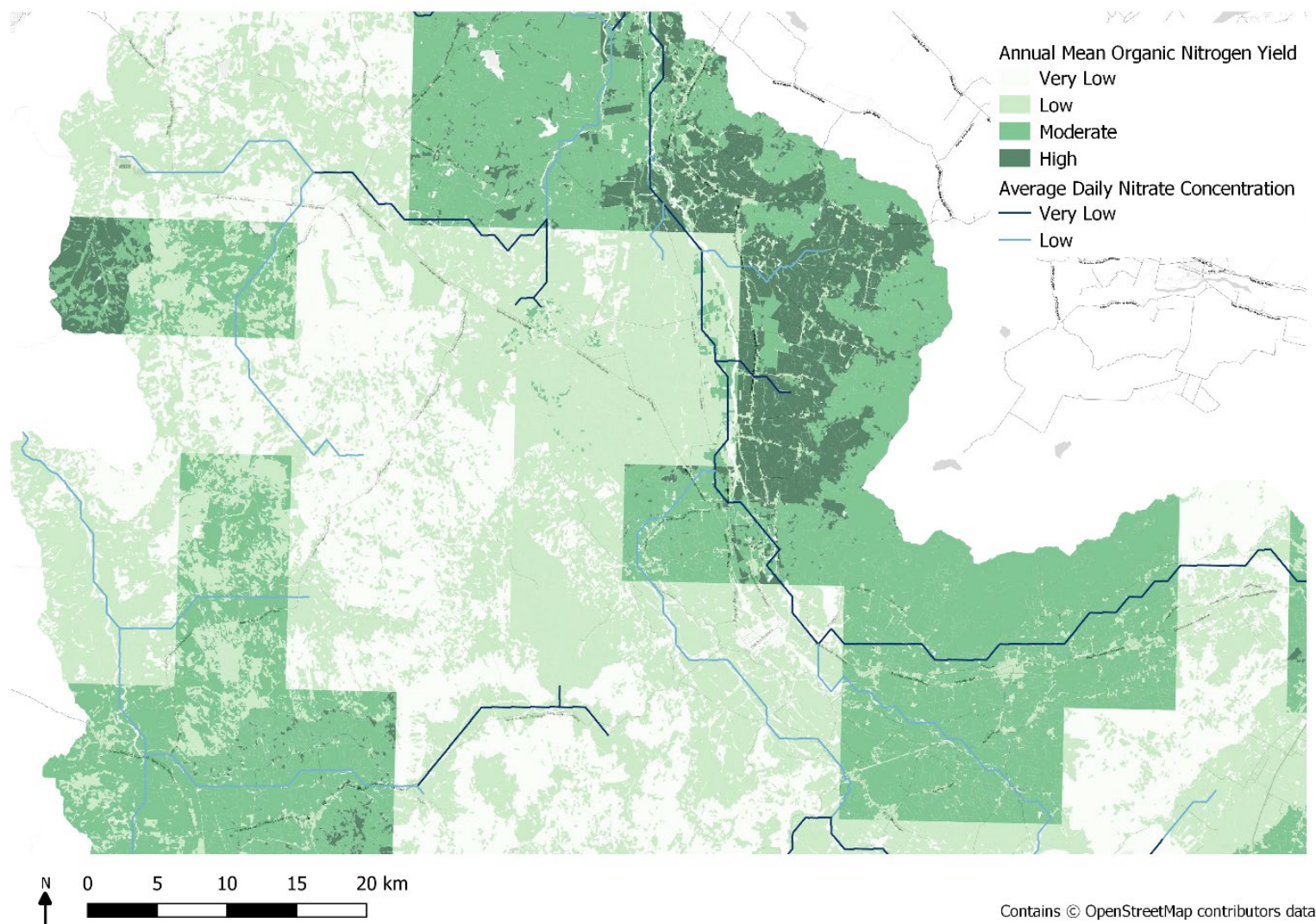


Figure 5.8. Modelled map of organic nitrogen loading rates, where nutrients are leaving the Hydrological Response Units and entering the stream. This is mapped against the natural levels of nitrate present in the water within each stream reach. These are estimations of natural levels without any additional management being applied to the landscape.

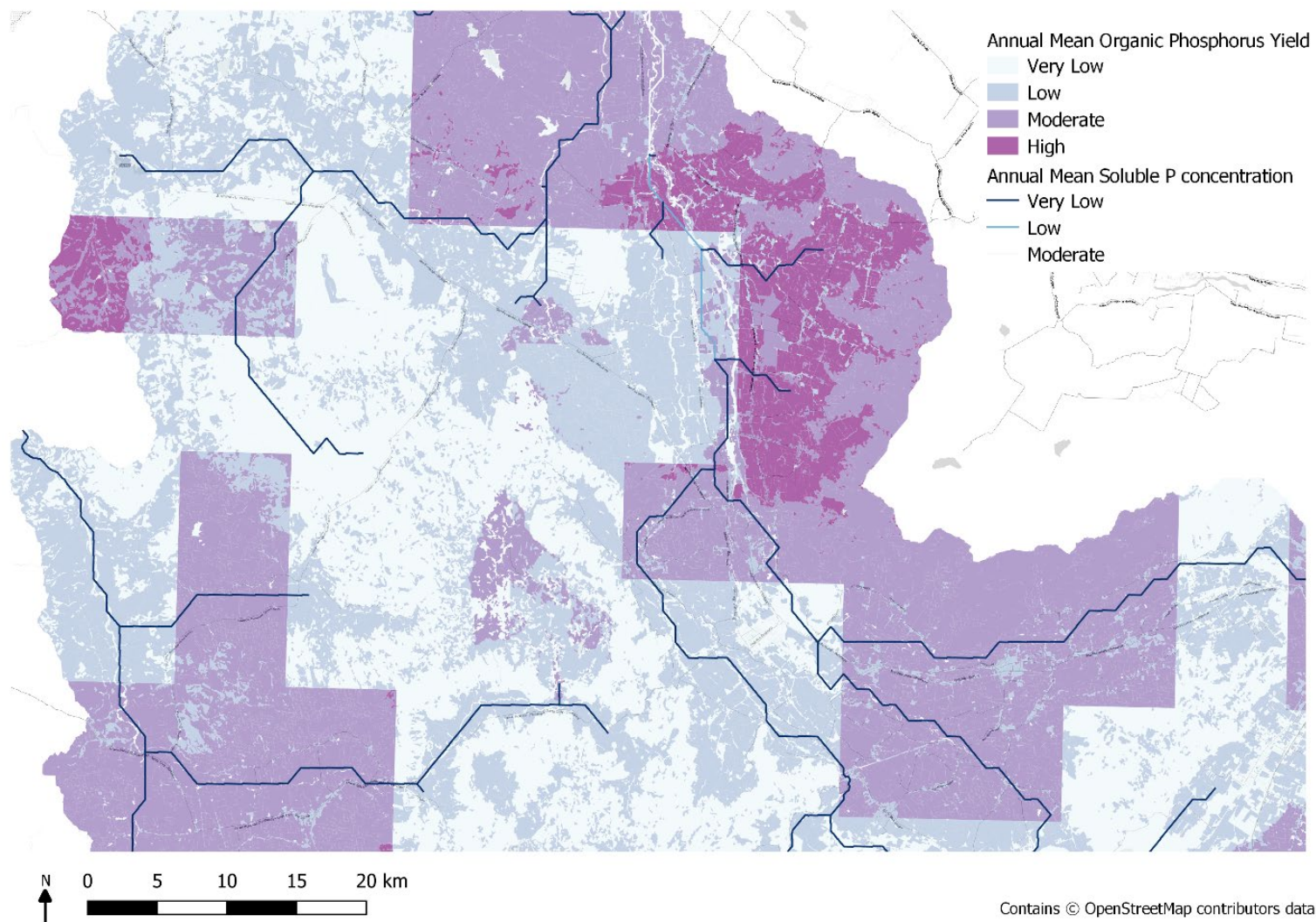


Figure 5.9. Modelled map of organic phosphorus loading rates, where nutrients are leaving the Hydrological Response Units and entering the stream. This is mapped against the natural levels of soluble phosphorus present in the water. These are estimations of natural levels without any additional management being applied to the landscape.

Table 5.2. Summary of baseline maps produced with output details extracted from the SWAT documentation (Arnold *et al.* 2012; Neitsch *et al.* 2012). The categorical ranges are denoted as Very Low = VL, Low = L, Low-Moderate = LM, Moderate = M, Moderate-High = MH, High = H, Very High = VH.

Ecosystem Service	SWAT variable	Metric	Description	Categorical boundaries
Water Supply	WYLD	Water yield	Total amount of water leaving the HRU and entering the main channel. Calculated from surface water runoff, lateral flow, groundwater flow, transmission losses through tributary channels and water abstractions.	(mm H ₂ O) VL:0-200, L:200-350, M:350-500, H:>500
	(Calculated)	Mean daily streamflow	Mean water flow within a reach (the continuous extent of water within a subbasin) calculated from the average of daily streamflow into and out of the reach.	(m ³ /s) L:0-10, M:10-20, H: 20-30, VH:>30
	PERC	Percolation	Water that percolates past the root zone. This is based on the rooting depth associated with the crop type and is calculated average annual value per HRU.	(mm H ₂ O) VL: 0-50, L:50-150, M:150-250, H:250-350, VH:>350
	SW_INIT	Soil water content -start of the day	Soil water content as the amount of water in the soil profile at the start of the day, averaged across the modelled time period.	(mm H ₂ O) VL: 0-30, L:30-60, M:60-90, H:>90
	SW_END	Soil water content – end of the day	Soil water content as the amount of water in the soil profile at the end of the day, averaged across the time period. The soil water loss from start of the day is a function of initial soil water content, time, precipitation, surface runoff, evapotranspiration, the soil profile characteristics and return flow.	(mm H ₂ O) VL: 0-30, L:30-60, M:60-90, H:>90
	(Calculated)	Average daily soil water content	Average daily soil water content calculated from the average values at the start and end of the day (SW_INIT & SW_END).	(mm H ₂ O) VL: 0-30, L:30-60, M:60-90, H:>90
	W_STRS	Water Stress days	The number of days the plant experiences water stress. Water stress is considered 0 if under optimal water conditions for the crop and ranges closer to 1 as soil water conditions vary from the optimal. This is determined through comparisons of actual and potential plant transpiration, detailed in Neitsch et al. 2012.	(days) 0-50, 50-100, 100-150, 150-200
Water quality	ORGN	Organic nitrogen yield	The amount of organic nitrogen transported out of the HRU and into the reach during the time step. In the baseline scenario, these are modelled nutrient values based on the land use and soil types without any additional input from management.	(kg N/ha) VL:0-10, L: 10-25, M: 25-35, H: >35
	ORGP	Organic phosphorus yield	Organic phosphorus transported with sediment out of the HRU and into the reach during the timestep. These are modelled nutrient values based on the land use and soil types without any additional input from management.	(kg N/ha) VL:0-1.5, L:1.5-3.0, M:3.0-4.5, H: >4.5
	NO3_OUT	Nitrate concentration	The average daily concentration of nitrate leaving the reach.	(mg N/L) VL: 0-5, L: >5
	SOLP_OUT	Soluble Phosphorus concentration	The annual mean soluble phosphorus concentration leaving the reach	(ug P/L) VL:0-30, L:30-50, M:>50

5.5 Climate change scenarios

Two climate change scenarios were run using the same weather generator as the baseline model (section 5.4). Daily precipitation and minimum and maximum temperatures were used under the HadGEM2-ES RCP 4.5 and 8.5 simulations (see section 3.4.2). The scenarios were run with a three-year warm-up period from 2066 to 2068 and then modelled for three years from 2069 to 2071.

Figure 5.11 shows a comparison of monthly discharges for a particular reach (reach 63) between the baseline scenario and the modelled data from the two climate change simulations and how streamflow varies under these scenarios. Reach 63 is selected as it is located within the central valley near to several stakeholder vineyards and upstream of the main watershed outlet.

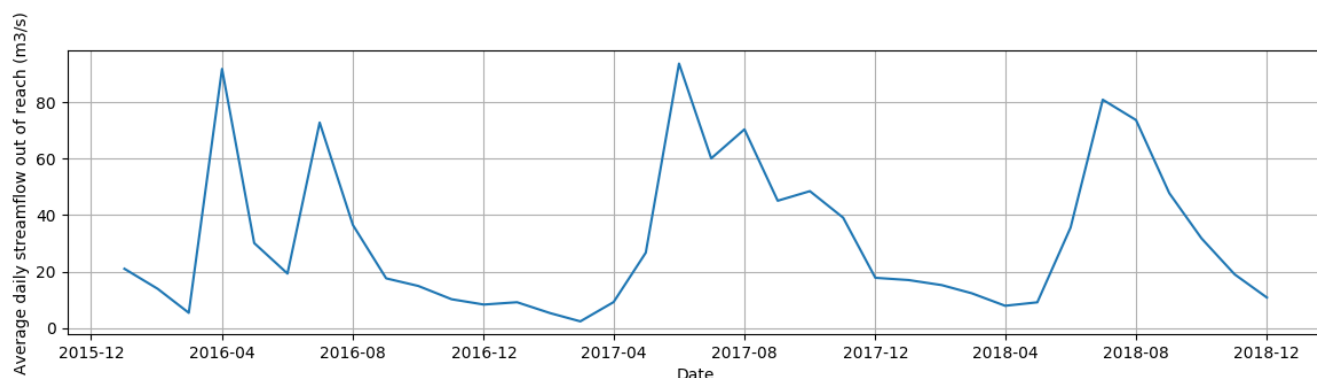


Figure 5.10. River discharge for reach 63 from the baseline model.

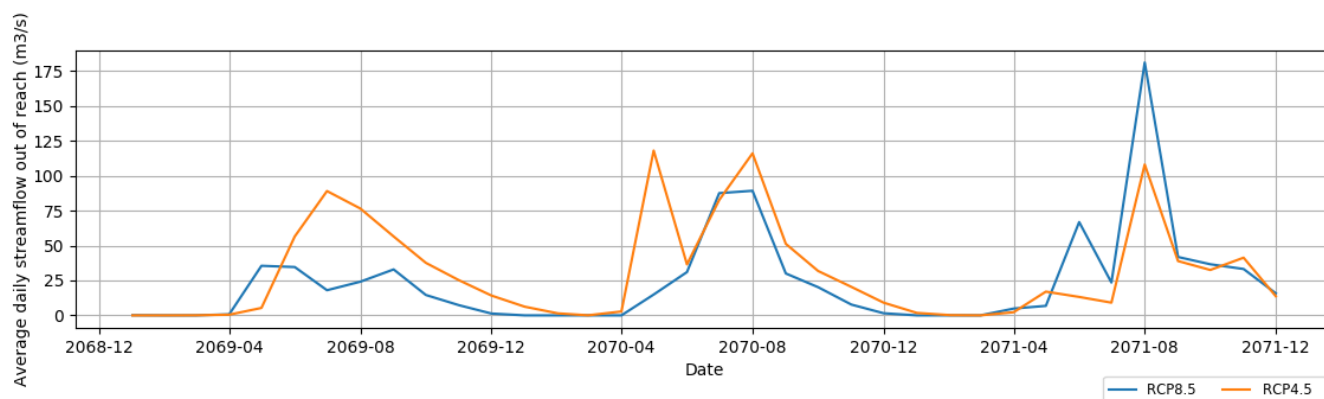


Figure 5.11. River discharge for reach 63 from the future scenarios under climate change scenarios RCP4.5 and RCP8.5 (bottom).

Figure 5.12 shows how water stress days of vegetation vary under the two climate change scenarios in the lowland region where the stakeholder vineyards are located. These were produced to help inform vineyard owners on how water availability may change in the future to gauge the potential impact this can have on vines. Water stress is used in viticulture to increase the fruit quality of berries, however if crops are in irrigation deficit then this can significantly reduce the production yield (Jara *et al.* 2017).

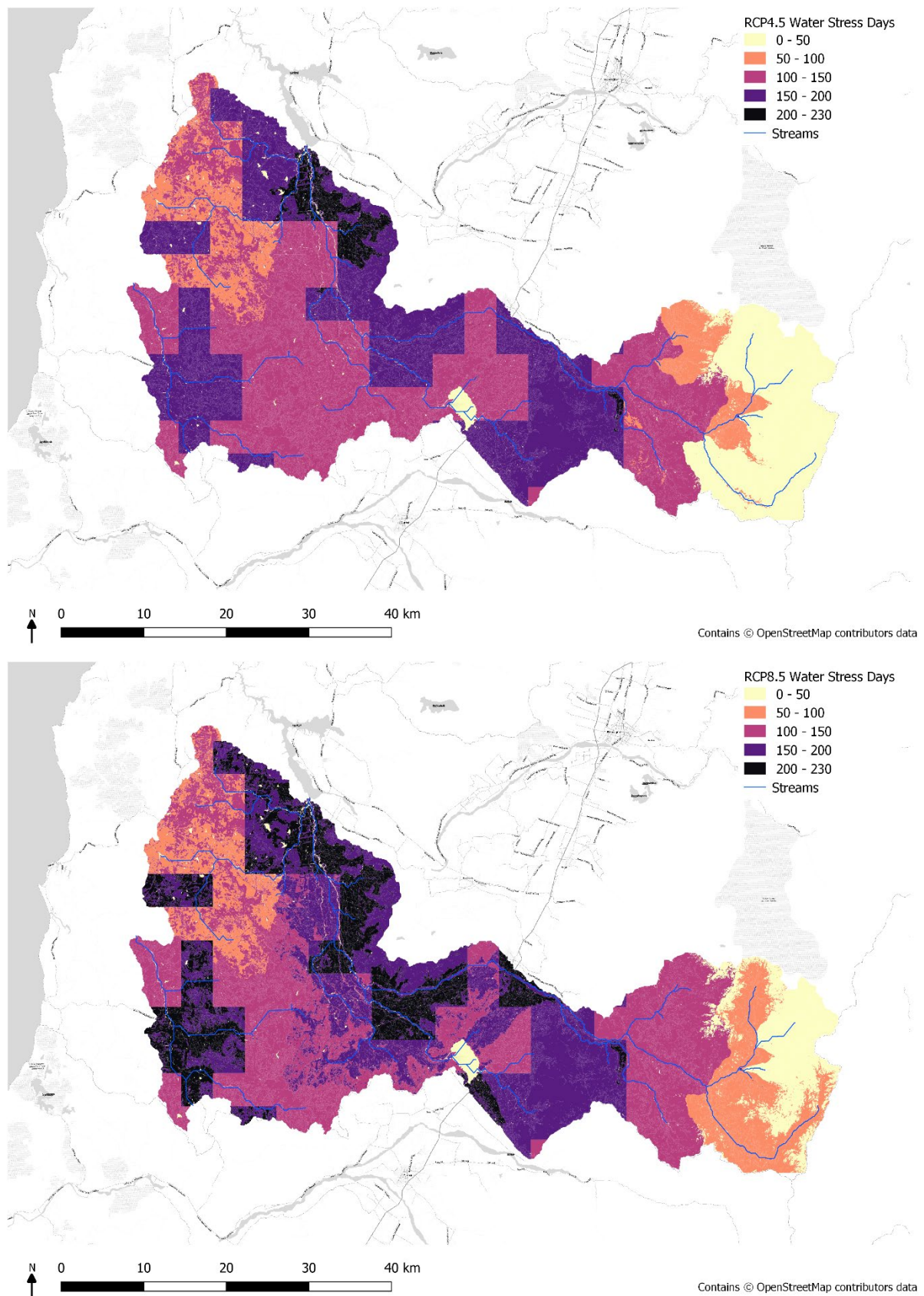


Figure 5.12. Modelled maps showing the water stress days experienced under climate change scenarios RCP4.5 (top) and RCP 8.5 (bottom). Water stress is calculated as a function of the amount of water uptake of the plant during the day and the maximum amount of transpiration.

5.6 Management scenarios to inform the BBN

VCCB encourages their stakeholders to use a variety of sustainable management practices to improve the ecosystem service provision of their land and minimise the negative impacts practices such as fertiliser and pesticide use can have upon the environment (Barbosa & Godoy 2014). Of the suggested management practices; creation of buffer strips, the application of organic fertiliser, chemical fertiliser, herbicide and fungicide, and winter grazing within vineyards by cattle were assessed with the SWAT model. Each management measure was applied to the vineyards and modelled both individually and in combination with each other compare how different management strategies can influence the water quality. To decrease computation time because of project time constraints, the model HRUs were rebuilt, applying threshold values to filter the considered HRUs to cover a minimum of 2% of the sub-basin (2% soil type, 2% land use), generating 615 HRUs used to run the scenarios. The outputs from modelling the different management combinations were used to inform the knowledge underpinning the Bayesian Belief Network relationships between management and downstream water quality (see section 6).

5.6.1 Buffer strips

Management scenarios were run to explore how planting buffer strips of native vegetation within the vineyards could increase nutrient uptake by plants and aid in improving water quality, as suggested in the guidance to stakeholders from VCCB (Barbosa & Godoy 2014). As detailed in section 3.4.3, this was assessed through modifying the land use layer to create 9 m buffer strips of native trees within the vineyard habitats. To apply this in the SWAT model the HRUs were rebuilt using the modified land use layer, with the same parameters as the baseline model, and rerun to simulate the effect of adding buffer strips.

5.6.2 Fertiliser and Pesticide use

Agricultural pesticide and fertiliser use can have a large impact on water quality and are consequently a large concern in countries where there are high application rates. In 2016, Chile used 152.7 kg/ha of nitrogen-based fertilisers and 5.69 kg/ha of pesticide per area of cropland annually, which are relatively high in comparison to usage in other countries (FAO 2017).

Scenarios of high, moderate and low pesticide and fertiliser applications were based on FAO global averages for national fertiliser and pesticide use per area of cropland in 2016 (FAO 2017). From the stakeholder questionnaires, fertilisers used in current management practices included organic sources: compost, humus and seaweed and chemical sources: urea, nitrogen, potassium and phosphorus-based fertilisers. The types of pesticides used by stakeholders tended to focus on herbicides as a form of weed control and fungicides to control the spread of the common mildew fungus on vines. In the scenarios, 'Basta' a Glufosinate Ammonia herbicide and 'Botran' a DCNA (Dicloran) fungicide were applied to the vineyards, which are both pesticides commonly used in grape production (Bayer 2019; Washington State University Extension 2019). Each treatment was applied to the vineyards once annually after the harvest period, with the quantities summarised in Table 5.3. To assess the impact of application to the vineyards, the herbicide and fungicide was only applied to the vineyard land classes within the catchment and outputs were compared with the baseline model. To inform the BBN, the model was run with different high, moderate and low scenarios of each type of fertiliser and pesticide applied to fields. To inform the chemical concentration node of the BBN (see section 6), all possible combinations of herbicide and fungicide were run with and without buffers being applied to fields under the baseline and climate change scenarios. To inform the nutrient concentration node, combinations of organic fertiliser, chemical fertiliser, herbicide, winter grazing by cattle and planting buffer

strips were run to produce outputs encompassing all possible combinations of inputs in the BBN.

To assess the fertiliser treatments, the percentage of the fertiliser applied to each vineyard that leached into the reach was calculated on a HRU level using the equation:

$$PFLeach = \frac{NO_3L_{(sim)} - NO_3L_{(base)}}{N_APP} \times 100$$

where *PFLeach* is the percentage of the total N fertiliser that was applied that has leached below the soil profile, $NO_3L_{(sim)}$ is the amount of nitrate leached per HRU in the management scenario, $NO_3L_{(base)}$ is the amount of nitrate leached per HRU in the baseline scenario and N_APP is the amount of Nitrogen fertilizer applied in kg N/ha. The amount of nitrate leached from the soil profile is calculated in SWAT using numerous algorithms detailed in Neitsch *et al.* 2011) and simultaneously equate nitrate losses through surface water and lateral flow.

Table 5.3. Management scenarios modelled with the SWAT baseline model repeated annually

Management	Chemical Id name	Scenario	Amount applied (kg/ha)	Amount applied (kg N/ha)	Day	Month
Fertiliser - organic	Cattle (beef) manure	Low	625	25	10	4
		Moderate	1250	50	10	4
		High	2500	100	10	4
Fertiliser - chemical	Urea	Low	54.35	25	10	4
		Moderate	108.70	50	10	4
		High	217.40	100	10	4
Herbicide	Glufosinate Ammonia	Low	1	-	10	4
		Moderate	3	-	10	4
		High	6	-	10	4
Pesticide/ fungicide	DCNA (Dicloran)	Low	1	-	10	4
		Moderate	3	-	10	4
		High	6	-	10	4

For these scenarios, as shown in Figure 5.13, the percentage change in nitrate load in the stream (PNO3Load) was also calculated from the difference between the simulated and baseline nitrate load transported out of the reach:

$$PNO3Load = (NO3_OUT_{(sim)} - NO3_{OUT_{(base)}}) / NO3_{OUT_{(base)}} \times 100$$

To assess the pesticide scenarios, the percentage of the applied chemical that entered the reach was calculated on a sub-basin level by:

$$PPLeach = \frac{SOLPST_OUT_{(sim)}}{\sum PST_APP} \times 100$$

where *PPLeach* is the percentage of the total amount of pesticide applied to the sub-basin that is present as dissolved pesticide in the reach during the timestep, $SOLPST_OUT$ is the amount of soluble pesticide in the reach and $\sum PST_APP$ is the sum of the amount of pesticide applied to the sub-basin.

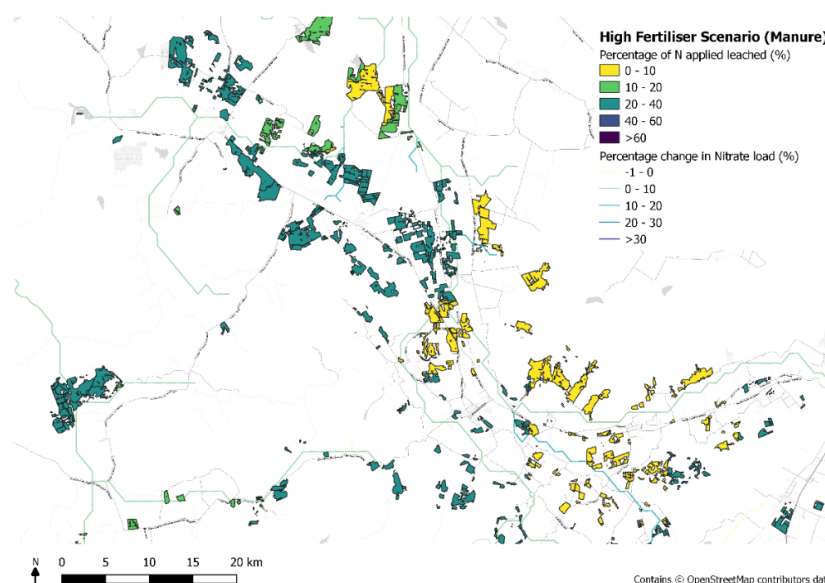


Figure 5.13. A map showing the amount of nitrogen applied to vineyards that has leached below the soil profile and the change in nitrate loading within the reach, under a high organic fertiliser scenario.

5.6.3 Winter grazing by cattle

Winter grazing by livestock is suggested as a sustainable management measure within vineyards for maintaining biodiversity, soil fertilisation and weed management through winter grazing. Chile has a lower stocking rate of cattle compared with other South American countries, at 0.19 LSU (livestock asset) per hectare (FAO 2019). For assessing the impact of cattle management, manure deposition estimations were calculated from FAO statistics of total manure excreted by non-dairy cattle divided by the area of agricultural land. Statistics from Chile in 2006 were used in the moderate cattle stocking scenario and statistics for New Zealand were used in the intensive stocking simulation, where the density of cattle is amongst the highest globally at 0.82 LSU/ha. Manure statistics were calculated for each country using the following equations:

$$TOTH = \frac{\text{Total Cattle stock (LSU)}}{\text{LSU conversion coefficient}}$$

$$\text{Daily manure excreted (kg ha}^{-1} \text{ day}^{-1}) = \frac{TOTH}{\text{AREA(ha)}} \times \left(\frac{TOTM(\text{kg})}{TOTH} \times 365 \right)$$

where TOTH is the total number of cattle heads and TOTM is the Annual total N cattle manure on a countrywide level.

Estimations of dry matter consumption were obtained from IPCC guidelines based on the minimum and maximum estimates of consumption of low-quality forage (Dong *et al.* 2006). Grazing was assumed to occur on vineyards only during the winter period in Chile (19 June to 10 September) (Ruiz-Albarrán *et al.* 2016). The parameters used in the simulations are shown in Table 5.4, with the day and month denoting when the operation began in the model.

Table 5.4. Cattle grazing scenarios modelled with the SWAT baseline model.

Management	Scenario	Consumed biomass (kg/ha/day)	Deposited manure (kg/ha/day)	Grazing days	Day	Month
Winter grazing	Moderate	3.5	0.94	83	19	6
	Intensive	5.5	4.60	83	19	6

6 Bayesian Belief Network modelling

6.1 Introduction

The lead partners at VCCB work with viticulture businesses to develop sustainable environmental management practices that work with the natural environment and deliver benefits by enhancing the quality of the grapes and wine produced. To graphically demonstrate how an ecosystem responds to land management and other environmental variables, a Bayesian belief network (BBN) approach was adopted to relate management practices to ecosystem service outcomes. This was developed using training data from the ecosystem service modelled outputs under the different management and climate scenarios (sections 3-5), as well as literature reviews and local knowledge obtained from interviews and workshops with the vineyard stakeholders.

The BBN approach was chosen as it allows a flexible approach to integrate knowledge from the different modelling outputs. It can account for the uncertainty in the relationships between management practices, environmental components and ecosystem services, by using probability tables. Therefore, confidence in a relationship informed here by literature, modelled data and stakeholder knowledge can be accounted for in the conditional probability values. Once fitted with the informed conditional probability tables, the BBN could then be queried to explore how changes in management affected the probable service delivery of the key ecosystem services of interest to stakeholders.

To communicate these decisions to stakeholders in a user-friendly interactive way, an R-shiny application was developed using R shiny dashboard. This allows users to select management practices and see how these impact upon the ecosystem service delivery of their vineyards on an individual field scale. This lets them explore the relationships between management and ecosystem service delivery and the different trade-offs that could impact their businesses on a scale relevant to their operations and future management decisions.

6.2 Conceptual Ecological Model

Discussions with the VCCB team and a master's thesis by their student Journet (2016) provided an understanding of the different management approaches undertaken by vineyards and the types of sustainable practices landowners are encouraged to consider. This also provided an insight into how viticulturists in the region viewed relationships between management and ecosystem services (Figure 6.1). Through discussions and workshops, stakeholders identified the following ecosystem services as most relevance to their business:

- Natural biocontrol of pest species
- Biodiversity
- Aesthetic appeal
- Prevention of fire spread
- Reduction in topsoil loss
- Avoidance of natural nutrient enrichment
- Water supply and water quality regulation

A conceptual model was developed to integrate these factors and provide the structure for the directed acyclic graph (DAG) (Figure 6.3). This shows diagrammatically how interactions between the promoted management practices and the environment caused changes in the delivery of ecosystem services.

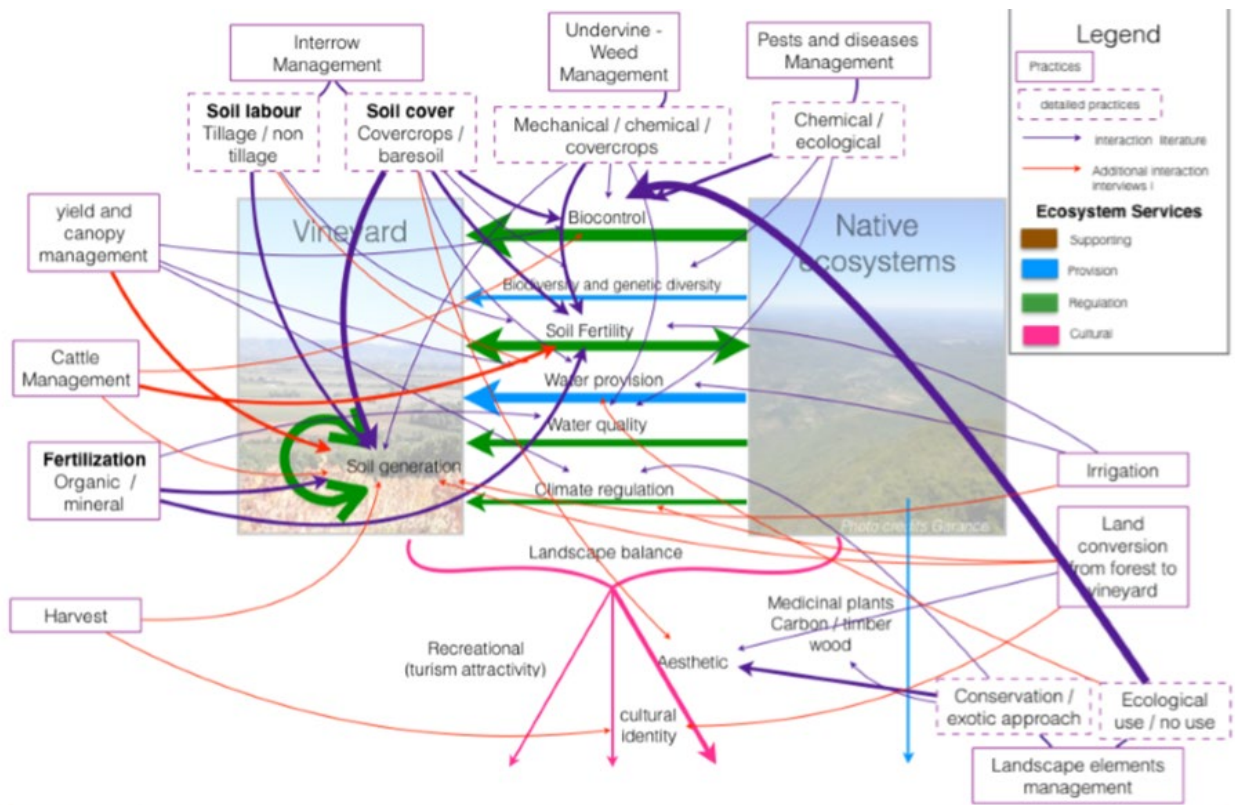


Figure 6.1. Boxes denote management interventions in vineyards that have direct and indirect interactions with natural ecosystems surrounding areas of production. It identifies ecosystem services provided by native ecosystems and how both managed and natural areas interact. Compared visions of literature and the viticulturists (Journet 2016).

6.3 Bayesian Belief Network Development

BBNs are a statistical modelling methodology used to infer probable relationships between elements using known relationships with intermediaries. A simple BBN diagram is displayed in Figure 6.2.

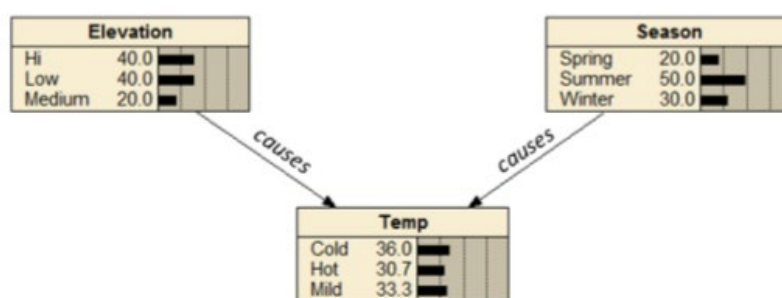


Figure 6.2. An example of a simple BBN diagram (Morgan *et al.* 2012).

Each component in the network is listed as an individual “node” in the diagram and the relationship between the nodes are termed an “edge”. The direction of the edge indicates causality, where one “parent” node can cause a change in state of the “child” node. In Figure 6.2, this is illustrated by the season and elevation nodes determining the temperature. A discrete network was developed by assigning each node with possible “states”, which categorises the data into bands of values (e.g., high, moderate or low). BBNs are probabilistic models where every possible state of a node is determined by an occurrence probability, collated into a single conditional probability table (CPT). Therefore, the probable

state of a child node will be determined by the states of the parent nodes. Using this logic, we can infer likely outcomes given known states of parent nodes and their relationships to child nodes and can develop larger networks to inform more complex problems.

BBNs were used in this project, to help deduce relationships between management practices and the ecosystem services. The suggested management practices by VCCB (Barbosa & Godoy 2014) and key ecosystem services highlighted by the stakeholders were each assigned to a node. This was developed into a directed acyclic graph (DAG) shown in Figure 6.3, by adding additional nodes for intermediate environment components and edges to denote the relationships between nodes, informed by the key variables required for the ecosystem service provision models used in sections 3-5 and expert opinion from ourselves and stakeholders. Information on the states of each node and their conditional probability tables were informed by a mixture of measured and modelled data, literature reviews and expert opinion, detailed in section 6.4. The R package 'bnlearn' (Scutari & Ness 2019) was used to build and fit the BBN in R and it was then queried using the package 'gRain' (Højsgaard 2016).

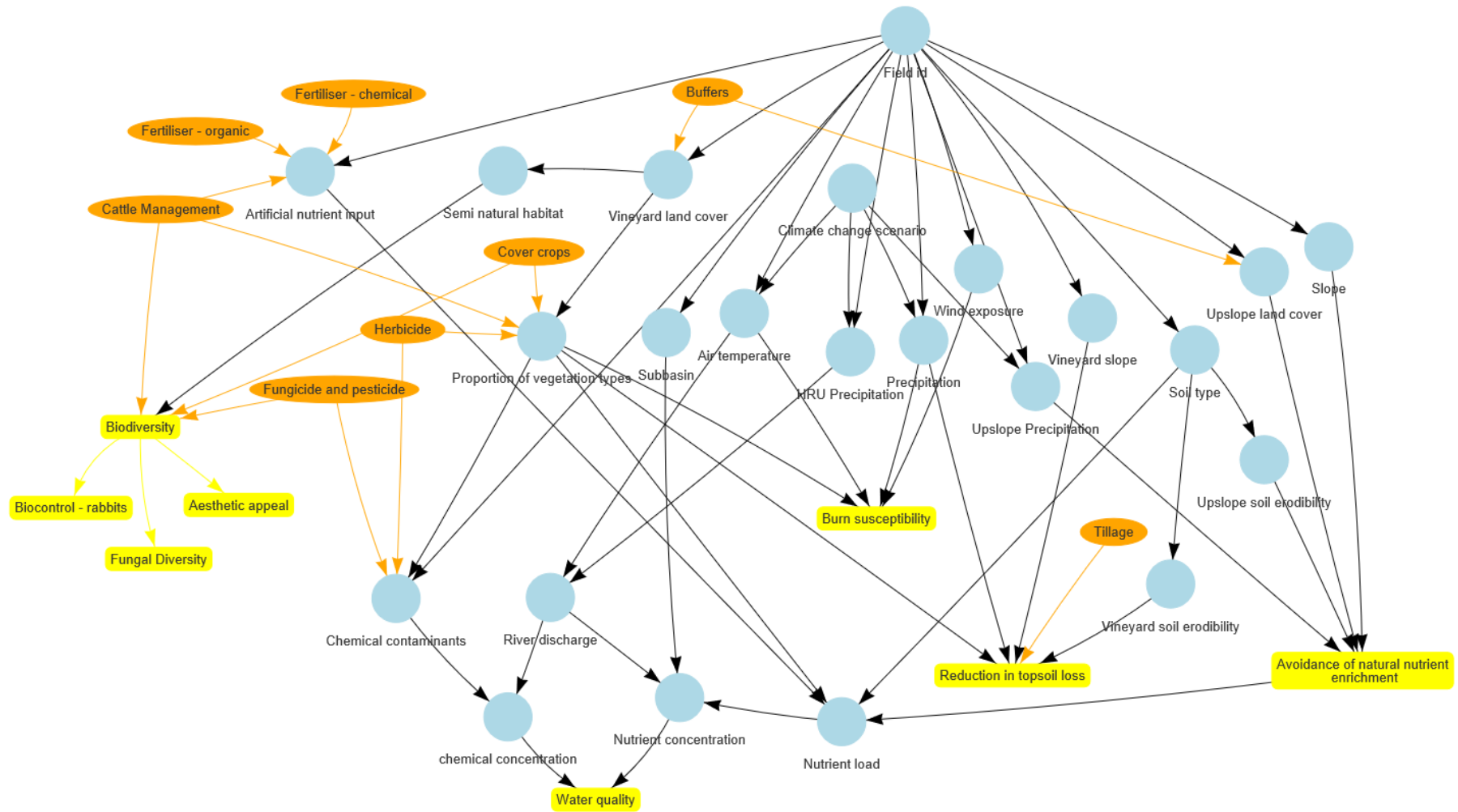


Figure 6.3. Bayesian Belief Network Directed Acyclic Graph (DAG). The orange nodes represent vineyard management practices. Blue nodes represent ecosystem components/features where data can be added to explore these factors on a spatial scale. Yellow nodes highlight the key ecosystem services that can be delivered by the vineyards.

6.4 Relationship Evidence

6.4.1 Measured and modelled data

The data inputs and modelled outputs from the ecosystem service models described in sections 3-5 were used to inform the BBN relationships, summarised in Table 6.1.

Table 6.1. A summary of the nodes informed by either input data sources used in the ecosystem service provision models or output data produced by the models, detailed in sections 3-5.

Model	Described in Section	Scenarios modelled	BBN node informed	Measured data input or modelled output data
INVEST Sediment Delivery Ratio (SDR) model	3	Baseline, Climate change scenarios, Cover crops, Tillage, Buffer strips	Field id	Measured
			Vineyard land cover	Measured
			Air temperature	Measured
			Precipitation	Measured
			Slope	Measured
			Upslope land cover	Measured
			Soil type	Measured
			Vineyard slope	Measured
			Upslope Precipitation	Measured
			Vineyard soil erodibility	Modelled
			Upslope soil erodibility	Modelled
Fire Susceptibility model	4	Baseline, Buffer strips	Field id	Measured
			Vineyard land cover	Measured
			Wind exposure	Measured
			Precipitation	Measured
			Air temperature	Measured
			Burn Avoidance	Modelled
SWAT model	5	Baseline, Climate change scenarios, Buffer strips, Organic Fertiliser, Chemical Fertiliser, Fungicide, Herbicide, Winter Grazing by Cattle	Field id	Measured
			Vineyard land cover	Measured
			Sub-basin	Measured
			Soil type	Measured
			HRU Precipitation	Measured
			Air temperature	Measured
			River discharge	Modelled
			Artificial nutrient input	Modelled
			Nutrient load	Modelled
			Nutrient concentration	Modelled
			Chemical contaminants	Modelled
			Chemical concentration	Modelled

Due to a lack of available data on current management practices applied to the stakeholder vineyards, conditions were modelled without considering practices already in place. Each vineyard is looked at in isolation and it is assumed that management from one vineyard does not impact the management at another. As this is a *proof of concept* project, this was designed to give an indication of the potential impacts that certain management could have upon the landscape. Given more data about the current landscape and working closer with stakeholders to design parameters this could be further developed to provide more accurate results.

Data were extracted from the models at three different scales, as follows:

- **Vineyard scale** – Shape files of stakeholder vineyard boundaries were supplied by VCCB. These were used to extract information specific to each individual field, such as the proportion of land cover, slope, climate variables.
- **Upslope catchment** – The upslope catchment was defined as the contributing area of flow for soil movement into the vineyard habitats within field boundaries. This was calculated by the TauDEM Python applications, which use elevation data to calculate

flow directions of soil and water movement across the landscape. By assessing the flow pathways against the field boundaries, the applications can be used to calculate the flow contribution area upslope of the field. Figure 6.4 displays the calculated upslope contributing area for one of the stakeholder vineyards. These were cropped to a distance of 50 m to represent the contributing area of soil which enters the vineyards, as described in the Natural Capital Project's (2019) InVest Sediment Delivery Ratio documentation. The upslope catchment area was used to extract data from the soil loss model to inform the BBN node 'Avoidance of natural nutrient enrichment'.

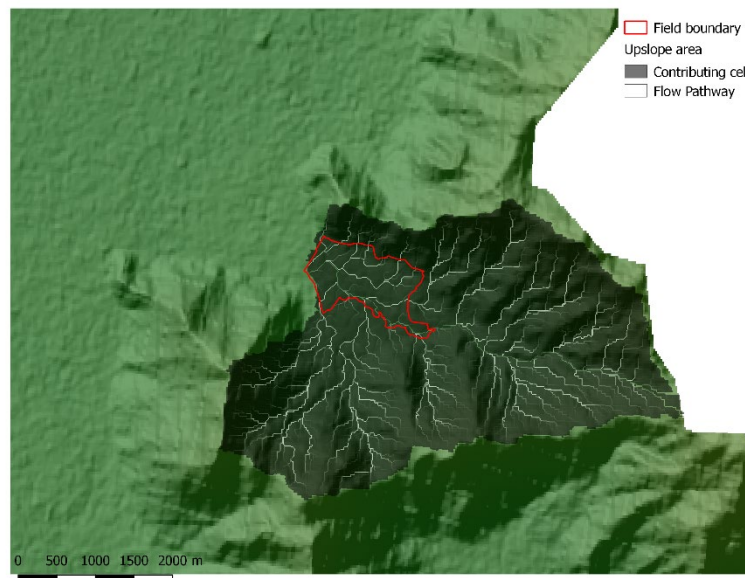


Figure 6.4. The upslope contributing area to a stakeholder vineyard calculated using the TauDem functions.

- **Sub-basin level** – Data were extracted at the sub-basin level to inform the nodes relating to water quality, as the chemical and nutrient levels within a stretch of the river is dependent upon the land use and management within the whole sub-basin drainage area. Contributing values could be obtained per vineyard and therefore their contribution toward the water quality could then be extrapolated.

6.4.2 Literature review and stakeholder workshops

For nodes which could not be informed directly by the models, information from the stakeholder workshops and studies carried out by the VCCB research team were valuable in informing the remaining BBN relationships.

The thesis by Journet (2016) as part of the VCCB research group explored how vineyard management practices can impact upon ecosystem services by conducting interviews with stakeholders in the region and literature reviews. This provided an overview of the suggested measures encouraged by VCCB and their impact upon vineyard vegetation. This along with satellite images from Google Earth and expert opinion helped to inform the "Proportion of vegetation types" node and relationships to management. This node simplifies the Vineyard land cover by categorising the states into vegetation type classes, the states of which were based upon high level FAO land cover classification (Di Gregorio 2005). The conversion table for these classes are displayed in Table 6.2. This simplification reduces the dimensions required in the child nodes captures the differences in vegetation biomass between habitats.

Planted cover crops and interrow planting between vines were highlighted by Journet (2016) as a method to enhance soil fertility and reduce topsoil loss, as well as encouraging natural biodiversity within the vineyard. Cover crops mentioned in the region were mostly exotic species such as vetches, clovers and mustards, herbaceous crops, captured in the BBN by increased proportions of the “grass” vegetation type. Cattle management was also highlighted by Journet as a key practice used to enrich soil and manage pests and disease. Winter grazing from livestock is used to manage weed control within vineyards, reducing the proportion of grass between vines through trampling and consumption, which has shown to have an impact upon fire risk impacting the amount of mid-to-low-level vegetation (Journet 2016).

Table 6.2. Land cover class conversion table from habitat map classes to proportion of vegetation type states.

Vineyard Land Cover classes	Bare	Bare soil	Grass	Shrub	Trees – native	Trees – non-native
Agricultural land	-	50%	5%	15%	30%	-
Alluvial plain	80%	10%	10%	-	-	-
Central Andean steppe	-	34%	33%	33%	-	-
Crop grassland	-	-	100%		-	-
Glaciers	100%	-	-	-	-	-
Lakes	100%	-	-	-	-	-
Native forest	-	-	-	-	100%	
Plantation	-	50%	-	-	-	50%
Rivers	100%	-	-	-	-	-
Rocky outcrops	80%	20%	-	-	-	-
Scrubland	-	-	-	100%	-	-
Seasonal meadows	-	-	100%	-	-	-
Snowcover	100%	-	-	-	-	-
Trees & Scrub		-	-	50%	50%	-
Urban	100%	-	-	-	-	-
Vineyard	-	40%	10%	50%	-	-

Similarly, the “semi-natural habitat” node was used for simplification within the network, simplifying the states of the “Vineyard land cover” by categorising the information into three categories instead of sixteen. These were denoted as agriculture, semi-natural and urban habitats, and were categorised using expert opinion with the classification shown in Table 6.3.

Table 6.3. Land cover class conversion table from habitat map classes to semi-natural habitat states.

Categories	Habitat classes
Agriculture	Agricultural land, Crop grassland, Plantation, Seasonal meadows, Vineyards
Semi natural	Alluvial plain, Central Andean steppe, Glaciers, Lakes, Native Forest, Rivers, Rocky outcrops, Scrubland, Snowcover, Trees & Scrub
Urban	Urban

Biodiversity within vineyards has been explored in a number of studies and has shown to increase with increasing proximity to nearby semi-natural habitat, as opposed to disturbed land such as urban or agricultural land (Grashof-Bokdam & van Langevelde 2005; Márquez-García *et al.* 2018). Biodiversity is key for ecosystem functions within a vineyard such as maintaining the fungal diversity and pest control within fields. It is key with regards to encouraging the natural yeasts and fungal species diversity as part of the ‘terroir’

characteristic in growing biodynamic wines. Fungal diversity and maintaining a correct balance of yeast species within the environment is important to the flavour and quality of the wine produced and has been linked to plant diversity and the distance of the vines to the surrounding semi-natural habitat (Castañeda *et al.* 2018).

Pest species are key concerns for vineyards, stakeholder identify rabbits, vine fake red spider, Oiddio and vine wood fungi as particular pest species in the region. Guidance from VCCB (Barbosa & Godoy 2014) highlights how creating ecological corridors by using buffer strips and cover crops can help reduce pest pressures by encouraging natural predators, whereas monoculture vineyard fields are more susceptible to pests and disease.

Cattle management is also seen to aid in pest prevention, in addition to fire prevention; as shorter grasses are maintained reducing ignition potential and fuel availability (Journet 2016; Márquez-García 2018). Pesticide and fertiliser application have shown to negatively impact upon vineyard biodiversity, especially where use is excessive as well as downstream impacts within lakes and streams (Puig-Montserrat *et al.* 2017). Another benefit of encouraging biodiversity in vineyards is the aesthetic value species add to the landscape, increasing values associated to community identity and human well-being (Tribot *et al.* 2018).

6.4.3 Constructing the Conditional Probability Tables (CPTs)

The data collated for each node detailed in section 6.4.1 was used along with the two simplification nodes “proportion of vegetation types” and “semi-natural habitat” (described in section 6.4.2) to create training data for four of the ecosystem services; reduction in topsoil loss, avoidance of natural nutrient enrichment, fire avoidance and water quality. This training data was then used to fit smaller sections of the BBN in Figure 6.3. This was partitioned to reduce processing power and computation time. These smaller BBNs generated the conditional probability tables for the majority of nodes, informing their relationships based upon the training data. The CPT for the end service node for water quality was calculated as a combination of the nutrient and chemical concentration nodes, where these were both of a high status the water quality was denoted as poor. The remaining node CPTs for biodiversity, fungal diversity, aesthetic appeal and natural pest control were equated using knowledge from literature reviews detailed in section 6.4.2 and expert opinion. All the CPTs were then compiled to populate the larger Bayesian belief network, linking all of the modelled ecosystem services together with management decisions.

6.5 Applying the BBN

The extracted data were collated, and the BBN network was fitted with the informed conditional probability tables. This allowed it to be queried under the different scenarios with functions in the “bnlearn” package.

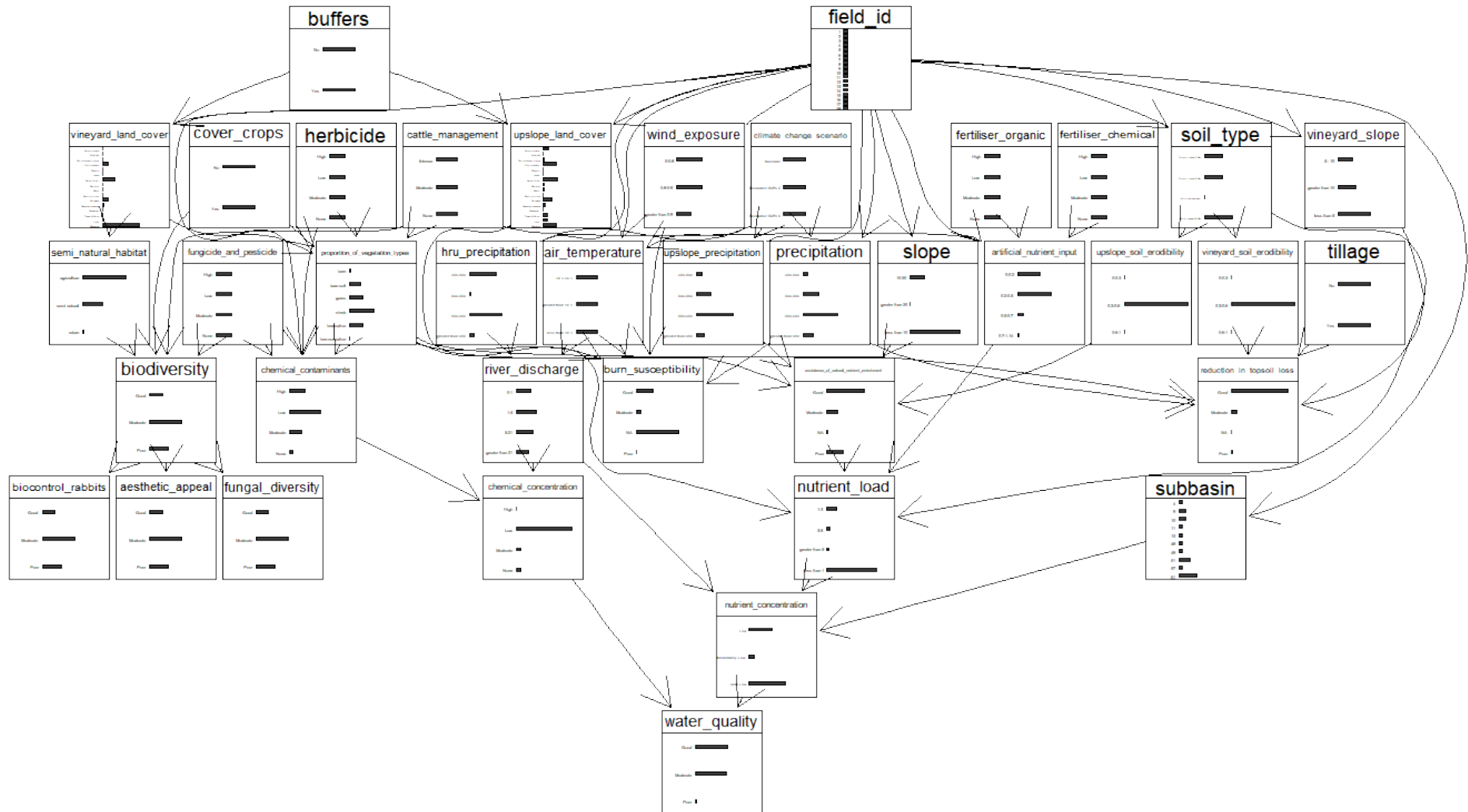


Figure 6.5. A diagram of the fitted BBN displaying the conditional probability tables as bar graphs for each node.

To make this more accessible for stakeholders, an R shiny application was developed using R shiny dashboard to allow users to view the outcomes of management decisions in a user-friendly display (see Figure 6.6 to Figure 6.8). The Viticulture ImplemeNting Ecosystem Services (VINES) app was developed to display specific land parcels managed by particular stakeholders, displaying a map of their vineyards' location in relation to the surrounding landscape using 3D renders of their fields and surrounding area, and data from their individual crop fields.

The app consists of three tabs, shown in the screenshots in Figure 6.6 to Figure 6.8. The App landing page (Figure 6.6) displays a 3D rendered image of the Colchagua valley, developed using the R package 'rayshader' (Morgan-Wall 2019). On this page the user should select their winery and field. This information then feeds into the second tab 'Management', which allows stakeholders to view and query the data for their selected field, plotting the ecosystem service delivery in a coloured bar plot (Figure 6.7). Here they can select different management options and climate change scenarios, which queries the BBN directly outputting how this changes the resulting ecosystem services and their relative probabilities of being either 'Good', 'Moderate' or 'Poor'. This is visualised by changes in the proportional bar plot, with the state having the largest area representing the most likely state of ecosystem service delivered. This plot is interactive, allowing users to hover over areas of the graph to retrieve probability values, as well as show and hide legend entries by clicking them. There is also an option to download a .csv file of the plot data and reset all management options to default. The final tab 'Network' displays the BBN DAG, showing the user the mechanisms by which each scenario is affecting the ecosystem services and allows them to visualise the underlying BBN network.

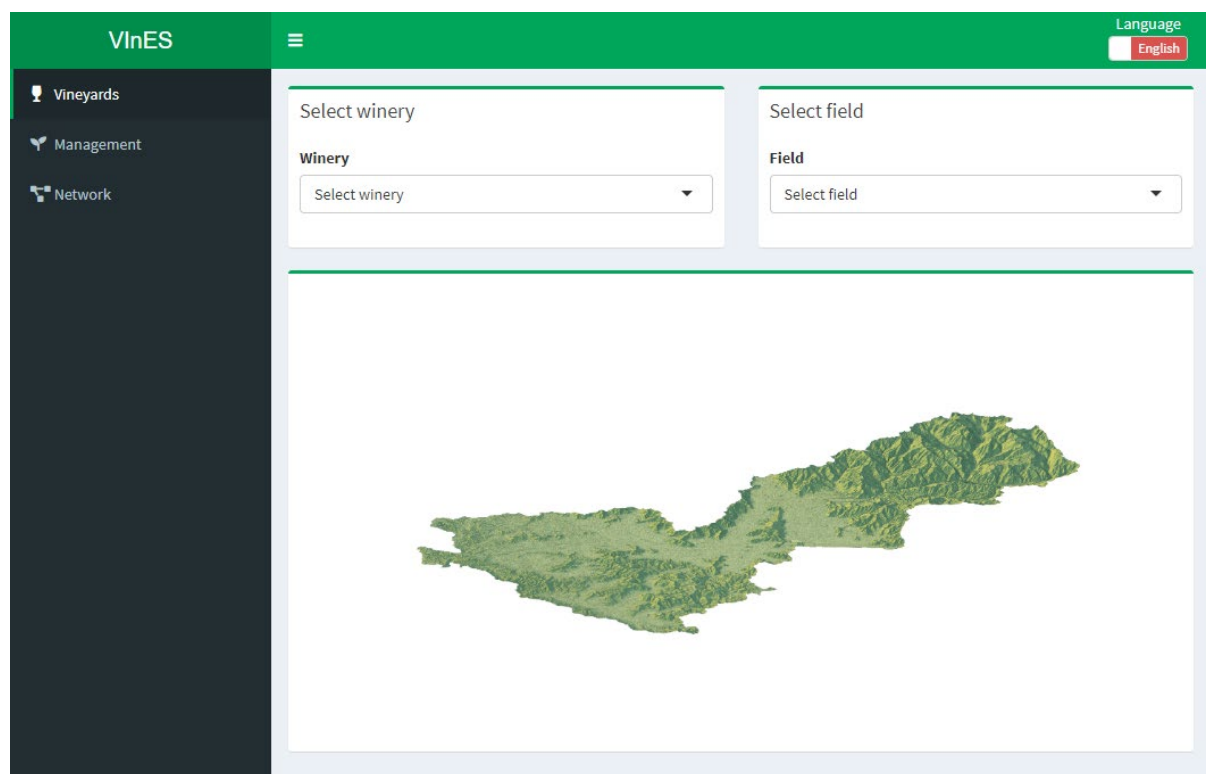


Figure 6.6. App landing page.

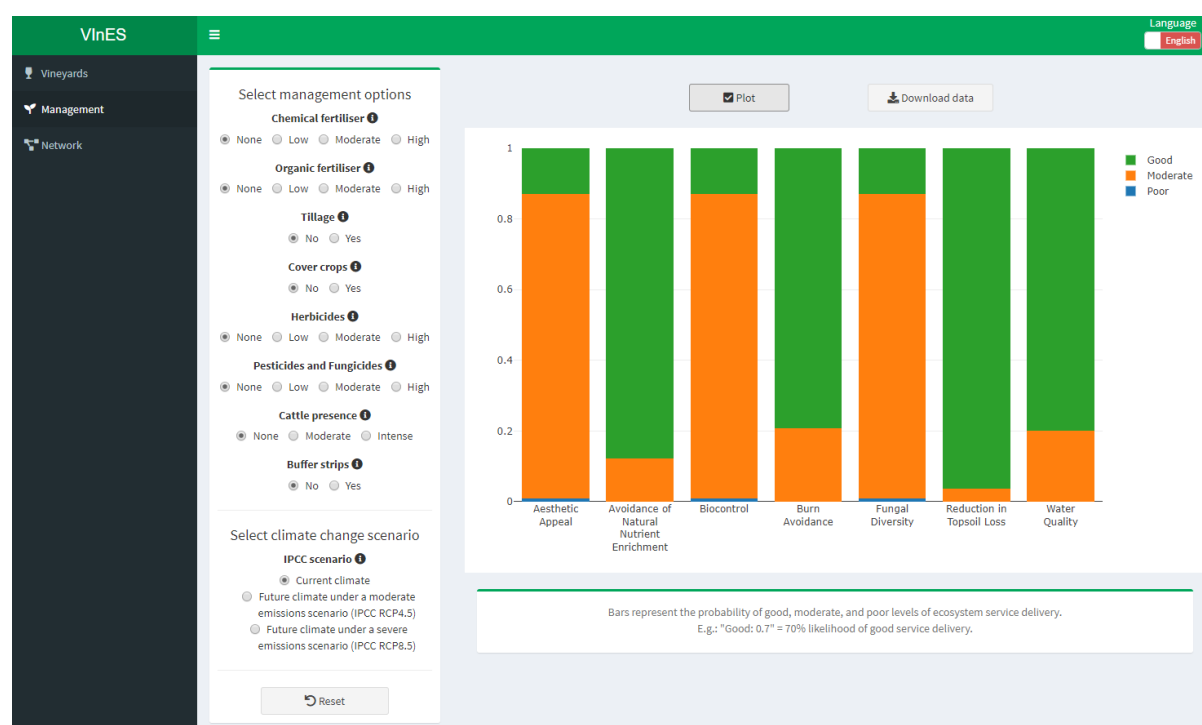


Figure 6.7. Example plot displayed in the app, with default management and climate change options.

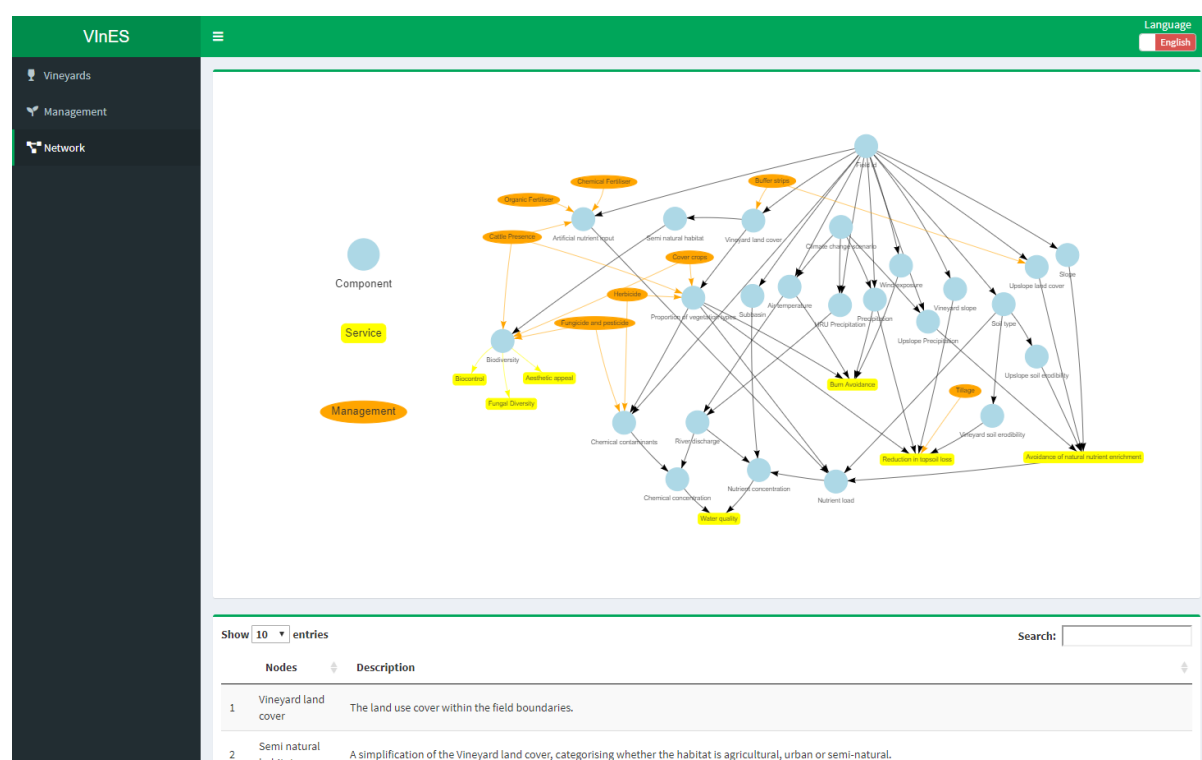


Figure 6.8. BBN DAG visualisation.

7 Conclusion and next steps

The Natural Capital Approach to Landscape Planning: a Pilot Project in Colchagua Valley, combines industry knowledge with ecosystem sciences and seeks to disentangle and quantify the interactions between land management, biotic and abiotic factors and the effect on business-critical ecosystem services. The project ran for five months, and within that time initial iterations have developed, showing how models can be established in-line with user

requirements, providing tools that help bring environmental data into decision making processes. The use of Bayesian Belief Networking (BBN) helps to clarify the trade-offs associated with land use planning and management.

Environmental risk management is critical for avoiding supply chain disruption and potential infrastructure damage; such as identifying fire risks and implementing avoidance strategies. Better understanding of catchment processes can lead to better informed land planning. Predicting factors such as water stress and pollution risk are vital to the future success of any business. The most important next steps are to test the applicability of these concepts and identify how they may be applied in this context or scaled to accommodate other scenarios.

7.1 Potential Steps for Model Improvement

Working more closely with vineyards to gather and apply local data and gain a more detailed understanding of the links between management decisions, ecosystem responses, abiotic variables and impacts, which would improve the BBN. This would provide more advanced information, enabling models to be adapted, to inform local management and monitoring of outcomes. The scalability of the models could be assessed to identify management unit specific applications, at finer scales.

Due to a lack of available data on current management practices adopted by the focal vineyards, conditions were modelled without considering practices already in place. Each vineyard was reviewed in isolation, and it is assumed that management from one vineyard does not impact management at another. Improved understanding of current interventions implemented by vineyards and other land users would provide a better picture of inter-play between different activities; potentially identifying opportunities for cooperative management, to maximise ecosystem services and minimise environmental impacts.

The use of high-resolution satellite imagery would improve habitat mapping, as would conducting further ground validation across a wider area, this would improve the accuracy of the classification of different land use and regional habitats; helping to identify more features delivering ecosystem services, improving modelling at the local and landscape level, and to detect change over time.

Due to a lack of local soil data, a low-resolution Food and Agriculture Organisation (FAO) soils data layer has been used, which does not accurately reflect how the soil compositions may vary spatially across the landscape. Soil data could be improved with the provision of local data or sampling, especially in terms of biophysical characteristics and rates of soil loss.

Local crop characteristics and measurements were unavailable and were matched to the nearest crop type in the models' crop databases, which are based upon temperate US crop types. Information on local crop characteristics would improve the accuracy of assessing factors such as water demand and stress and soil permeability.

With more time, a sensitivity analysis could assess the relative influence the data layers have on the responses in the Soil and Water Assessment Tool (SWAT) models.

Local weather station data from the Colchagua Valley was only available as point data, and at inconsistent time intervals. There is value in exploring how local meteorological data could be better collected to improve local accuracy of models.

Due to time and resource constraints, it was not possible to cover all ecosystem services identified as 'important' by stakeholders. Future work could explore natural biocontrol of pest species, and even cultural values associated with the vineyards and landscape.

Biodiversity is of utmost importance to the terroir of the wine growing region. Researching organisms such as wild yeasts and soil microbial communities could be explored in relation to land management and spatial planning, to maintain or restore unique characteristics of the landscape.

The models and BBNs can be used to inform monitoring schemes, assess outcomes in real terms (e.g., does reduced cattle stocking density impact soils or water quality), there is also the potential to explore how this type of information can be quantified and used by companies to improve and report on environmental performance.

The approaches developed can be adapted to other scenarios, ecosystem services and land use. The main proviso being the availability of data.

8 References

2W2E – Weather Water Energy Ecosystem. 2019. Climate Change Data for SWAT model (CRU). Available from: <https://www.2w2e.com/home/CRU> [Accessed 04/02/2019].

ADAS. 2007. Nitrates in water – the current status in England. ADAS report to Defra – supporting paper D1 for the consultation on implementation of the Nitrates Directive in England. July 2007.

Abatzoglou, J.T., Dobrowski, S.Z., Parks, S.A. & Hegewisch, K.C. 2018, Terraclimate, a high-resolution global dataset of monthly climate and climatic water balance from 1958-2015, Scientific Data,

Alcamo, J., Flörke, M. & Märker, M. 2007. Future long-term changes in global water resources driven by socio-economic and climatic changes. *Hydrological Sciences Journal* **52**(2): 247-275. DOI: 10.1623/hysj.52.2.247

Alexander, M.E., Lawson, B.D., Stocks, B.J. & van Wagner, C.E. 1984. User Guide to the Canadian Forest Fire Behaviour Prediction System: Rate of Spread Relationships; (Interim Edition). Environment Canada, Canadian Forestry Service, Northern Forest Research Centre, Edmonton, Alberta

Allen, R.G., Pereira, L.S., Raes, D. & Smith, M. 1998. Crop evapotranspiration - Guidelines for computing crop water requirements - FAO Irrigation and drainage paper 56: Chapter 3 Meteorological data. Available from: <http://www.fao.org/3/X0490E/x0490e07.htm> [Accessed 20/01/2019].

Almendinger, J. 2016. Google Groups. ArcSWAT topic: How to set up warm-up period in SWAT. Available from: <https://groups.google.com/forum/#!msg/arcswat/c19Li5ATNvY/1QM8gnvZAwAJ> [Accessed 14/02/2019]

Alvarez-Garreton, C., Mendoza, P.A., Boisier, J.P., Addor, N., Galleguillos, M., Zambrano-Bigiarini, M., Lara, A., Puelma, C., Cortes, G., Garreaud, R., McPhee, J. & Ayala, A. 2018. The CAMELS-CL dataset: catchment attributes and meteorology for large sample studies – Chile dataset. *Hydrology and Earth System Sciences* **22**: 5817-5846. <https://doi.org/10.5194/hess-22-5817-2018>

Anderson, B., Peng, R. & Ferreri, J. 2016. Package 'weathermetrics': Functions to Convert Between Weather Metrics. Version 1.2.2. Available from: <https://cran.r-project.org/web/packages/weathermetrics/weathermetrics.pdf> [Accessed 29/01/2019].

Arnold, J.G., Kiniry, J.R., Srinivasan, R., Williams, J.R., Haney, E.B. & Neitsch, S.L. 2012. SWAT Water Assessment Tool: Input/Output Documentation Version 2012. Texas Water Resources Institute TR-439. Available from: <https://swat.tamu.edu/media/69296/swat-io-documentation-2012.pdf> [Accessed 07/01/2019].

Barbet-Massin, M., Jiguet, F., Albert, C.H. & Thuiller, W. 2012. Selecting pseudo-absences for species distribution models: how, where and how many? *Methods in Ecology and Evolution* **3**: 327-338.

Barbosa, O. & Godoy, K. 2014. Conservación biológica en viñedos: conceptos claves y actividades prácticas. Programa Vino Cambio Climático y Biodiversidad Chile. *Universidad Austral de Chile* 2014

Bayer (Pty) Ltd. 2019. Basta®. Available from: <https://www.cropscience.bayer.co.za/en/Products/Herbicides/Basta.aspx> [Accessed:11/03/2019].

Boisier, J.P., Alvarez-Garretón, C., Cordero, R.P., Damiani, A., Gallardo, L., Garreaud, R.D., Lambert, F., Ramallo, C., Rojas, M. & Rondanelli, R. 2018. Anthropogenic drying in central-southern Chile evidenced by long-term observations and climate model simulations. *Elementa Science of the Anthropocene* **6**: 74. DOI: <https://doi.org/10.1525/elementa.328>

Braithwaite, R.J. 2008. Temperature and Precipitation Climate at the Equilibrium-Line Altitude of Glaciers Expressed by the Degree-Day Factor for Melting Snow. *Journal of Glaciology* **54** (186): 437-444.

Bravo, C., Loriaux, T., Rivera, A. & Brock, B.W. 2017. Assessing glacier melt contribution to streamflow at Universidad Glacier, central Andes of Chile. *Hydrology and Earth System Sciences* **21**(7):3249-3266.

Castañeda, L.E., Miura, T., Sánchez, R. & Barbosa, O. 2018. Effects of agricultural management on phyllosphere fungal diversity in vineyards and the association with adjacent native forests. *Peer J* **6**: e5715; DOI 10.7717/peerj.5715

CONAF. 2018. Estadísticas históricas. Available from: <http://www.conaf.cl/incendios-forestales/incendios-forestales-en-chile/estadisticas-historicas/> [Accessed 11/02/2019].

Copernicus Global Land Service. 2019. Fraction of green Vegetation Cover. Available from: <https://land.copernicus.eu/global/products/fcover> [Accessed 10/01/2019].

Di Gregorio, A. 2005. Land Cover Classification System: Classification concepts and user manual. Software version (2). Food and Agriculture Organization of the United Nations. Available from: <http://www.fao.org/3/y7220e/y7220e00.htm#Contents> [Accessed 28/02/19].

Didan, K., Huete, A. & MODAPS SIPS. 2015. MOD13A3 MODIS/Terra Vegetation Indices Monthly L3 Global 1km SIN Grid. NASA LP DAAC. <http://doi.org/10.5067/MODIS/MOD13A3.006>

Dile, Y., Srinivasan, R. & George, C. 2018. QGIS Interface for SWAT(QSWAT) Version 1.7 October 2018 User Manual. Available from: https://swat.tamu.edu/media/116095/qswat-manual_v17.pdf [Accessed 06/01/2019]

Dirección General de Aguas (DAG), Ministerio de Obras Públicas. 2019. Información Oficial Hidrometeorológica y de Calidad de Aguas en Línea. Available from: [http://snia.dga.cl/BNAConsultas/ reportes 2015-2018](http://snia.dga.cl/BNAConsultas/reportes%202015-2018) [Accessed 13/01/2019].

Duane, A., Piqué, M., Castellnou, M. & Brotons, L. 2015. Predictive modelling of fire occurrences from different fire spread patterns in Mediterranean landscapes. *International Journal of Wildland Fire* **24**: 407-418

FAO. 2006. Guidelines for soil description, Fourth edition. Food and Agriculture Organization of the United Nations, Rome. Available from: <http://www.fao.org/3/a0541e/a0541e.pdf> [Accessed 03/01/2019]

FAO/UNESCO. 2003. The Digital Soil Map of the World. Available from: http://www.waterbase.org/data/Global_Soil_Data/readme.pdf [Accessed 06/01/2019].

Fick, S.E. & Hijmans, R.J. 2017. Worldclim 2: New 1-km spatial resolution climate surfaces for global land areas. *International Journal of Climatology*.

Food and Agriculture Organization of the United Nations (FAO). 2017. FAOSTAT: Fertilizers. Available from: <http://www.fao.org/faostat/en/?#data/EF> [Accessed 25/02/2019].

Gassman, P.M., Reyes, M.R., Green, C.H. & Arnold, J.G. 2007. The Soil and Water Assessment Tool: Historical development, applications and future research directions. *American Society of Agricultural and Biological Engineers*. **50**(4): 1211-1250.

Gharibdousti, S.R., Kharel, G. & Stoecker, A. 2018. Modelling the impacts of agricultural best management practices on runoff, sediment, and crop yield in an agriculture-pasture intensive watershed. *Peer J Preprints* (Not peer-reviewed). Available from: [https://doi.org/10.7287/ peerj.preprints.27452v1](https://doi.org/10.7287/peerj.preprints.27452v1) [Accessed 06/01/2019].

Giglio, L., Justice, C., Boschetti, L. & Roy, D. 2015. MCD64A1 MODIS/Terra+Aqua Burned Area Monthly L3 Global 500 m SIN Grid V006. 2015, distributed by NASA EOSDIS Land Processes DAAC. Available from: <https://doi.org/10.5067/MODIS/MCD64A1.006> [Accessed 06/01/2019].

GLIMS. 2018. Global Land Ice Measurements from Space glacier database. Compiled and made available by the international GLIMS community and the National Snow and Ice Data Center, Boulder CO, U.S.A. DOI:10.7265/N5V98602

Gómez-González, S., González, M.E., Paula, S., Díaz-Hormazábal, I., Lara, A. & Delgado-Baquerizo, M. 2019. Temperature and agriculture are largely associated with fire activity in Central Chile across different temporal periods. *Forest Ecology and Management* **433**: 535-543.

Grashof-Bokdam, C. J. & van Langevelde, F. 2005. Green veining: landscape determinants of biodiversity in European agricultural landscapes. *Landscape Ecology* **20**: 417-439.

Hajek, E.R. & Gutiérrez, J.R. Growing seasons in Chile: Observation and prediction. *International Journal of Biometeorology* **23**(4): 311-329.

Harris, I., Jones, P.D., Osborn, T.J. & Lister, D.H., 2013. Updated high-resolution grids of monthly climatic observations - the CRU TS3.10 Dataset. *International Journal of Climatology* **34**(3): 623e642

Hijmans, R.J. & Elith, J. 2019. Spatial Distribution Models. Available from: <https://rspatial.org/sdm/SDM.pdf> [Accessed 07/01/2019].

Hijmans, R.J., Phillips, S., Leathwick, J. & Elith, J. 2017. dismo: Species Distribution Modelling. R package version 1.1-4. Available from: <https://CRAN.Rproject.org/package=dismo> [Accessed 07/01/2019].

Hijmans, R.J., Cameron, S.E., Parra, J.L., Jones, P.G. & Jarvis, A. 2005. Very high-resolution interpolated climate surfaces for global land areas. *International Journal of Climatology* 25: 1965-1978.

Højsgaard, S. 2016. Package 'gRain': Graphical Independence Networks. Version 1.3-0. Available from: <https://cran.r-project.org/web/packages/gRain/gRain.pdf> [Accessed 03/01/2019].

ISRIC. 2019. Harmonized continental SOTER-derived database (SOTWIS). Available from: <https://www.isric.org/index.php/projects/harmonized-continental-soter-derived-database-sotwis> [Accessed 03/01/2019].

Jara, J., Holzapfel, E.A., Billib, M., Arumi, J.L., Lagos, O. & Rivera, D. 2017. Effect of water application on wine quality and yield in 'Carménère' under the presence of a shallow water table in Central Chile. *Chilean Journal of agricultural research* 77(2): <http://dx.doi.org/10.4067/S0718-58392017000200171>

Johnston, J.M., Wheatley, M.J., Wooster, M.J., Paugam, R., Davies, G.M. & DeBoer, K.A. 2018. Flame-front rate of spread estimates for moderate scale experimental fires are strongly influenced by measurement approach. *Fire* 1: 16.

JNCC. 2018. JNCCsdms: Functions to Generate Species Distribution Models using the JNCC SDM Framework. R package version 0.1.0. <https://github.com/jncc/sdms>

Jones, T., Wicks, D., Agass, S. & Bunting, P. 2017. Developing standards and automated production for Sentinel-2 Analysis Ready Data. Evidence Project SD1707

Journet, G. 2016. Viticulture and ecosystem services: from myths to reality with Chilean vine growers. Master's Thesis 2016 30 ECTS. Department of Plant Sciences, Norges Miljø- og biovitenskapelige universitet.

Kilcoyne, A.M. Alexander, R., Cox, P. & Brownnett, J. 2017. Living Maps: Satellite based Habitat Classification. Evidence Project SD1705

Lehner, B. & Grill, G. 2013. Global river hydrography and network routing: baseline data and new approaches to study the world's large river systems. *Hydrological Processes*, 27(15): 2171–2186.

Márquez-García, M., Jacobson, S.K. & Barbosa, O. 2018. Wine with a Bouquet of Biodiversity: Assessing Agricultural Adoption of Conservation Practices in Chile. *Environmental Conservation* page 1 of 9. doi:10.1017/S0376892918000206

Martínez, E. 2014. Proyecto Monitoreo de cambios, corrección cartográfica y actualización del catastro de bosque native en las regiones de Valparaíso, Metropolitana y Libertador Bernardo O'Higgins. Ciren Informe Técnico Final Diciembre 2013.

Mattiuzzi, M. & Detsch, F. 2018. MODIS: Acquisition and Processing of MODIS Products. R package version 1.1.4. Available from: <https://CRAN.R-project.org/package=MODIS> [Accessed 07/01/2019].

McWethy, D.B., Pauchard, A., García, R.A., Holz, A., Veblen, T.T., Stahl, J. & Currey, B. 2018. Landscape drivers of recent fire activity (2001-2017) in south- central Chile. *PLoS ONE* **13**: e0201195.

Meyer, D., Dimitriadou, E., Hornik, K., Weingessel, A., Leisch, F., Chang, C.C. & Lin, C.C. 2019. Package 'e1071' Version 1.7-0.1: Misc Functions of the Department of Statistics, Probability Theory Group (Formerly: E1071), TU Wien. Available from: <https://cran.r-project.org/web/packages/e1071/e1071.pdf> [Accessed 14/02/2019].

Minchella, A. 2018. JNCC Sentinel-1 Backscatter Data Provision Service. SAR processing Methodology

Moeys, J. 2018. soiltexture: Functions for Soil Texture Plot, Classification and Transformation. R package. Available from: <https://cran.r-project.org/web/packages/soiltexture/index.html> [Accessed 11/02/2019].

Morgan, J.D., Hutchins, M.W., Fox, J. & Rogers, K.R. 2012. A Methodological Framework focused on integrating GIS and BBN Data for Probabilistic Map Algebra Analysis. *7th International Conference, GIScience, Columnus, OH*.

Morgan-Wall, T. 2019. Package 'rayshader': Create and Visualize Hillshaded Maps from Elevation Matrices. Version 0.10.1. Available from: <https://cran.r-project.org/web/packages/rayshader/rayshader.pdf> [Accessed 10/03/2019].

National Center for Atmospheric Research Staff (Eds)(NCEP-CFSR). 2017. The Climate Data Guide: Climate Forecast System Reanalysis (CFSR). Available from: <https://climatedataguide.ucar.edu/climate-data/climate-forecast-system-reanalysis-cfsr> [Accessed 14/01/2019].

Neitsch, S.L., Arnold, J.G., Kiniry, J.R., Williams, J.R. & King, K.W. 2002. Soil and water assessment tool theoretical documentation. Version 2000. Texas Water Resources Institute, College Station, Texas. TWRI Report TR-191. Available from: <https://swat.tamu.edu/media/1290/swat2000theory.pdf> [Accessed 11/02/2019].

Neitsch, S.L., Arnold, J.G., Kiniry, J.R. & Williams, J.R. 2011. Soil and Water Assessment Tool Theoretical Documentation Version 2009. *Texas Water Resources Institute Technical Report No.406*. September 2011.

OMAFRA Factsheet. 2015. Universal Soil Loss Equation (USLE). Available at: <http://www.omafra.gov.on.ca/english/engineer/facts/12-051.htm> [Accessed 03/01/2019].

Omani, N. 2014. Impact Assessment of Climate Change on Glaciers and Runoff Using SWAT. A Dissertation. Doctor of Philosophy: Biological and Agricultural Engineering. Graduate and Professional Studies of Texas A&M University.

Omani, N., Srinivasan, R., Karthikeyan, R. & Smith, P.K. 2017. Hydrological modelling of highly glacierized basins (Andes, Alps, and Central Asia). *Water* **9** (111): doi:10.3390/w9020111.

Palmer, W.C. 1965. Meteorological Drought. Research Paper No. 45. Office of Climatology, US Weather Bureau, Washington DC.

Panagos, P., Borrelli, P., Meusburger, K., Alewell, C., Lugato, E. & Montanarella, L. 2015. Estimating the soil erosion cover-management factor at the European scale. *Land Use Policy* **48**: 38-50.

Puig-Montserrat, X., Stefanescu, C., Torre, I., Palat, J., Fábregas, E., Dantart, J., Arrizabalaga, A. & Flaquer, C. 2017. Effects of organic and conventional crop management on vineyard biodiversity Agriculture, Ecosystems and Environment. *Agriculture, Ecosystems and Environment* **243**: 19–26.

QGIS Development Team. 2019. QGIS Geographic Information System. Open Source Geospatial Foundation Project. Available from: <http://qgis.osgeo.org>

R Core Team. 2018. R: A Language and Environment for Statistical Computing. Vienna, Austria. Available from: <https://www.R-project.org/>

Renard, K.G. & Freimund, J.R. 1994. Using monthly precipitation data to estimate the R-factor in the revised USLE. *Journal of Hydrology* **157**: 287-306 Available from: <https://eurekamag.com/pdf/002/002728247.pdf> [Accessed 14/01/2019].

Renard, K.G., Foster, G.R., Weesies, G.A., McCool, D.K., & Yoder, D.C. 1997. Predicting soil erosion by water: a guide to conservation planning with the Revised Universal Soil Loss Equation (RUSLE). United States Department of Agriculture, Agricultural Research Service. Agriculture Handbook Number 703. Available from: https://www.ars.usda.gov/ARSUserFiles/64080530/rusle/ah_703.pdf [Accessed 10/01/2019].

Ruiz-Albarrán, M., Balocchi, O., Wittwer, F. & Pulido, R. 2016. Milk production, grazing behaviour and nutritional status of dairy cows grazing two herbage allowances during winter. *Chilean Journal of Agricultural Research* **76**(1): <http://dx.doi.org/10.4067/S0718-58392016000100005>

Scutari, M. & Ness, R. 2019. Package ‘bnlearn’: Bayesian Network Structure Learning, Parameter Learning and Inference. Version 4.4.1. Available from: <https://cran.r-project.org/web/packages/bnlearn/bnlearn.pdf> [Accessed 04/01/2019].

Srinivasan, R. 2013. Google Group: SWAT-user: Custom Weather Generator: RAINHHMX (Maximum 0.5 h rainfall) Problem, Available from: <https://groups.google.com/forum/#!topic/swatuser/kpZMCKe3BvU> [Accessed 4/02/2019].

Stanford University. 2019. Integrated Valuation of Ecosystem Services and Tradeoffs. Available from: <https://naturalcapitalproject.stanford.edu/invest/> [Accessed 14/01/2019].

Stehr, A. & Aguayo, M. 2017. Snow cover dynamics in Andean watersheds of Chile (32.0-39.5 S) during the years 2000-2016. *Hydrology and Earth System Sciences* **21**:5111-5126.

Stehr, A., Debels, P., Romero, F. & Alcayaga, H. 2008. Hydrological modelling with SWAT under conditions of limited data availability: evaluation of results from a Chilean case study. *Hydrological Sciences- Journal – des Sciences Hydrologiques* **53**(3):588-600

Strauch, M. & Volk, M. 2013. SWAT plant growth modification for improved modelling of perennial vegetation in the tropics. *Ecological Modelling* **269**: 98-112.

SWAT. 2019. Global Weather Data for SWAT. Available from: <https://globalweather.tamu.edu/> [Accessed: 25/2/2019]

The Natural Capital Project. 2019. InVest Sediment Deliver Ratio (SDR) model documentation. Available from: <http://releases.naturalcapitalproject.org/invest-userguide/latest/sdr.html> [Accessed 2/1/19]

Tribot, A.S., Deter, J. & Mouquet, N. 2018. Integrating the aesthetic value of landscapes and biological diversity. *Proc Biol Sci.* **285**(1886):2018.0971.

Trimaille, E. 2019. QuickOSM QGIS Plugin Version 1.4.15. Available from: <https://plugins.qgis.org/plugins/QuickOSM/> [Accessed 4/2/2019]

UK Technical Advisory Group (UKTAG) on the Water Framework Directive (WFD). 2008. UK Environmental Standards and Conditions (Phase 1) Final report April 2008 (SR1 – 2006). Available from: http://www.wfduk.org/sites/default/files/Media/Environmental%20standards/Environmental%20standards%20phase%201_Finalv2_010408.pdf [Accessed 09/04/2019]

UNU-INWEH. 2019. WaterBase: World Data Grids. Available from: http://www.waterbase.org/download_data.html [Accessed: 14.12.2018]

Urrutia-Jalabert, R., González, M.E., González-Reyes, Á., Lara, A. & Garreaud, R. 2018. Climate variability and forest fires in central and south-central Chile. *Ecosphere* **9**: e02171.

Vaghefi, S.A., Abbaspour, N., Kamali, B. & Abbaspour, K.C. 2017. A toolkit for climate change analysis and pattern recognition for extreme weather conditions – Case study: California-Baja California Peninsula. *Environmental Modelling & Software*. **96**: 181-198. ISSN 1364-8152. <https://doi.org/10.1016/j.envsoft.2017.06.033>.

Valdés-Pineda, R., Pizarro, R., García-Chevesich, P., Valdés, J.B., Olivares, C., Vera, M., Balocchi, F., Pérez, F., Vallejos, C., Fuentes, R., Abarza, A. & Helwig, B. 2014. Water governance in Chile: Availability, management and climate change. *Journal of Hydrology* **519**: 2538-2567.

Van Vuuren, D.P., Edmonds, J., Kainuma, M., Riahi, K., Thomson, A., Hibbard, K., Hurtt, G.C., Kram, T., Krey, V., Lamarque, J.F., Masui, T., Meinshausen, M., Nakicenovic, N., Smith, S.J. & Rose, S.K. 2011. The representative concentration pathways: an overview. *Climate Change* **109**: 5-31. DOI 10.1007/s10584-011-0148-z.

Viñas de Colchagua, A.G. 2012. Colchagua Vina & Ruta: Colchagua Wineries. <http://www.colchaguavalley.cl/en/> [Accessed 21/05/2019].

Washington State University Extension. 2019. Pest Management Guide for Grapes in Washington—2019 EB0762. Available from: http://cru.cahe.wsu.edu/CEPublications/-EB0762/EB0762_19.pdf [Accessed 11/03/2019].

Williams, J.R. 1975. Sediment routing for agricultural watersheds. *Journal of the American Water Resources Association* **11**(5): 965-975.

Wischmeier, W.H. & Smith, D.D. 1978. Predicting rainfall losses: A guide to conservation planning. USDA Agricultural Handbook No 537. U.S. Gov. Print. Office, Washington, D.C.

WorldPop. 2016. Chile 100 m Population. Alpha version 2010, 2015 and 2010 estimates of numbers of people per pixel (ppp) and people per hectare (pph), with national totals adjusted to match UN population division estimates (<http://esa.un.org/wpp/>) and remaining unadjusted. www.worldpop.org, School of Geography and Environmental Science, University of Southampton

World Wildlife Fund (WWF). 2019. HydroSHEDS Available from:
<https://www.worldwildlife.org/pages/hydrosheds> [Accessed:12.12.2018]

Appendix 1 – Implementing the Living Maps Method (LMM) in the Colchagua Valley

1 Datasets

A summary of each of the datasets used for input to the habitat classification is listed below. All data were georeferenced to the map projection that is most suitable to the region, which is WGS 84 / UTM zone 19S (EPSG:32719) and were resampled to 10 m unless otherwise specified.

1.1 Sentinel-1

Sentinel-1 is a polar-orbiting, all weather, day-and-night radar imaging mission for land and ocean services. The mission is part of the European Union (EU) Copernicus Programme and is operated by the European Space Agency (ESA). The mission consists of a two-satellite constellation providing orbit revisit times of six days. The radar instrument transmits and receives in C-band (5.405 GHz) at a resolution of 5 x 20 metres in interferometric wide-swath mode. This is the most common mode that is used over land masses. The data is processed and stored as Level 1 Single Look Complex (SLC) and Level 1 Ground Range Detected (GRD) products by the ground segment of ESA. The SLC product contains the intensity of returns and phase information, whereas the GRD product does not contain the phase information, due to the enhanced processing that it receives. This GRD data is multi-looked and projected to ground range using the earth ellipsoid model.

Sentinel-1 data are transformed into backscatter products from data collected in the Interferometric Wide (IW) swath mode and processed from the Ground Range Detected (GRD) version of the data. These Sentinel-1 data contain data in both VV and VH polarisations. The raw scenes were terrain corrected, radiometrically normalised and processed to Gamma-0 backscatter coefficient in decibels (dB) using the SNAP Toolbox (<http://step.esa.int/main/toolboxes/snap/>). An example Sentinel-1 ARD product is shown in Figure A1.1.

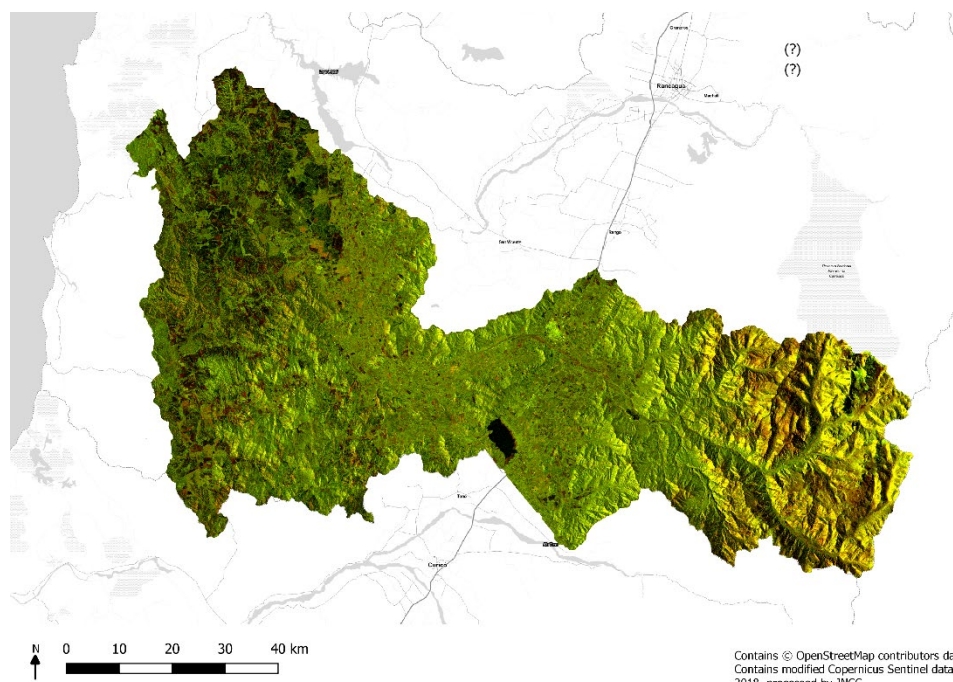


Figure A1.1. Sentinel-1 ARD product, captured on the 25th March 2018, for the Colchagua Valley.

1.2 Sentinel-2

Sentinel-2 is a polar-orbiting, multispectral high-resolution imaging mission for land monitoring. The mission is also part of the EU's Copernicus Programme and operated by ESA. The mission consists of a two-satellite constellation providing orbit revisit times 10 days at the equator with one satellite, and five days with two satellites under cloud free conditions which results in 2-3 days at mid-latitudes. The optical instrument payload samples 13 spectral bands: four bands at 10 metres six bands at 20 metre and three bands at 60 metre spatial resolution. The orbital swath width is 290 kilometres.

Sentinel-2 data are transformed to produce a topographically corrected surface reflectance product with cloud and topography mask that can be applied to the imagery provided separately. The Atmospheric and Radiometric Correction of Satellite Imagery (ARCSI) software (<http://www.rsgislib.org/arcsi>) was used to produce this product, as this is the software that has been used during the automation process in the UK (Jones *et al.* 2017). This process, although developed for UK processing, can be deployed globally, and this saves time in cost and effort while deploying the processing chain to other areas globally. During the processing the 20 m image bands are sharpened to 10 m through application of linear regression models. The 60 m bands are primarily used for atmospheric aerosol correction and processes and are therefore removed from the final surface reflectance product.

ESA's SNAP toolbox was used to create Linear Spectral Unmixing (LSU) layers for productive vegetation, non-productive vegetation, and shade and water for all four Sentinel-2 scenes. The rationale behind LSU is that the signal detected by Sentinel-2 into a pixel is frequently a combination of numerous disparate signals. Figure A1.2 shows a visualisation of this. To overcome the mixed pixels, modelling is implemented in the SNAP toolbox (<http://step.esa.int/main/toolboxes/snap/>) to identify the percentage of each material present per pixel. The user defines "pure" pixels for the productive vegetation, non-productive

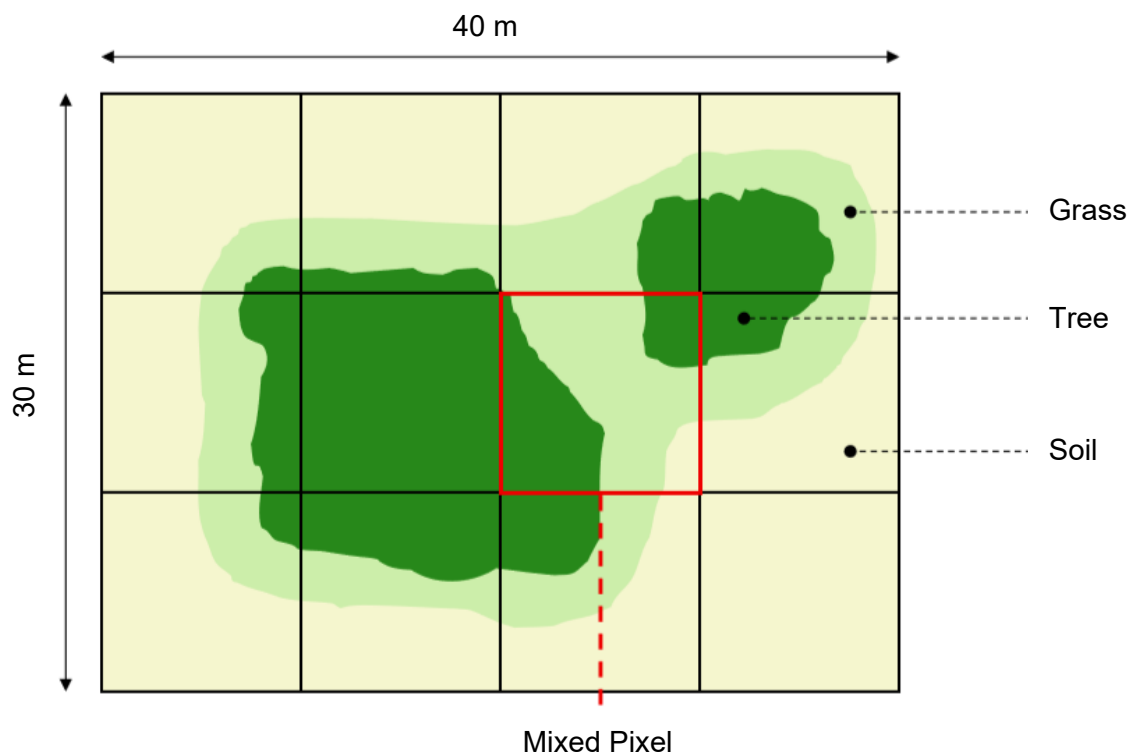


Figure A1.2. An example diagram showing a mixed pixel composed of grass, trees and soil (Kilcoyne *et al.* 2017).

vegetation, shade and water layers. The relative abundance of these materials are then highlighted based on the materials spectral characteristics. By identifying pure pixels of desired criteria, each pixel is attributed with affinity to the training pixels. For more detail on the LSU process see Living Map Method Report (Kilcoyne *et al.* 2017).

1.3 Digital Elevation Model (DEM)

A DEM provided by NASA's Shuttle Radar Topography Mission (SRTM) in 2000 was used in the classification process. The SRTM data is open source and is available at a resolution of 1 arc-second, or about 30 metres. Data were downloaded from Earth Resources Observation and Science (EROS) Center website (<https://www.usgs.gov/centers/eros>). Layers of slope, aspect and hill shade were also created, and all layers were resampled to 10 metre spatial resolution.

1.4 Bioclim

Maximum temperature, minimum temperature and annual rainfall was downloaded as freely available raster layers at ~1 km spatial resolution (30 arc-seconds) from WorldClim (<http://worldclim.org/bioclim>).

1.5 Open Street Map data

OpenStreetMap® are open data, licensed under the Open Data Commons Open Database License (ODbL) by the OpenStreetMap Foundation (OSMF). The data were downloaded through a QGIS plugin (https://wiki.openstreetmap.org/wiki/QGIS_OSM_Plugin) and included layers on buildings and roads.

2 Training Data

There were limited data available from the field for use in this project for habitat mapping. A 2013 land cover map was available and was used as a baseline. Training data created based on the location and distribution of classes as mapped in 2013; albeit on a coarser scale. Within each class distribution, an equal number of points were generated per class on a random basis. All these points were used to train the random forest algorithm only.

3 Method

A summary of steps is outlined in the flowchart in Figure A1.3.

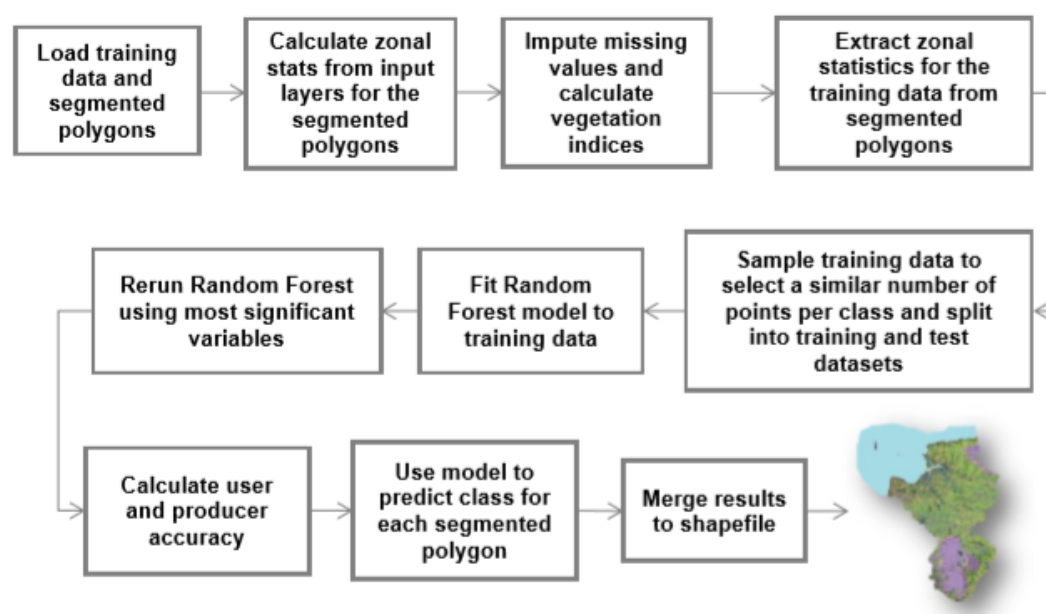


Figure A1.3. Flowchart of classification process (Kilcoyne *et al.* 2017).

The method follows the steps of the Living Maps Method. More detail on the steps can be seen in the technical report (Kilcoyne *et al.* 2017). The only difference to the method outlined in this report is the segmentation process, and the number of significant variables identified to improve the model fit of Random Forest, which is outlined below in Appendix section 3.1.

3.1 Segmentation

The segmentation was applied in the commercial image analysis software package, Trimble eCognition version 9.2.1. At the time of writing, eCognition produces a better object characterisation of the landscape than open-source software alternatives. The processing of the segmentation used the Sentinel-2 images from December. The segmentation algorithm used was a combination of the multispectral segmentation and spectral differences algorithm. The multispectral segmentation algorithm was first used to generate objects, while the spectral difference algorithm was used to eliminate small objects by combining spectrally similar objects into one. The parameters used are outlined in Table A1.1

Table A1.1. Parameters used for object generation.

Multiresolution Segmentation	Parameters
Image band weights	Blue = 1; Green = 1; Red = 2; Red Edge 5 = 1; Red Edge 6 = 1; Red Edge 7 = 1; Red Edge 8A = 1; NIR = 3; SWIR1 = 4; SWIR2 = 4
Scale parameter	18
Shape	0.6
Compactness	0.4

3.2 Random Forest Classifier most significant variables

Random Forest was selected as the most successful statistical classification method. A multinomial classifier, Random Forest is a fast and parallelisable algorithm (compared to other statistical classification methods such as Support Vector Machines). Random Forest has a low computation requirement and can therefore be rerun without large time investment. The method is extremely flexible, able to deal with continuous and categorical variables, and able to discern interactions between variables (Kilcoyne *et al.* 2017).

A Random Forest is built out of a large number of decision trees, which have been trained on a subset of the training data and a subset of the training variables. Trees are built by making a series of sequential partitions of the training data, each one based on the value of a single variable, until the data has been separated into groups with identical classes, or a maximum number of partitions are reached. New data points can then be fed through each tree to produce a prediction. The predictions from each tree are aggregated, and the class with the most “votes” is considered the best overall prediction. Each of the individual trees is a weak predictor of class, but together the forest has stronger predictive power (Kilcoyne *et al.* 2017).

The number of variables required to produce an accurate classification varies per project and the final number is determined when the overall accuracy of the map does not increase with additional variables. The final list of variables is available in Table A1.2

Table A1.2. Final list of variables used in the mapping and their significance values as determined by the random forest algorithm.

Variable name	Significance Value
Slope – Mean	72.54760129
Waterways – Open Street Map – Mean	71.24787397
Height – Mean	59.63962917
Roads – Open Street Map – Mean	55.58142176
Sentinel-2 – March – Roughness – Mean	49.51739453
Difference Index – Sentinel-2 – October – Green Band – SWIR1 Band	46.80663597
Sentinel-2 – October – Blue Band – Mean	40.00953466
Sentinel-2 – December – Blue Band – Median	39.42202805
Sentinel-2 – December – Red Edge [8A] Band – Median	36.3874349
Sentinel-2 – December – Blue Band – Mean	36.28038398
Sentinel-1 – July – Backscatter – VH – Mean	35.75198425
Difference Index – Sentinel-2 – December – Green Band – SWIR1 Band – Mean	35.20160931
Difference Index – Sentinel-2 – March – Green Band – SWIR1 Band – Mean	35.18408674
Sentinel-1 – July – Backscatter – VV – Mean	34.48999362
Difference Index – Sentinel-2 – October – Red Band – SWIR2 Band – Mean	33.71149407
Sentinel-2 – December – Red Edge [8A] Band – Standard Deviation	32.86976039
Difference Index – Linear Spectral Unmixing – March – Non-Photosynthetic Vegetation – Linear Spectral Unmixing – October – Non-Photosynthetic Vegetation – Mean	32.59380616
Sentinel-2 – October – Blue Band – Median	32.47969091
Sentinel-1 – July – Backscatter – VV – Median	32.19519016
Linear Spectral Unmixing – October – Water/Shade – Mean	32.11183534
Sentinel-2 – July – NDWI (Green) – Mean	32.05935048
Difference Index – Sentinel-2 – October – Red Band – SWIR1 Band - Mean	32.02550816
Sentinel-2 – March – Blue Band – Median	31.87871294
Difference Index – Sentinel-2 – December – Red Band – Red Edge [5] Band – Mean	31.60258527
Sentinel-1 – October – Backscatter – VV – Mean	31.15906736
Sentinel-2 – October – Green Band – Mean	30.70047368
Sentinel-1 – July – Backscatter – VH - Median	30.22784791
Sentinel-2 – October – Red Edge [8A] Band – Median	29.94324594
Sentinel-2 – March – Blue – Mean	29.84671631

Sentinel-2 – October – Blue Band – Standard Deviation	29.53510312
Sentinel-2 – October – NIR – Median	28.75321749
Sentinel-2 – October – Red Band – Mean	28.1821866
Sentinel-2 – October – Red Edge [7] Band – Mean	28.11684533
Sentinel-2 – October – SWIR2 Band – Median	28.08480935
Difference Index – Sentinel-2 – December – Red Band – Red Edge [5] Band – Mean	28.08058611
Plantations – O'Higgins 2013 – Mean	27.03271549
Sentinel-2 – October – Green Band – Median	26.78671136
Sentinel-2 – December – Green Band – Mean	26.67012603
Sentinel-2 – October – Red Edge [5] Band – Mean	24.49036896
Sentinel-2 – December – Red Edge [6] Band – Standard Deviation	24.1995114
Sentinel-2 – December – NIR Band – Standard Deviation	23.50938571
Sentinel-2 – December – Red Edge [7] Band – Standard Deviation	22.76341942

Appendix 2 – SWAT modelling HRU parameters

Various model parameters were required to create the Hydrological Response Units (HRUs) of the SWAT model. To create unique soil and land use combination from the data layers, a lookup table was created to relate the land classes of the habitat map (section 2) to the crop databases within SWAT (Table A2.1). Glaciers and Snow cover are classed as water, with the snowmelt parameters determining its physical state when the SWAT is run. As explained in section 4, as detailed crop characteristics and measurements were unavailable, the habitat classes were matched to the nearest crop type in SWAT's inbuilt crop databases, which are based upon temperate US crop types. Managed agricultural habitats of crop grassland and plantations were classed as Cropland/Grassland Mosaic and Cropland/Woodland Mosaic respectively, capturing the differences in their vegetative structure. However, this caused some inaccuracies in the modelling process where for instance although the Central Andean steppe and Southwestern US (Arid) Range may share some characteristics of grassy/shrubby regions intermixed with bare exposed rock, the crop species present will vary and therefore may not accurately represent plant characteristics such as average rooting depth.

Table A2.1. The land use lookup table comparing habitat classes from the produced habitat map (see Chapter 1) with classes within the SWAT crop and urban databases. Further descriptions of the SWAT classes are noted in Appendix A of the SWAT documentation in Arnold *et al.* (2012)

Raster Id	Habitat class	SWAT class	SWAT class name
1	Agricultural land	AGRL	Agricultural Land - Generic
2	Alluvial plain	WEHB	Herbaceous wetland
3	Central Andean steppe	SWRN	Southwestern US (Arid) Range
4	Crop grassland	CRGR	Cropland/Grassland Mosaic
5	Glaciers	WATR	Water
6	Lakes	WATR	Water
7	Native forest	FRST	Forest – Mixed
8	Plantation	CRWO	Cropland/Woodland Mosaic
9	Rivers	WATR	Water
10	Rocky outcrops	BSVG	Barren or Sparsely Vegetated
11	Scrubland	SHRB	Shrubland
12	Seasonal meadows	GRAS	Grassland
13	Snow cover	WATR	Water
14	Trees & shrub	SHRB	Shrubland
15	Urban	URBN	Residential
16	Vineyard	GRPE	Vineyard

1 Plant growth definitions

Once the HRUs were defined in the model, management operation parameters were used to establish cycles in plant growth. These are determined in SWAT by the crop characteristics of the land use class and by the operations applied to each HRU. These operations define the start period when growth begins and the end of the growth period for natural habitats or when harvest occurs for managed land.

As SWAT was developed for temperate regions, operations are usually scheduled by heat day units and the algorithms rely on a dormancy period, which is absent in regions in the tropics and the southern hemisphere (Strauch & Volk 2013). To overcome this, management operations for all land use classes were scheduled instead by date, following the start and end of the growing season in September and April, as noted for Curico, in Hajek and Guitierrez (1979). Managed agricultural habitats and vineyards were scheduled according to

information provided by stakeholders at a pre-project workshop; vineyard harvest season was set as taking place in March.

2 Snow parameters

Glacier boundaries were denoted in the habitat map. Using the GLIMS Glacier database, visual comparisons with the habitat map (described in appendix section 1) showed they followed a similar outline with the same sub-basins impacted by both datasets. Following the approach of Omani *et al.* (2017), these boundaries were used to help determine the equilibrium line altitude (ELA), a theoretical line separating the accumulation and ablation zone of a glacier, and different snow melt parameters were assigned to areas of ice and snow present in the relevant zones. The ELA was estimated through comparisons of the habitat map and DEM to extract the minimum elevation for glaciated habitats within each sub-basin, assuming below which snow cover would be seasonal. Sub-basins exceeding a threshold elevation of 2000 m were subdivided into 10 elevation bands, with bands evenly spaced throughout each sub-basin's minimum and maximum elevations (see Table A2.3). Glacier bands were denoted as those where at least 50% of the elevation band exceeded the ELA.

The GLIMS database had few complete records falling within our study region and was lacking seasonal snow line data, therefore the seasonal snow line was instead presumed to be equivalent to the minimum elevation of the snow cover denoted by the habitat map. This had a lower accuracy as the full seasonality of snow cover was not assessed in the creation of the habitat map but provided an indication of areas that experience some snow cover throughout the year.

From the literature, melt factors have been reported higher for ice (6-8 mm per day) than snow (3-5 mm per day) (Braithwaite 2008). Snow melt parameters were extracted from Table 1.15 in Omani's (2014) dissertation study where SWAT was used to model a similar glaciated watershed study region in Central Chile. The average snowmelt parameters across the total basin were applied across the 10 elevation bands, with maximum melt factors and minimum lag times applied where elevations were highest, shown in Table A2.2.

The initial snow storage was required for each individual band, denoted with the 'SNOEB' parameter in SWAT as the equivalent water content within the band. Local snow depth records and observations of mean ice thickness within the catchment region of Libertador Bernardo O'Higgins were unavailable from the World Glacier Inventory (WGI 2019). As a result, snow depths for the elevation bands were estimated from glacial experiments conducted in the Chilean Andes by Stehr and Aguayo (2017). Data obtained from the supplementary section of their 2017 study contained mean snow depth records for three stations installed at varying elevations in the Biobío region in Central Chile, a region just south of Libertador Bernardo O'Higgins with a similar climate that has been studied in greater detail than the Colchagua region of interest. Their experimental stations provided an indication of the varying snow depth and were applied to the elevation bands in the watershed model where elevations exceeded that of the station (Portillo alt. 3005 m, mean depth: 473.5091 mm, Laguna Negra alt. 2709 m, mean depth: 376.3265 mm, Volcan Chilan alt. 1964 m, mean depth: 262.366 mm).

Table A2.2. The snowmelt parameters used within defined elevation bands, from Omani (2014).

Snow melt parameter	SWAT parameter	Lower elevation bands (below snow cover)	Snow bands	Glacier bands (avg)	Glacier bands (max)
Temperature lapse rate (°C/km)	TLAPSE	-4.3	-4.3	-4.3	-4.3
Precipitation lapse rate (mm H ₂ O/km)	PLAPSE	-17	-17	-17	-17
Snowfall temperature (°C)	SFTMP	0.77	1.01	1.14	1.14
Snowmelt base temperature (°C)	SMTMP	0.42	0.90	1.66	5
Melt factor for snow on June 21 (°C)	SMFMX	4.68	4.64	5.38	7
Melt factor for snow on December 21 (°C)	SMFMN	4.07	4.06	4.93	8
Snowpack temperature lag factor (°C)	TIMP	0.78	0.74	0.50	0.01

Table A2.3. Sub-basins exceeding a threshold elevation of 2000 m were divided into 10 elevation bands, with the threshold elevations noted for each band (ELEV1-10). The minimum snow cover elevation and glacier elevations were extracted from comparisons with the Digital Elevation Model and habitat map layers along with the maximum elevation for each sub-basin. Where there was no overlap between the snow and glacier habitats within a sub-basin boundary this is denoted as n/a*.

Sub-basin	Maximum elevation (m)	Minimum snow cover elevation (m)	Minimum glacier elevation (m)	ELEVB1 (m)	ELEVB2 (m)	ELEVB3 (m)	ELEVB4 (m)	ELEVB5 (m)	ELEVB6 (m)	ELEVB7 (m)	ELEVB8 (m)	ELEVB9 (m)	ELEVB10 (m)
13	3567	2443	2655	1466.55	1687.65	1908.75	2129.85	2350.95	2572.05	2793.15	3014.25	3235.35	3456.45
14	4971	2495	2542	1690.65	2035.95	2381.25	2726.55	3071.85	3417.15	3762.45	4107.75	4453.05	4798.35
15	3752	2385	2416	1475.8	1715.4	1955	2194.6	2434.2	2673.8	2913.4	3153	3392.6	3632.2
18	3918	2657	2860	1121.2	1415.6	1710	2004.4	2298.8	2593.2	2887.6	3182	3476.4	3770.8
19	4971	2379	2474	1686.85	2032.55	2378.25	2723.95	3069.65	3415.35	3761.05	4106.75	4452.45	4798.15
22	2059	n/a*	n/a*	374.65	551.95	729.25	906.55	1083.85	1261.15	1438.45	1615.75	1793.05	1970.35
26	2535	n/a*	n/a*	754.7	942.1	1129.5	1316.9	1504.3	1691.7	1879.1	2066.5	2253.9	2441.3
27	4686	2717	3037	1602.3	1926.9	2251.5	2576.1	2900.7	3225.3	3549.9	3874.5	4199.1	4523.7
28	4207	2781	2991	1578.35	1855.05	2131.75	2408.45	2685.15	2961.85	3238.55	3515.25	3791.95	4068.65
30	4676	2439	2426	1253.15	1613.45	1973.75	2334.05	2694.35	3054.65	3414.95	3775.25	4135.55	4495.85
32	2062	n/a*	n/a*	375.75	553.25	730.75	908.25	1085.75	1263.25	1440.75	1618.25	1795.75	1973.25
33	3056	2410	2480	779.8	1019.4	1259	1498.6	1738.2	1977.8	2217.4	2457	2696.6	2936.2
38	3028	2499	2579	1079.55	1284.65	1489.75	1694.85	1899.95	2105.05	2310.15	2515.25	2720.35	2925.45
40	2939	2489	2663	793.9	1019.7	1245.5	1471.3	1697.1	1922.9	2148.7	2374.5	2600.3	2826.1
43	3838	2513	2939	1458.25	1708.75	1959.25	2209.75	2460.25	2710.75	2961.25	3211.75	3462.25	3712.75
47	3706	2778	2994	1208.45	1471.35	1734.25	1997.15	2260.05	2522.95	2785.85	3048.75	3311.65	3574.55
52	2057	n/a*	n/a*	552.2	710.6	869	1027.4	1185.8	1344.2	1502.6	1661	1819.4	1977.8
54	3911	2717	2837	840.6	1163.8	1487	1810.2	2133.4	2456.6	2779.8	3103	3426.2	3749.4
60	2243	n/a*	n/a*	568.15	744.45	920.75	1097.05	1273.35	1449.65	1625.95	1802.25	1978.55	2154.85

Appendix 3 – Stakeholder workshops

The stakeholder vineyards provided meteorological station data from 2018 along with information on the management practices they use on their fields shown in the tables below:

Table A3.1. Pest questionnaire.

Field	Type of treatment	Insects	Fungus	Rabbits	Birds	Others	None
a	Chemical	Insects	Fungus				
a	Biocontrol	Insects					
b	Chemical	Insects	Fungus				
b	Biocontrol	Insects					
c	Chemical	Insects	Fungus			Mite	
c	Biocontrol			Rabbits			
d	Chemical	Insects	Fungus				
d	Biocontrol	Insects					
e	Chemical	Insects	Fungus				
e	Biocontrol	Insects	Fungus				
f	Chemical	Insects	Fungus				
f	Biocontrol	Insects	Fungus				
g	Chemical	Insects	Fungus			Mite	
g	Biocontrol						None
h	Chemical	Insects	Fungus				
h	Biocontrol						None
i	Chemical	Insects	Fungus				
i	Biocontrol						None
j	Chemical		Fungus				
j	Biocontrol						None
k	Chemical	Insects	Fungus				
k	Biocontrol			Rabbits	Birds		
l	Chemical	Insects	Fungus			Mite	
l	Biocontrol	Insects					
m	Chemical	Insects	Fungus				
m	Biocontrol	Insects					
n	Chemical	Insects	Fungus				
n	Biocontrol						None
o	Chemical	Insects	Fungus			Mite	
o	Biocontrol						None
p	Chemical	Insects	Fungus				
p	Biocontrol	Insects					
q	Chemical	Insects	Fungus				
q	Biocontrol	Insects					
r	Chemical	Insects	Fungus				
r	Biocontrol	Insects		Rabbits			

Table A3.2. Weed management.

Field	Most damaging weeds	Scientific name	Where the weed grows	Type of management (Chemical, Mechanical, Both, Cover crop)	Frequency (times per year)	Information used to decide frequency
a	Chepica	Paspalum paspalodes	Inter-row, under-vine	C	2	Monitoring
a	Correhuela	Convolvulus arvensis	Inter-row, under-vine	C	2	Monitoring
b	Chepica	Paspalum paspalodes	Inter-row, under-vine	C	2	Monitoring
b	Correhuela	Convolvulus arvensis	Inter-row, under-vine	C	2	Monitoring
c	Conyza	Conyza bonariensis	Inter-row, top-vine	B	2	Monitoring
c	Correhuela	Convolvulus arvensis	Inter-row, top-vine	B	2	Monitoring
c	Acacia caven	Acacia caven	Inter-row, under-vine	M	1	Monitoring
d	Chepica	Paspalum paspalodes	Under-row	B	12	Monitoring
d	Zanahoria silvestre	Daucus carota	Under-row	B	4	Monitoring
d	Falso te	Bidens aurea	Under-row	B	4	Monitoring
e	Chepica	Paspalum paspalodes	Everywhere	M	12	Monitoring
e	Galega	<i>Galega officinalis</i>	Everywhere	M	12	Monitoring
e	Maicillo	Sorghum halepense	Everywhere	M	12	Monitoring
f	Chepica	Paspalum paspalodes	Everywhere	M	12	Monitoring
f	Galega	<i>Galega officinalis</i>	Everywhere	M	12	Monitoring
f	Maicillo	Sorghum halepense	Everywhere	M	12	Monitoring
g	Correhuela	Convolvulus arvensis	Everywhere	B	12	Monitoring
g	Ballica	Lolium sp.	Everywhere	C	4	Monitoring
g	Malva	Malva nicaensis	Everywhere	B	12	Monitoring
h	Conyza	Conyza bonariensis	Inter-row, top-vine	B	2	Monitoring
h	Loteria	Lotus corniculatus	Inter-row, top-vine	M		Monitoring
h	Meloza	Madia sativa	Inter-row, top-vine	C	3	Monitoring
i	Conyza	Conyza bonariensis	Everywhere	C	3	Monitoring
i	Meloza	Madia sativa	Everywhere	C	3	Monitoring
j	Chepica	Paspalum paspalodes	Inter-row, under-vine	C	1	Calendar
j	Galega	<i>Galega officinalis</i>	Inter-row, under-vine	M	1	Monitoring
j	Correhuela	Convolvulus arvensis	Inter-row, top-vine	C	1	Monitoring
k	Grass		Inter-row, under-vine	M	1	Monitoring
k	Correhuela	Convolvulus arvensis	Everywhere	C	12	Monitoring
k	Chepica	Paspalum paspalodes	Inter-row, under-vine	C	1	Monitoring
l	Correhuela	Convolvulus arvensis	Inter-row	M	1	Monitoring
l	Qinguilla	Chenopodium album	Inter-row	M	1	Monitoring
l	Yuyo	Brassica campestris	Inter-row, top-vine	B	1	Monitoring
m	Correhuela	Convolvulus arvensis	Everywhere	B		Monitoring
m	Epilodyum	Epilobium sp	Everywhere	B		Monitoring
m	Qinguilla	Chenopodium album	Everywhere	B		Monitoring
n	Chepica	Paspalum paspalodes	Inter-row	M, Cover crop	12	Monitoring
n	Meloza	Madia sativa	Inter-row, under-vine	M, Cover crop	12	Monitoring
o	Correhuela	Convolvulus arvensis	Under-vine	C	12	Monitoring
o	Ballica	Lolium sp.	Under-vine	M	12	Monitoring
p	Conyza	Conyza bonariensis	Inter-row, under-vine	M	8	Monitoring
p	Ballica	Lolium sp.	Inter-row, under-vine	C	8	Monitoring
p	Malva	Malva nicaensis	Under-vine	C	8	Monitoring
q	Conyza	Conyza bonariensis	Inter-row, under-vine	M	8	Monitoring
q	Ballica	Lolium sp.	Inter-row, under-vine	C	8	Monitoring
q	Malva	Malva nicaensis	Under-vine	C	8	Monitoring
r	Conyza	Conyza bonariensis	Inter-row, under-vine	M	8	Monitoring
r	Ballica	Lolium sp.	Inter-row, under-vine	C	8	Monitoring
r	Malva	Malva nicaensis	Under-vine	C	8	Monitoring

Table A3.3. Tillage practices.

Field	Type of interrow management (Tillage, Covercrop, Both)	When tillage present (Mechanical, Animal, Both, Other)
a	Both	Mechanical
b	Both	Mechanical
c	Tillage	Mechanical
d	Tillage	Mechanical
e	Covercrop	
f	Covercrop	
g	Both	Both
h	Tillage	Both
i	Covercrop	
j	Tillage	Both
k	Tillage	Mechanical
l	Both	Mechanical
m	Both	Mechanical
n	Tillage	Mechanical
o	Both	Mechanical
p	Both	Mechanical
q	Both	Both
r	Both	Both

Table A3.4. Fertiliser application practices.

Field	Type of fertilizer	Frequency (Times per year)	Name	Field	Type of fertilizer	Frequency (Times per year)	Name
a	Chemical	2	Urea	i	Organic	0	
a	Chemical	2	Muriate of potassium	j	Chemical	2	Urea
a	Organic	1	Compost	j	Chemical	2	UAN 32
b	Chemical		Urea	j	Chemical	2	Nitrato K
b	Chemical	2	Muriate of potassium	j	Chemical	1	Muriato K
b	Organic	1	Compost	j	Organic	0	
c	Chemical	2	Urea	k	Chemical	2	
c	Chemical	2	Muriate of potassium	k	Chemical	2	
c	Chemical	1	monoammonium phosphate	k	Chemical	2	
c	Organic	1	Compost	k	Organic	0	
c	Organic	1	Fontsoil	l	Chemical	28	Not specified
c	Organic	1	Iberhumus	l	Chemical	28	Foliasa
d	Chemical	1	Nitrogen	l	Organic	12	Seaweed
d	Chemical	1	Potassium	m	Chemical	2	Not specified
d	Chemical	1	Phosphorus	m	Chemical	28	Not specified
d	Chemical	2	Magnesium	m	Organic	12	Not specified
d	Chemical	1	Boron	n	Organic	28	Humus
d	Organic	0	NA	n	Organic	1	Compost
e	Chemical	0	NA	n	Organic	12	Seaweed
f	Chemical	0	NA	o	Chemical	Not specific	Nitrogen
e	Organica	1	Compost	o	Chemical	Not specific	Magnesium
f	Organica	1	Compost	o	Chemical	Not specific	Potassium
g	Chemical	12	Urea	o	Chemical	Not specific	Boron and Zinc
g	Chemical	12	Cloruro de	o	Chemical	Not specific	Phosphorus
g	Chemical	24	Potasio	o	Organic	Not specific	Compost
g	Chemical	24	Nitrato de	o	Organic	Not specific	Guano
g	Chemical	24	Potasio	p	Chemical	20	Nitrogen
g	Chemical	24	Sulfato de Mg	p	Chemical	20	Potassium
g	Chemical	1	Zin, Boro	p	Chemical	32	Magnesium
g	Organic	1	Guano	p	Chemical	4	Boron
g	Organic	12	Cal	p	Chemical	4	Zinc
g	Organic	24	Magnesium	p	Chemical	4	Phosphorus
h	Chemical	2	Nitrogen	q	Chemical	20	Nitrogen
h	Chemical	2	Potassium	q	Chemical	20	Potassium
h	Chemical	1	Phosphorus	q	Chemical	32	Magnesium
h	Chemical	2	Boron	q	Chemical	4	Boron
h	Chemical	2	Zinc	q	Chemical	4	Zinc
h	Organic	0		q	Chemical	4	Phosphorus
i	Chemical	3	Uaal 32	r	Chemical	20	Nitrogen
i	Chemical	2	Muriato Potasio	r	Chemical	20	Potassium
i	Chemical	2	Sulfato Potasio	r	Chemical	32	Magnesium
i	Chemical	4	Acido Fosforico	r	Chemical	4	Boron
i	Chemical	4	Acido Borico	r	Chemical	4	Zinc
i	Chemical	2	Sulfato de Mg	r	Chemical	4	Phosphorus

Table A3.5. Organic management practices.

Field	Other organic practices (Yes/No)	Number of additional organic practices	Practice 1	Practice 2	Practice 3
a	Yes	3	Protection of fauna that controls rabbits	Controlled hunt of rabbits	Vinegar traps of wasps
b	Yes	3	Protection of fauna that controls rabbits	Controlled hunt of rabbits	Vinegar traps of wasps
c	Yes	2	Mecanical control of weeds	Pheromons for pests	
d	Yes	2	Biological corridors	Hummus application in soil	
e	Yes	3	Biodynamic products	Covercrops	Biological corridors
f	Yes	3	Biodynamic products	Covercrops	Biological corridors
g	Yes	1	Organic control of pests		
h	Yes	2	Use of livestock to control weeds in winter	Use of guano as fertilization	
i	Yes	1	Compost		
j	No	0			
k	No	0			
l	Yes	3	Use of livestock to control weeds in winter	Hummus application in soil	Seaweed
m	Yes	3	Use of livestock to control weeds in winter	Covercrops	Seaweed
n	Yes	3	Compost	Control of pest with organic products	Control of weed mechanically
o	Yes	2	Pheromons for pests	Compost	
p	Yes	3	Pheromons for pests	Compost	Use of livestock to control weeds in winter
q	Yes	3	Pheromons for pests	Compost	Use of livestock to control weeds in winter
r	Yes	3	Pheromons for pests	Compost	Use of livestock to control weeds in winter